THE MULTIVESICULAR BODY PATHWAY AND THE ENDOSOMAL SORTING COMPLEXES REQUIRED FOR TRANSPORTS: ESCRT-II RECRUITMENT AND CARGO SORTING MECHANISMS

by

Elizabeth Mary Ott

A dissertation submitted to the faculty of
The University of Utah
in partial fulfillment of the requirements for the degree of

Doctor of Philosophy

Department of Biology

The University of Utah

August 2011

The University of Utah Graduate School

STATEMENT OF DISSERTATION APPROVAL

The dissertation of **Elizabeth Mary Ott**

has been approved by the following supervisory committee members:

Markus Babst	, Chair	**6/17/2011** Date Approved
David Gard	, Member	**6/17/2011** Date Approved
Julie Hollien	, Member	**6/17/2011** Date Approved
Michael Shapiro	, Member	**6/17/2011** Date Approved
Jordan Gerton	, Member	**6/17/2011** Date Approved

and by **Neil Vickers**, Chair of the Department of **Biology**

and by Charles A. Wight, Dean of The Graduate School.

ABSTRACT

The ESCRT (endosomal sorting complexes required for transport) protein complexes are required for the sorting of proteins into the MVB (multivesicular body) pathway, a protein trafficking pathway that is critical for the degradation of plasma membrane proteins. As a result, the ESCRTs plays an important role in the regulation of nutrient import and cell signaling events by influencing the expression of nutrient transporters and signaling receptors on the surface of the cell. In this study we present a novel *in vitro* technique based on SFG (sum-frequency generation) capable of analyzing the dynamic assembly of the ESCRT complexes on planar supported lipid bilayers. We present evidence to support that this novel approach has the potential to provide information about the dynamics of the ESCRT network and to obtain data regarding the function of these protein complexes. Furthermore, we elucidated a regulatory connection between the nutrient sensing system, TORC1 (target of rapamycin complex 1), and the MVB pathway. Our results demonstrate that the MVB pathway functions to degrade non-essential biomass during starvation to replenish depleted amino acid levels. We further propose that ESCRT-dependent protein turnover is regulated by the metabolic state of the cell through TORC1 signaling. Surprisingly, we found indications that endocytosis and subsequent degradation

of plasma membrane proteins is regulated by a novel starvation pathway that acts independently of TORC1. Based on our results, we present a model in which during starvation TORC1, together with an unknown regulatory pathway, increases the sorting efficiency and degradation of cargo proteins through the MVB pathway by suppressing recycling pathways. The increase in protein turnover replenishes the free amino acid pool, which allows the cell to produce stress-response proteins required to adapt to starvation conditions.

This thesis is dedicated to my parents, Jennifer Baade, Trevor Ott and Matt Crowther, for all of their love and support.

TABLE OF CONTENTS

LIST OF TABLES

LIST OF FIGURES

LIST OF ABBREVIATIONS

Defining Term	Abbreviation
Multivesicular body	MVB
Endosomal sorting complex required for transport	ESCRT
Intralumenal vesicles	ILVs
Vacuolar protein sorting	VPS
Endoplasmic reticulum	ER
Epsin N-terminal homology	ENTH
Class c core vacuole/endosome transport	CORVET
Endosome to Golgi retrieval complex	Retromer
Sorting nexin	SNX
Phox domain	PX
Homotypic vacuolar fusion and protein sorting	HOPS
Fab1, YGL023, Vps27 and EEA1	FYVE
Ubiquitin interacting motifs	UIM
Vps27, Hrs, STAM	VHS
GGAs and Tom	GAT
Ub E2 variant	UEV
GRAM-like-ubiquitin binding in EAP45	GLUE
BIN1/amphiphysin,Rvs167	BAR

Myotubularin-like 1 ..... Ymr1

Synaptojanin-like 1 ..... Sjl1

Microtubule interacting and transport ..... MIT

Microtubule interacting motifs one and two ..... MIM

RNA interfering silencing complex ..... RISC

Soluble NSF attachment protein receptor ..... SNARE

Phosphatidylinositol ..... PI

Phosphatidylinositol 3-phosphate ..... PI(3)P

Arrestin related trafficking ..... ART

Homologous to E6-AP COOH terminus ..... HECT

Coatomer protein I ..... COPI

Guanine nucleotide exchange factor ..... GEP

GTPase activating proteins ..... GAP

Epidermal growth factor receptor ..... EGFR

GTPase activating proteins ..... GAP

ACKNOWLEDGMENTS

I would first like to express my sincerest gratitude to my advisor, Dr. Markus Babst, for providing numerous hours of guidance throughout my education over the past 6 years. Thank you for your kindness, understanding, and endless patience you provide as a mentor and friend. I would also like to thank my committee, Drs. John Conboy, Jordan Gerton, Mike Shapiro, Dave Gard and Julie Hollien, for providing feedback and assistance while pursuing my research endeavors. I wish to acknowledge members of the John Conboy Lab, Trang Nguyen, Kathryn Smith and Nilanjana Biswas for their assistance with the SFG experiments. A special thanks to Matt Curtiss and all of the Babst Lab members: Anna Shestakova, Charlie Jones, Shrawan Mageswaran and Jay Keener for providing support and input on a daily basis. I thank my husband and companion, Matt Crowther for his love, friendship, and kind heart. Finally, I would like to thank my friends and family who have been the source of much appreciated encouragement throughout my life.

CHAPTER 1

EUKARYOTIC MEMBRANE TRAFFICKING AND THE MVB PATHWAY

1.1 *Introduction*

Membrane trafficking pathways facilitate a plethora of cellular functions including cell signaling, cell motility, nutrient uptake, and organelle maintenance to name a few. Membrane based trafficking pathways are executed through basic conserved functions, many of which were first described in yeast. The unicellular eukaryotic organism *Saccharomyces cerevisiae*, also known as Baker's yeast, is a powerful model organism for the study of basic cellular processes. We use yeast to study membrane trafficking pathways because of the simplicity of their trafficking pathways and the high degree of homology between trafficking mechanisms in yeast and higher eukaryotes (Conibear, 2010). Unless specifically noted, the following introduction to the trafficking pathways of eukaryotic cells will focus on the yeast system.

1.2 *Membrane Trafficking Pathways*

Membrane trafficking pathways transport proteins and lipids between subcellular membranes. Essential proteins required for organelle function are delivered through membrane trafficking pathways. For example, transporters and receptors are delivered to the cell surface by a membrane trafficking pathway (Conibear, 2010). Proteins that function in the lumen of organelles, such as Golgi and endosomal proteins are delivered to the target organelle through membrane trafficking.

Three major membrane trafficking routes have been well characterized: the biosynthetic, the secretory, and the endocytic pathways (Figure 1.1). Most of the steps involved in membrane trafficking pathways are conserved between

Figure 1.1 Membrane Trafficking Pathways. Transmembrane proteins are synthesized in the ER (1) followed by vesicle transport to the Golgi (2). The Golgi membrane is enriched in PI(4)P (phosphatidylinositol 4-phosphate). Vesicles from the Golgi are delivered via the secretory pathway (3) to the plasma membrane (4), which is enriched in $PI(4,5)P_2$. Golgi-derived vesicles are trafficked via the biosynthetic pathway (5) to the endosome (6), which is enriched in PI(3)P. The early endosome receives endocytic vesicles delivered by the endocytic pathway (7). Recycling pathways traffic plasma membrane proteins back to the surface from the early endosome. Early endosomes mature into late endosomes/MVBs (multivesicular bodies) (8) as proteins are added and removed from the endosome. Recycling from late endosomes to the Golgi also occurs. Cargo sorting at the MVB produces ILVs as part of the MVB pathway (9). MVBs are trafficked to and fuse with the vacuolar membrane (10), which is enriched in $PI(3,5)P_2$. ILVs are degraded and biosynthetic cargoes are delivered to the lumen of the vacuole.

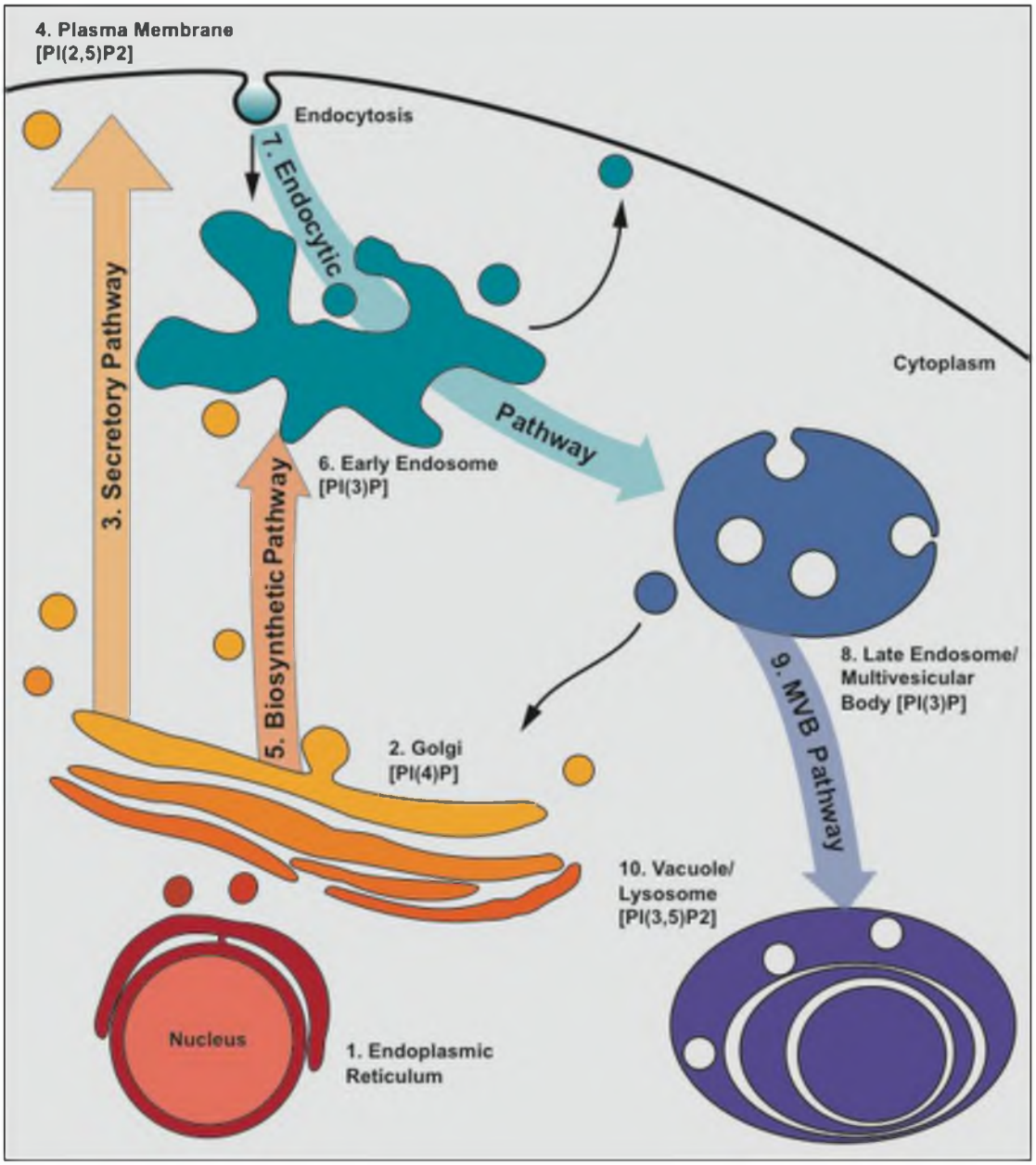
4. Plasma Membrane
[PI(2,5)P2]
Endocytosis
7. Endocytic
Pathway
Cytoplasm
3. Secretory Pathway
6. Early Endosome
[PI(3)P]
5. Biosynthetic Pathway
8. Late Endosome/
Multivesicular
Body [PI(3)P]
9. MVB Pathway
2. Golgi
[PI(4)P]
10. Vacuole/
Lysosome
[PI(3,5)P2]
Nucleus
1. Endoplasmic
Reticulum

pathways and through eukaryotes. In the following paragraphs, the importance of each pathway is discussed briefly and is followed by a general synopsis of the mechanism underlying eukaryotic membrane trafficking pathways.

The proteins trafficked through membrane trafficking pathways are synthesized in the ER (endoplasmic reticulum) (Chen et al., 2010). ER chaperones located in the lumen aid in the folding of nascent peptides by stabilizing hydrophobic regions, unfolded domains and transmembrane domains until they are folded or inserted into the membrane (Chen et al., 2010). Posttranslational modifications including disulfide bond formation and glycosylation are catalyzed in the ER, prior to trafficking to the Golgi (Feige and Hendershot, 2011). ER glycosylations are edited and finalized in the Golgi producing mature proteins. At this point, the biosynthetic and secretory pathways diverge. The biosynthetic pathway delivers cargo to the endosomal system. The secretory pathway is important for both the release of soluble proteins into the extracellular milieu and the delivery of transmembrane proteins and lipids to the plasma membrane.

The endocytic pathway is required for the internalization of plasma membrane proteins and the import of molecules from the environment. Endocytic vesicles are formed at the plasma membrane and are delivered to the endosome. Here, reusable proteins from the plasma membrane and biosynthetic pathway are sorted into recycling pathways for further rounds of cargo delivery. The remaining cargoes are delivered to the vacuole. The vacuole is an acidified compartment containing peptidases and hyrdrolases that degrade proteins in its

lumen (Matile and Wiemken, 1967). The MVB (multivesicular body) pathway is important for the trafficking of membrane proteins to the vacuolar lumen. Cargoes trafficked through the MVB pathway consist of plasma membrane proteins marked for degradation and biosynthetic cargoes, such as vacuolar hydrolases. The MVB pathway sorts cargoes into vesicles, called ILVs (intraluminal vesicles), within the endosome (Piper and Katzmann, 2007). The MVB is then transported to the vacuole where fusion between the MVB and vacuolar limiting membranes releases the ILVs into the lumen of the vacuole, resulting in degradation of protein and lipids. Cargoes that remain on the MVB limiting membrane are inserted into the vacuolar membrane upon MVB fusion. The delivery of cargo protein through vesicle-mediated trafficking pathways occurs through a common sequence of events in all membrane trafficking pathways.

1.3 *Vesicle-Mediated Membrane Trafficking*

The general mechanism of vesicle transport involves four basic steps: cargo selection and budding at the donor membrane, vesicle abscission, motor-based transport and fusion to the acceptor or target membrane (Stenmark, 2009)(Figure 1.2). These steps are highly regulated to ensure the delivery of proteins to the proper membrane and to prevent vesicles from fusing to random membranes.

Figure 1.2 Vesicle Transport. 1. The first step of vesicle transport is cargo selection. Cargo adaptors bind to proteins at the donor membrane and recruit coat proteins like Clathrin. 2. Coat polymerization induces budding and aids in vesicle abscission. 3. Vesicles are uncoated to enable Rabs and their effectors to bind, including myosin type motor proteins. Myosin motors walk along actin filaments moving the vesicle to the target membrane. 4. Vesicles make initial contacts with tethering factors near the target membrane. 5. SNARE (soluble NSF attachment protein receptor) complex formation leads to membrane fusion.

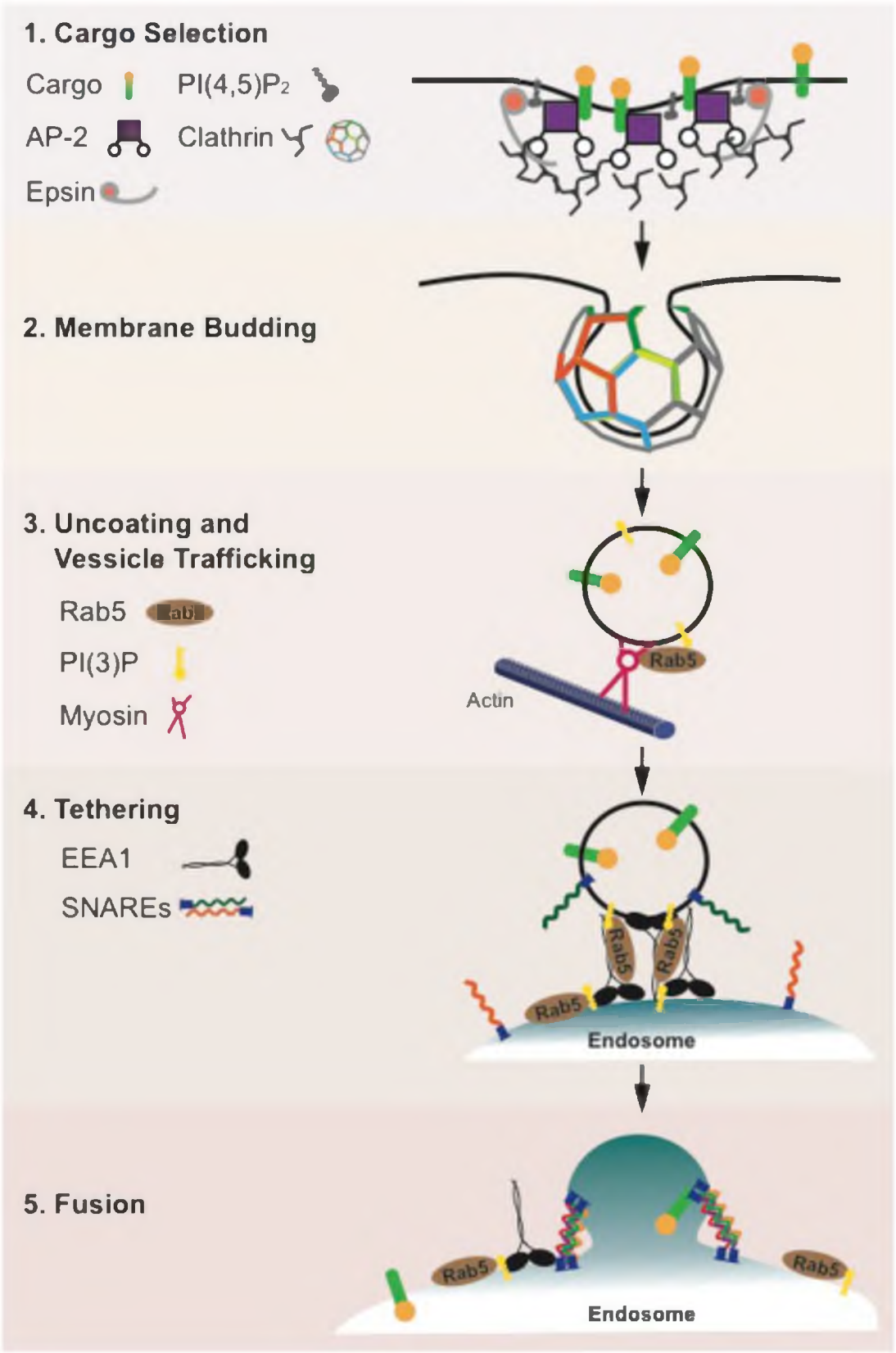
1. Cargo Selection
Cargo
PI(4,5)P2
AP-2
Clathrin
Epsin
2. Membrane Budding
3. Uncoating and
Vessicle Trafficking
Rab5
PI(3)P
Myosin
Actin
Rab5
4. Tethering
EEA1
SNAREs
Rab5
Rab5
Rab5
Endosome
5. Fusion
Rab5
Rab5
Endosome

1.3.1 *Cargo Selection and Budding*

There are a variety of cargo adaptors that function in cargo recognition and clustering at the donor membrane. Some adaptors, like the AP (adaptor protein complexes), bind specific sequences in cargoes whereas other adaptors, like the Epsins, bind to a common endocytosis signal, ubiquitin (Reider and Wendland, 2011). The recruitment of adaptors to cargoes initiates the polymerization of coat proteins, stabilizing and promoting vesicle formation (Reider and Wendland, 2011). Clathrin is one of the most well characterized coat proteins and is involved in the vesicle formation at the plasma membrane, *trans*-Golgi network and endosomes (Conibear, 2010; Conner and Schmid, 2003).

Other coat proteins contain curved BAR (BIN1/amphiphysin,Rvs167) domains that bind to negatively charged lipids and disrupt lipid packing by inserting amphipathic domains into the bilayer, inducing membrane curvature (Madsen et al., 2010). The COPI (coatomer protein I) and COPII coat proteins, which both contain BAR domains, function to form vesicles involved in retrograde and anterograde trafficking between the Golgi network and the ER, respectively (Hughson and Reinisch, 2010; Stenmark, 2009). Often, the recruitment of adaptors and coat proteins to membranes is influenced by the activity of the GTP-ase family of Rab proteins. Rabs cycle through active and inactive states where the GTP-bound active state is catalyzed by GEFs (guanine nucleotide exchange factors) and GAPs (GTPase activating proteins) promote hydrolysis, forming the GDP-bound inactive state (Angers and Merz, 2011). The interaction of Rabs with GDI (guanine dissociation inhibitor), a cytosolic chaperone,

regulates Rab localization between the membrane and the cytoplasm. When Rab is bound by GDI, the prenylation moiety is stabilized and the Rab is soluble. Dissociation of GDI promotes the localization of Rab to membranes through non-specific membrane interaction and by Rab binding to unique lipids or proteins in the membrane (Soldati et al., 1994). Membrane-associated Rabs in the active GTP-bound state recruit effector proteins that enact a variety of functions including membrane identity, vesicle budding and attachment to motor proteins required for motility (Stenmark, 2009).

1.3.2 Vesicle Abscission

Scission of the vesicle neck is required for vesicle detachment. Many of the proteins involved in abscission also contain BAR domains. The binding of BAR domains around the neck of vesicles constricts the membrane inducing lipid mixing and membrane abscission. Disassembly of the coat superstructure occurs during or quickly following abscission prior to intracellular transport, although recent analyses suggest part of the coat remains in tact during transport and might aid in vesicle recognition (Trahey and Hay, 2010). Removal of the coat is necessary to enable trafficking factors to access and bind to the vesicle membrane. Coat disassembly is facilitated by factors that recognize and induce instability in the coat proteins, resulting in uncoating (Xing et al., 2010).

1.3.3 Vesicle Transport

The third step is intracellular trafficking of the vesicle to the target membrane by binding to motor proteins. The myosin family of motor proteins has

been implicated in many of the vesicular trafficking pathways and moves along actin filaments towards the cell periphery, with exception of Myosin VI in mammals, which moves towards the minus end of actin and is involved in vesicle transport during endocytosis (Aschenbrenner et al., 2003; Dance et al., 2004). In yeast, the myosin type 1 motors, Myo3 and Myo5, function during endocytosis in collaboration with the actin cytoskeleton (Grosshans et al., 2006; Jonsdottir and Li, 2004). Kinesin motors move along microtubules towards the cell interior and are involved in organelle transport, mRNA movement and endocytic vesicle trafficking (Bananis et al., 2000; Hirokawa et al., 2009). Attachment of vesicles to the motor protein facilitates motor activation and movement (Sweeney and Houdusse, 2010). In some cases, Rabs, which are localized to distinct compartments, recruit specific motors to the membrane for intracellular transport (Seabra and Coudrier, 2004).

1.3.4 Vesicle Tethering

Initial contact between the vesicle and the target membrane is mediated by tethering factors. Tethering factors are large multisubunit complexes that extend from target membranes and make initial interactions with the vesicle, stabilizing the vesicle at the membrane (van den Bogaart and Jahn, 2011).

1.3.5 Vesicle Fusion with Target Membrane

Rabs recruit the tethering complexes to the target membrane and function in membrane specificity and vesicle binding. Vesicle tethering allows for the formation of the SNARE (soluble NSF attachment protein receptor) protein

complexes, which function in promoting membrane fusion. Binding between the vesicle SNARE complex and the target membrane SNARE complex is required for fusion. The SNARE proteins are anchored to the membrane through a C-terminal transmembrane domain and contain one (R-SNAREs) or two (Q-SNAREs) long sequences of 60-70 amino acids that form αhelices upon SNARE-SNARE interactions (Sutton et al., 1998). One R-SNARE from the vesicle and two Q-SNAREs from the target membrane interact to form a four helix bundle termed a trans-SNARE complex (Sudhof and Rothman, 2009). The formation of the four-helix bundle brings the two membranes close together, initiating membrane fusion and completing vesicle transport (Yu and Hughson, 2010).

1.4 *Phosphoinositides and Membrane Identity*

The enrichment of a specific lipid is used to indicate the identity of subcellular membranes and is required for the recruitment cargo adaptor complexes and Rabs, among other trafficking factors. Often, the lipid enriched in the membrane is a phosphorylated derivative of PI (phosphatidylinositol), such as PI(3)P phosphatidylinositol 3-phosphate, which is unique to the endosomal membrane (Kutateladze, 2010; Segev, 2011) (Figure 1. 3). Several other derivatives of PI are found in other subcellular membranes including $PI(4,5)P_2$ in the plasma membrane, PI(4)P in the Golgi membrane, and $PI(3,5)P_2$ in the vacuolar membrane (Kutateladze, 2010). Vps34, the only phosphoinositol-3-kinase in yeast, forms a complex with Vps15, Vps30 and Vps38 and regulates Vps34 membrane association and kinase activity (Kihara et al., 2001). Vps34 is

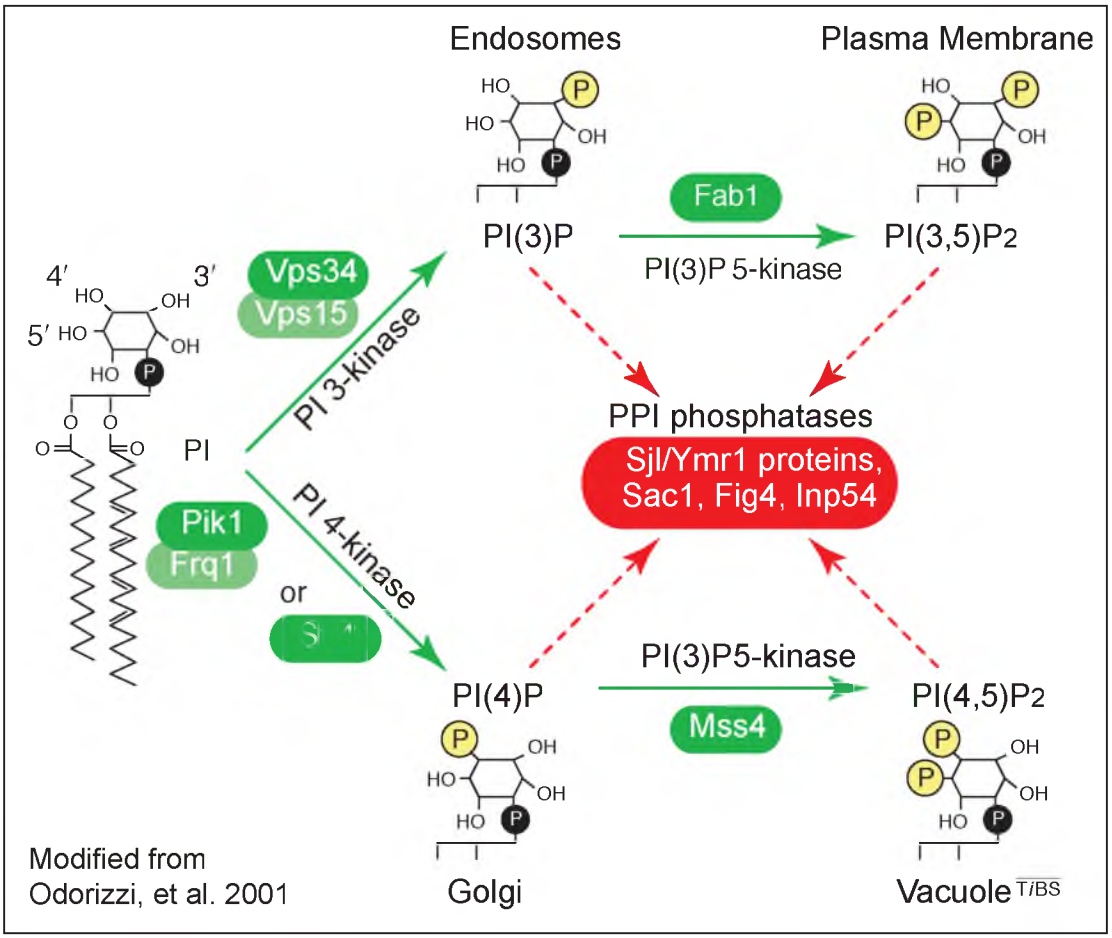

Figure 1.3. PI Kinases and Phosphateses. The different kinases and phosphatases that help regulate membrane identity. The membrane enriched in each lipid is labeled.

recruited to endosomes where it converts PI to PI(3)P which is essential for MVB protein sorting (Stack et al., 1995). Fab1 is required for vacuolar function and converts PI(3)P to PI(3,5)P_2 at the vacuole (Odorizzi et al., 1998; Yamamoto et al., 1995). The phosphoinositide phosphatases, Ymr1 (myotubularin-like 1), Sjl1 (synaptojanin-like 1), Sjl2 and Sjl3 remove 2', 3', 4' and 5' phosphates from phosphoinositides and play a critical role the regulation of organelle identification and function (Parrish et al., 2004; Singer-Kruger et al., 1998). Phosphoinositide kinases and phosphatases modify the lipid composition of membranes as lipids flow in and out to maintain membrane identity (Stenmark, 2009).

The four general vesicle trafficking steps also regulate membrane trafficking through the endocytic pathway and are discussed in more detail in the following sections as they are of particular importance to the work presented in this thesis.

1.5 *Membrane Trafficking in the Endocytic Pathway*

A key function of the endocytic pathway is the removal and trafficking of plasma membrane proteins to the vacuole for degradation. Plasma membrane proteins are degraded for a plethora of reasons, ranging from receptor mediated downregulation, which is necessary to terminate signaling, to degradation of misfolded or damaged proteins (Wollert et al., 2009). Proteins that enter the endocytic pathway from the plasma membrane are recognized by cargo adaptors.

1.5.1 *Cargo Selection and Budding at the Plasma Membrane*

There are a wide variety of cargo adaptors involved in the recognition and endocytosis of cargoes from the plasma membrane. AP-2 is localized to the plasma membrane by binding to $PI(4,5)P_2$ and recognizes two motifs in cargo proteins, the dileucine motif, ExxxLL (Glu, any, any, any, Leu, Leu), or the Yxxϕ (Tyr, any, any where ϕ can be Phe, Ile, Leu, Met or Val) motif (Owen and Evans, 1998; Pitcher et al., 1999). Another cargo adaptor Sla1, recognizes the NPFxD (Asp, Pro, Phe, Any, Asp) sequence in cargoes, facilitating cargo protein endocytosis (Tan et al., 1996). The Epsins, Ent1, Ent2, End3 and Ede1 are localized to the plasma membrane by an ENTH (epsin N-terminal homology) $PI(4,5)P_2$-binding domain and bind ubiquitinated cargoes through a ubiquitin interaction motif (Hofmann and Falquet, 2001; Wendland et al., 1999). The ENTH domain found in Epsins is essential for endocytosis as mutation or deletion of the domain significantly impairs endocytosis (Wendland et al., 1999).

The ubiquitnation of proteins at the plasma membrane is a particularly effective sorting signal and induces the rapid endocytosis of membrane proteins (Oliveira et al., 2010; Piper and Katzmann, 2007). Rsp5, an E3 ligase of the HECT (homologous to E6-AP COOH terminus) family, is required for the covalent attachment of ubiquitin to many plasma membrane proteins (Figure 1.4). HECT domain containing ubiquitin ligases catalyze the formation of a covalent bond between a cytoplasmic Lys residue of the substrate and Gly76 of ubiquitin (Dunn and Hicke, 2001b; Hicke, 2001). E3 ligases require the E1 and E2 enzymes to load the E3 ligase with ubiquitin. The conserved N-terminal domain

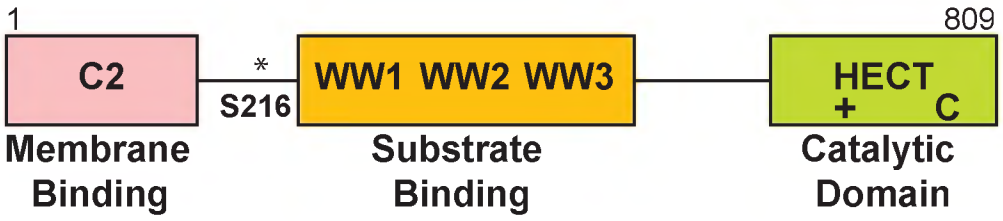

Figure 1.4. Domains of Rsp5. The C2 domain is required for phosphoinsoitide interaction and membrane binding. The three WW domains recognize and bind to protein substrates. The HECT catalyzes formation of the covalent bond between ubiquitin and the substrate. S216 is phosphorylated by Npr1. The (+) is the rsp5-1 mutation site. The (C) is the active cite cystein required for catalysis.

of Rsp5 contains a lysine-rich patch required for membrane localization, which binds to phosphoinositides (Dunn and Hicke, 2001a). The three WW domains of Rsp5, bind to proline-rich PPxY (Pro, Pro, any, Tyr) or PPxK (Pro, Pro, any, Lys) motifs in cargoes, which is important for substrate recognition (Kay et al., 2000).

Cargoes lacking the Rsp5-binding motif require an adaptor protein that binds to the cargo and contains an Rsp5-binding motif. Recently, a collection of roughly 10 ART (arrestin related trafficking) adaptor proteins that recruit Rsp5 to cargo proteins were identified (Mittal and McMahon, 2009). Many Rsp5 adaptors bind to multiple cargoes, increasing the diversity of Rsp5 substrates (Leon et al., 2008; Lin et al., 2008).

1.5.2 *Vesicle Budding from the Plasma Membrane*

Adaptors also recruit clathrin complexes including the AP-2, Sla1 and Epsin proteins to form a clathrin-coated pit, initiating vesicle formation. Epsins were shown by live-cell imaging to be required for the movement of ligand-bound, ubiquitinated Ste2 to sites of clathrin-coated pits (Toshima et al., 2009). Recruitment of clathrin triskelia, a trimer of monomers, results in the polymerization of a dense clathrin coat superstructure on the membrane. Clathrin polymerization induces and stabilizes membrane curvature, promoting vesicle formation. The Epsins and other BAR containing proteins like the cargo adaptor Syp1, which contains an F-BAR (FCHo2) domain (Reider et al., 2009), and Sla1 aid in vesicle formation by stabilizing membrane curvature and drive vesiculation (Ferguson et al., 2009).

Clathrin-independent endocytosis plays a significant role in yeast endocytosis, as mutation of the clathrin heavy chain does not completely inhibit endocytosis (Payne et al., 1988). The mechanisms driving clathrin-independent enocytosis in yeast are not well characterized, however further progress in understanding clathrin-independent endocytosis has been made in mammalian systems. One pathway involves the cholesterol binding protein caveolin, which induces endocytosis by the formation of caveolae (Hayer et al., 2010). Caveolae induced endocytosis occurs from cholesterol rich lipid domains and is directly involved in the endocytosis of GPI-anchored proteins lacking a cytoplasmic domain and some toxins (Howes et al., 2010).

In contrast to the mammalian system, the activity of the actin cytoskeleton plays an important role in yeast endocytosis in both vesicle formation and scission. The cargo adaptor proteins, Sla1 and Syp1, are involved in the regulation of actin dynamics during endocytosis (Howard et al., 2002; Warren et al., 2002). Syp1 temporally represses actin polymerization during cargo selection in the early stage of endocytosis (Boettner et al., 2009). Once clathrin and Syp1 are localized to a clathrin-coated pit, actin filaments attach to the vesicle and to the plasma membrane. Syp1 interacts with the adaptor protein Ede1 and might function to further stabilize coat formation (Stimpson et al., 2009). Dissociation of Syp1 enables the polymerization of actin filaments to force the vesicle towards the cell interior and aid in vesicle formation (Boettner et al., 2009).

Abscission of the clathrin coated vesicles in mammalian cells has been elucidated and requires the recruitment of the GTPase and BAR-domain

containing protein dynamin (Ramachandran, 2011). GTP hydrolysis results in the polymerization of dynamin into spirals that wind around the neck of the vesicle, driving abscission (Pawlowski, 2010). The scission of the vesicle neck in yeast is poorly understood, although it involves the recruitment and assembly of BAR domain-containing proteins (Ferguson et al., 2009). It is hypothesized that these curvature inducing proteins function to constrict the vesicle neck and that together membrane constriction and the force from the actin cytoskeleton are sufficient to induce scission (Boettner et al., 2009; Stimpson et al., 2009). Recent studies suggest that the actin cytoskeleton destabilizes lipids in the plasma membrane during budding to promote scission (Romer et al., 2010).

Following vesicle detachment, the clathrin coat must be removed from the vesicle to expose the membrane, allowing the Rab Vps21 and myosin motor attachment (Horazdovsky et al.). The mechanism of uncoating involves the clathrin binding protein, Swa2, which induces the activity of the ATPase Hsc70, a protein required for uncoating in mammalian cells (Cyr and Douglas, 1994; Cyr et al., 1994; Gall et al., 2000). Swa2 is the yeast ortholog of auxilin, a protein required for uncoating in mammalian cells (Fotin et al., 2004; Rothnie et al., 2011). The yeast mechanism has not been as fully elucidated as the mammalian system, although the identification of Swa2 suggests that the basic mechanism is likely conserved from yeast to mammalian cells and is described below (Rothnie et al., 2011).

The uncoating of clathrin-coated vesicles begins with the recruitment of auxilin to the clathrin coat (Cyr and Douglas, 1994; Cyr et al., 1994). Auxilin, an

Hsp40 J domain family member, binds to the heavy chain of clathrin and recruits Hsc70 to the freshly budded vesicle (Cyr et al., 1994; Fotin et al., 2004; Rapoport et al., 2008). Auxilin stimulates Hsc70 ATP hydrolysis inducing a slight conformational change in clathrin that allows Hsc70 to bindto the C-terminus of the clathrin heavy chain (Rapoport et al., 2008; Ungewickell et al., 1995). This interaction is believed to stabilize a strained clathrin conformation as observed by cryo EM (Xing et al., 2010). The binding of many Hsc70 proteins is likely sufficient to destabilize the clathrin coat leading to the disassembly of the coat (Cyr et al., 1994).

1.5.3 *Intracellular Vesicle Transport*

The trafficking of vesicles from the plasma membrane to endosomes is not well characterized in either the yeast or mammalian system, but likely involves recruitment of a myosin family of motor proteins. The double deletion of myosin type I yeast proteins, Myo3 and Myo5, results in severe defects in growth and actin cytoskeleton organization (Geli and Riezman, 1996). Myo5 is recruited to sites of vesicle budding and possibly aids in the budding process (Geli and Riezman, 1996). Expression of a temperature-sensitive *myo5-1* allele inhibited receptor-mediated endocytosis in cells (Geli and Riezman, 1996) and contained an increased number of immature vesicles at the plasma membrane (Jonsdottir and Li, 2004). These data suggest that the motor protein might be involved in vesicle formation and membrane scission (Jonsdottir and Li, 2004).

1.5.3 *Vesicle Fusion with the Endosome*

Near the endosome, the vesicle interacts with the endosomal tethering complex called CORVET (class c core vacuole/endosome transport) complex. The CORVET complex is recruited to endosomes by binding to PI(3)P and to the Rab Vps21 (Markgraf et al., 2009). The CORVET complex and Vps21 add additional specificity to vesicle delivery as they have to interact to immobilize the vesicle at the endosome. Once tethered, the membranes are close enough to allow the formation of the trans-SNARE complex, initiating fusion. Fusion between the endocytic vesicle membrane and the endosomal membrane requires one of the Q-SNAREs, (Tlg2/Tlg1,Vti1) (Holthuis et al., 1998; von Mollard et al., 1997)and (Pep12/Tgl1, Vti1) complexes and one R-SNARE in the vesicle, Snc1 and Snc2 (Paumet et al., 2004). Formation of a *trans*-SNARE complex between the Q-SNARE and R-SNAREs is sufficient to induce membrane fusion (McNew et al., 2000; Parlati et al., 2002; Paumet et al., 2001; Paumet et al., 2004; Scales et al., 2000). Vps21, PI(3)P and endocytic SNAREs together regulate the fidelity of vesicle trafficking and fusion with the endosome (Stenmark, 2009).

1.5.4 *Cargo Sorting in the Endosome*

Vesicles from the plasma membrane deliver membrane proteins to the endosome upon fusion with the early endosome compartment. From the early endosome, some membrane proteins are rapidly recycled back to the plasma membrane. In yeast, the regulation of cargo recycling from early endosomes is not well understood, however, the cycling of several mammalian receptors

through the early endosome, such as the iron receptor, transferrin (Piper and Katzmann, 2007), epidermal growth factor receptor, and the growth hormone receptor (van Kerkhof et al., 2011) have been characterized. Biosynthetic cargoes are also delivered to the endosome from the Golgi through vesicle mediated transport.

Protein sorting machinery, called retromer (endosome to Golgi retrieval complex), recycles proteins to the ER and the Golgi and is recruited to the endosomal membrane by binding to Vps21 (Balderhaar et al., 2010). Retromer is a pentameric soluble complex composed of SNXs (sorting nexins), proteins that contain PX (phox domain) and BAR domains (Seaman and Williams, 2002). This combination of domains in the retromer complex targets retromer to the endosomal membrane where it facilitates membrane deformation and cargo sorting. Retromer was identified through its role in the cycling of the transmembrane Golgi receptor Vps10 between endosomes and is a highly conserved recycling pathway with homologs in *C. elegans*, mice and humans (Cooper and Stevens, 1996; Marcusson et al., 1994). Vps10 anchors soluble cargoes to the membrane so that they are delivered to the endosome through the biosynthetic pathway and not trafficked through the secretory pathway (Seaman et al., 1997). Vps10 dissociates from its cargo in the endosome and is recycled back to the Golgi by retromer for additional rounds of cargo trafficking (McGough and Cullen, 2011; Seaman et al., 1997). Early endosomes mature into late endosomes as recycling pathways cease. The proteins retained in the late endosome are eventually delivered to the vacuolar limiting membrane or to the

lumen through the MVB pathway (discussed in detail in the following section). The MVB is a late endosomal compartment containing MVB cargoes, which aresorted into ILVs prior to vacuolar fusion. MVB cargoes are degraded in the lumen of the vacuole upon fusion between the MVB and vacuolar limiting membranes.

Fusion of the MVB with the vacuole is preceded by MVB tethering to the HOPS (homotypic vacuolar fusion and protein sorting) complex (Hickey and Wickner, 2010). The HOPS complex binds to PI(3)P at the endosome and to the vacuolar Rab, Ypt7 (Balderhaar et al., 2010). It is currently unknown what regulates the Rab switch between Vps21 and Ypt7 during MVB trafficking. One model predicts that the Rab switch is dependent upon removal of ubiquitin from the surface of the MVB. Cargo sorting results in the recycling of ubiquitin, such that Ypt7 is recruited when MVB sorting is complete and the MVB is ready for vacuolar fusion. As cargo is sorted, ubiquitin is removed from the surface of the MVB initiating the Rab switch. Therefore Ypt7 association is concomitant with maturation and allows fusion with the vacuole only after cargo sorting is complete.

Membrane fusion is promoted by cooperation between the HOPS complex and the *trans*-SNARE complex (Hickey and Wickner, 2010; Piper and Katzmann, 2007; Wickner, 2010). The vacuolar *trans*-SNARE complex requires the three Q-SNAREs (Vam3, Vit1 and Vam7) and one R-SNARE (Ykt6, Snc2 or Nvy1) for formation and MVB-vacuolar fusion. Vam7 does not have an integral lipid anchor and instead localized to the membrane by binding to PI(3)P and HOPS (Fratti and Wickner, 2007). Fusion of the vacuolar and MVB limiting membranes

delivers plasma membrane proteins for degradation and biosynthetic proteins into the lumen.

1.6 *The MVB Pathway*

The MVB pathway delivers cargoes from the endocytic pathway to the vacuole for function or degradation (Piper and Katzmann, 2007) (Figure 1.1). The ESCRTs bind to ubiquitinated cargoes. The ESCRTs are also believed to form a protein network on the cytoplasmic face of the endosome that sorts proteins into vesicles which bud into the lumen of the MVB. The following section describes the current model of the ESCRT sorting mechanisms including cargo recognition, cargo concentration, membrane deformation and vesicle scission.

1.6.1 *Ubiquitin as a Sorting Signal*

Ubiquitination of transmembrane proteins not only serves as an internalization signal at the plasma membrane but is also a signal for sorting of membrane proteins into the MVB pathway (Galan and Haguenauer-Tsapis, 1997). In addition, ubiquitination functions as a retention signal that prevents cargoes from being recycled from the early and late endosomes. Monoubiquitination of cargo proteins has been shown to be sufficient to direct the trafficking of these cargoes into the MVB pathway, although polyubiqutination has been observed for some MVB cargoes. Polyubqiuitination is thought to temporally enhance the efficiency of cargo sorting into ILVs.

Polyubiquitination is not unique to the MVB pathway, however, and is also used by the proteasomal system to mark cytoplasmic proteins for degradation.

Chains of at least four ubiquitins are recognized by the proteasome resulting in the degradation of the protein they are attached to. The difference between polyubiqutination found in the proteasomal and MVB pathway is in the bond formed between the ubiquitin molecules. The proteasomal system recognizes Lys48 linked ubiquitin chains, where ubiquitins are covalently attached to the Lys48 residue of the preceding ubiquitin (Galan and Haguenauer-Tsapis, 1997). The ESCRT complexes specifically recognize monoubiqutinated or Lys63-linked ubiquitins on cargoes (Galan and Haguenauer-Tsapis, 1997). Rsp5 performs both monoubiquitination and Lys63-linked polyubiquitination, although the attachment of only one ubiquitin is required for endocytosis of MVB cargo proteins.

Deubiquitinating enzymes can remove ubiquitin-tags and thus ubiquitin-modification is rather short lived. One deubiquitinating enzyme is Ubp2, which associates with Rsp5 and counteracts the ubiquitination reaction of the E3 ligase (Kee et al., 2005). The balance between these two opposing reactions regulates sorting of cargoes where ubiquitination favors degradation by the MVB pathway, whereas deubiquitination supports protein recycling. Ultimately multiple rounds of ubiquitination and deubiquitination might be necessary to determine the fate of the cargo (Kee et al., 2005).

1.6.2 *The ESCRT Complexes*

There are at least 18 *VPS* (Vacuolar Protein Sorting) genes that encode the proteins required for MVB cargo sorting and ILV formation. A subset of these proteins form the four protein sorting complexes ESCRT-0, -I, -II, -III

(Hanson et al., 2009; Hurley, 2010; Wollert et al., 2009). The ESCRTs are sequentially recruited to the endosomal membrane through intra-ESCRT complex interactions, binding to PI(3)P and ubiquitinated cargoes (Table 1.1, Figure 1.5) (Hanson et al., 2009; Hurley; Raiborg and Stenmark, 2009). A current model for ESCRT sorting is that ESCRT-0 and ESCRT-I sort cargo whereas ESCRT-II and ESCRT-III are thought to concentrate cargoes and facilitate membrane deformation and ILV formation. Finally the ATPase Vps4 seems to function together with ESCRT-III in the scission reaction that releases the ILV from the membrane. Prior to vesicle closure, Vps4 catalyzes the dissociation and recycling the ESCRT machinery to the cytoplasm enabling further rounds of sorting.

1.6.2.1 ESCRT-0. The first complex recruited is ESCRT-0, a heterodimeric complex that contains Vps27 and Hse1 (Bilodeau et al., 2003). At the endosome ESCRT-0 is thought to function bind to ubiquitinated cargo, thereby sequestering these cargo proteins away from the endosomal recycling pathways (Bilodeau et al., 2002; Katzmann et al., 2003). Recruitment of ESCRT-0 to the endosomal membrane is mediated, in part, by binding to PI(3) with its FYVE (Fab1, YGL023, Vps27 and EEA1) domain in Vps27 (Burd and Emr, 1998; Katzmann et al., 2003). The FYVE domain is a 70 amino acid sequence conserved in several PI(3)P binding proteins and has been shown to bind to PI(3)P with high affinity (K_d=50 nM) (Burd and Emr, 1998; Gaullier et al., 1998; Patki et al., 1998). Vps27 also contains three ubiquitin binding domains: a VHS (Vps27, Hrs, STAM) domain and two UIMs (ubiquitin interacting motifs). Hse1 contains two additional ubiquitin

Table 1.1 The Proteins of the ESCRT Complexes. Yeast and human ESCRT protein homologs are listed. In addition, ubiquitin binding domains, lipid interactions, and interactions between proteins are listed.

Complex	Yeast	Human	Ubiquitin Binding Domains	Lipid Interaction Domains	Intercomplex Interactions
ESCRT-0	Vps27 Hsel	Hrs STAM1/2	UIM, VHS UIM, VHS	FYVE	Ub, PI(3)P, Vps23 Ub, Rsp5
ESCRT-I	Vps23 Vps28 Vps37 MVB12	Tsg101 Vps28 Vps38A, B, C hMVB12A, B	 UEV UBD		Ub, Vps27 Vps36
ESCRT-II	Vps22 Vps25 Vps36	EAP30 EAP20 EAP45	GLUE	GLUE	Vps20 Ub, PI(3)P, Vps28
ESCRT-III	Vps20 Snf7 Vps2 Vps24	CHMP6 CHMP4A, B, C CHMP2A, B CHMP3		Myristoyl Group	Vps25, Vps4 Bro1, Vps4 Did2
Vps4	Vps4 Vta1 Vps60	SKD1 LIP5 CHMP5			Vps20, Vta1, Did2, Snf7 Vps4, Vps60, Did2 Vta1
Other	Did2 Ist1 Doa4 Bro1	CHMP1A,B hIst1 AMSH, UBPY Alix			Vps4, Vta1, Vps24 Did2 Bro1, Ub Doa4, Snf7

Figure 1.5. ESCRT Assembly Model. ESCRT-0 is recruited to the membrane by binding to ubiquitinated cargoes and PI(3)P. ESCRT-0 recruits ESCRT-I, which also binds to ubiquitinated cargoes. These two complexes are thought to be the cargo recognition machinery. ESCRT-II also binds to ubiquitn and PI(3)P and interacts with ESCRT-I on the membrane, stimulating ESCRT-III localization and assembly. ESCRT-III is believed to concentrate cargoes on the membrane and also recruits Vps4. ATP hydrolysis by Vps4 recycles the ESCRTs prior to vesicle scission. This model is based on genetic analysis and reflects the epigenetic recruitment of the ESCRTs, as the structure of the ESCRT protein network is not known.

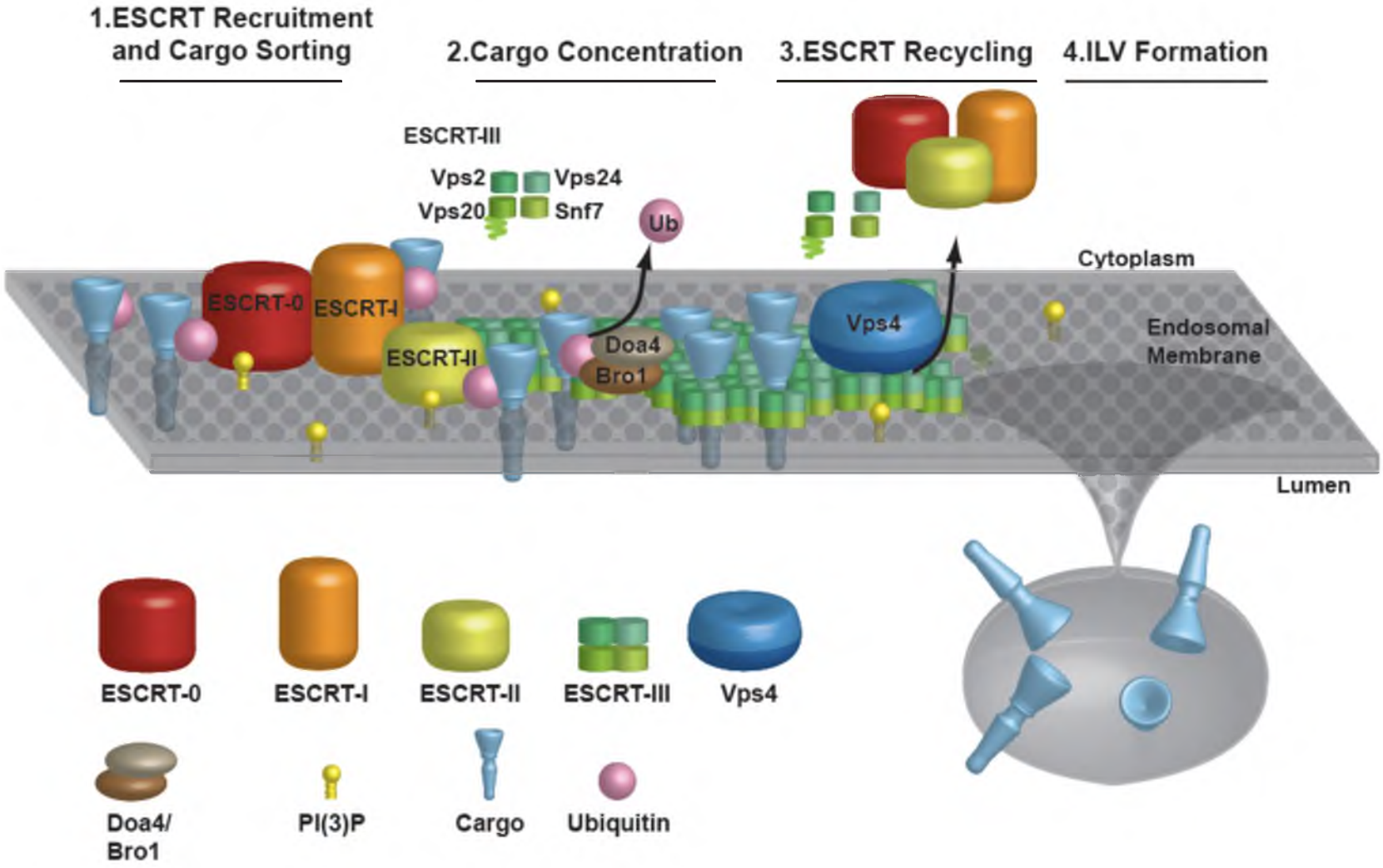
1.ESCRT Recruitment and Cargo Sorting
2.Cargo Concentration
3.ESCRT Recycling
4.ILV Formation
ESCRT-III
Vps2
Vps24
Vps20
Snf7
Ub
Cytoplasm
ESCRT-0
ESCRT-I
ESCRT-II
Doa4
Bro1
Vps4
Endosomal Membrane
Lumen
ESCRT-0
ESCRT-I
ESCRT-II
ESCRT-III
Vps4
Doa4/ Bro1
PI(3)P
Cargo
Ubiquitin

interacting domains: a VHS-type and a UIM (ubiquitin-interacting motif)-type domain. The crystal structure of ESCRT-0 shows that Vps27 and HSE1 are connected through intertwined GAT (GGAs and Tom) domains and form a 9 nm long barbell shape (Prag et al., 2007). Hydrodynamic studies of human ESCRT-0 demonstrate that the complex is flexible, possibly as a means to accommodate a variety of different cargo structures.

Endosome localized ESCRT-0 is predicted to interact with clathrin through a clathrin-box motif in Vps27 (Raiborg et al.). Planar clathrin patches have been observed on mammalian endosomes (Raiborg et al.) where they support protein a network containing ESCRT-0, and other ubiquitin-binding adaptors, including the GGA proteins (Kawasaki et al., 2005). These data further support a role for ESCRT-0 as a sorting receptor, directing ubiquitinated cargoes into the MVB pathway.

1.6.2.2 ESCRT-I. ESCRT-I is comprised of Vps23, Vps28, Vps37 and Mvb12 (Dimaano et al., 2008; Katzmann et al., 2001). Binding of the ESCRT-0 subunit Vps27 to the UEV (Ub E2 variant) domain in Vps23 recruits the ESCRT-I complex to membranes (Bilodeau et al., 2003; Katzmann et al., 2003). The UEV domain also binds to ubiquitinated cargoes on the endosomal membrane (Alam et al., 2004; Katzmann et al., 2001; Pornillos et al., 2002; Teo et al., 2004b). In addition, Mvb12 binds ubiquitin through a recently identified binding domain in the C-terminus of the protein (Shields et al., 2009; Tsunematsu et al., 2010). The potential for two ubiquitin binding sites on ESCRT-I supports a role for cargo sorting and recognition by this complex. The C-terminus of Vps28 is required for

interaction with downstream ESCRT-II on the endosomal membrane (Kostelansky et al., 2006; Teo et al., 2006). The crystal structure analysis of ESCRT-I determined that the heterotetramer is an extended stalk with the UEV domain and the ESCRT-II binding domain on opposite sides of the stalk (Kostelansky et al., 2007). These data indicate that ESCRT-I associates with the membrane such that the length of the complex is parallel to the membrane (Kostelansky et al., 2006). This conformation might afford the protein a long reach to connect distant ESCRT-0 and ESCRT-II complexes together on the membrane.

1.6.2.3 ESCRT-II. ESCRT-I interacts with the flexible GLUE (GRAM-like-ubiquitin binding in EAP45) domain in ESCRT-II (Kostelansky et al., 2006; Teo et al., 2006) (Vps22, two copies of Vps25 and Vps36) (Babst et al., 2002c). ESCRT-II forms a trilobal "Y" shape where the two subunits of Vps25 form the two arms. Tight binding between Vps36 and Vps22 form the center stalk connected by a flexible linker to the GLUE domain (Hierro et al., 2004; Im and Hurley, 2008; Teo et al., 2004b). ESCRT-II can localize to the endosomal membrane independent of the other ESCRTs through the PI(3)P binding domain and the two NZF (Npl1 zinc finger) ubiquitin binding domain, also in the GLUE domain (Alam et al., 2004; Babst et al., 2002a; Slagsvold et al., 2005; Teo et al., 2006). Despite biochemical data indicating that the NZF-1 domain binds ubiquitin (Alam et al., 2004), it not clear whether it is involved in cargo recognition. The current model suggests that interaction of the GLUE domain with ESCRT-I (Gill et al., 2007) results in the activation of ESCRT-II, which initiates the formation of

the downstream ESCRT-III complex (Teo et al., 2004a) (Babst et al., 2002c; Teis et al., 2010). Although ESCRT-II can localize to the membrane independently, it is only capable of initiating the localization of ESCRT-III, the next downstream complex upon overexpression (Babst et al., 2002c). This demonstrates that ESCRT-II functions downstream of ESCRT-I. Vps25 interacts with the Vps20 subunit of ESCRT-III and is essential to initiate ESCRT-III complex formation on the endosomal membrane (Babst et al., 2002a; Teo et al., 2004a).

1.6.2.4 ESCRT-III. The recruitment and assembly of the ESCRT-III protein complex on the membrane is thought to concentrate cargo and induce membrane deformation. The ESCRT-III complex is composed of four charged coiled-coil proteins: Vps20, Snf7, Vps2, Vps24 (Babst et al., 2002a). The crystal structure of the Vps24 mammalian homolog was determined to form a four helix bundle and a 5th helix attached by a flexible linker (Stuchell-Brereton et al., 2007). The first four helices form the core of the protein with the 5th bound to the core. All yeast ESCRT-III proteins are predicted to have a similar conformation. In solution, the 5th helix is bound to the core and the protein is in the "closed" or inactive conformation. Membrane binding of ESCRT-III proteins releases the 5th helix and is said to be in the "open" conformation enabling ESCRT-III complex formation (Stuchell-Brereton et al., 2007). ESCRT-III forms two subcomplexes on endosomal membranes: the Vps20-Snf7 complex and the Vps2-Vps24 (Babst et al., 2002b). Formation of the Vps20-Snf7 subcomplex on the membrane is promoted by a myristoyl group of Vps20 that anchors this subunit to the membrane and by interaction between the ESCRT-III subunit, Vps20, and Vps25,

a subunit of ESCRT-II (Babst et al., 2002b; Teo et al., 2004a; Wollert et al., 2009). Membrane-associated Vps20-Snf7 recruits the second subcomplex, Vps2-Vps24. ESCRT-III is predicted to form a large protein network on the endosomal membrane (Luhtala and Odorizzi, 2004). So far, ESCRT-III is the only ESCRT complex that does not contain a ubiquitin binding domain. Snf7 recruits Bro1, which in turn recruits Doa4 to the membrane. Doa4 is a deubiquitinating enzyme, which functions to remove ubiquitin from cargoes prior to vesicle closure (Hanson et al., 2009; Hurley, 2010; Wollert et al., 2009). The open conformations of membrane-associated ESCRT-III subunits recruit Vps4, a member of the *type-1* family of AAA ATPases (Babst et al., 1998).

1.6.2.5 Vps4 recruitment and assembly. Vps4 functions to remove the ESCRTs from the endosomal membrane, facilitating additional rounds of cargo sorting. Genetic and biochemical studies of this AAA ATPase have determined how the activity of this enzyme is directed to its substrate, ESCRT-III. Vps4 contains a single AAA-domain connected by a flexible linker to the N-terminal MIT (microtubule interacting and transport) substrate recognition domain and oligomerization domain in the C-terminal region (Babst et al., 1998; Scott et al., 2005a; Gonciarz et al., 2008;Vajjhala et al., 2008). Structural studies of purified Vps4 indicate that the active enzyme is a dodecameric double ring structure (Yu et al., 2008; Landsberg et al., 2009). Vps4 is thought to destabilize the ESCRT-III lattice by changing the conformation of the membrane bound ESCRT-III subunits. The energy necessary for this reaction is provided by ATP hydrolysis.

Vps4 assembly and localization is regulated by ESCRT-III and ESCRT-III associated factors. The localization and assembly of Vps4 on ESCRT-III requires interaction between the MIT domain in Vps4 and MIM1 and MIM2 (microtubule interacting motifs one and two) found in the four ESCRT-III proteins (Kieffer et al., 2008). The two types of MIM interactions with Vps4 can occur concomitantly as they bind to discrete regions within the MIT domain. Additional ESCRT-III-associated proteins assist in the assembly and stimulation of Vps4 activity. Did2 and Ist1 function to recruit Vps4 subunits to ESCRT-III (Rue et al., 2008). Vta1 is involved in the assembly of Vps4 and stimulation of ATPase activity. An additional protein, Vps60, is recruited to Vps4 through interaction with Vta1, although the function of this protein is not known (Azmi et al., 2008; Rue et al., 2008; Shim et al., 2008; Ward et al., 2005). The fully assembled Vps4 complex catalyzes ESCRT-III complex disassembly and membrane detachment using the energy released from ATP hydrolysis (Babst et al., 2002a; Babst et al., 1998; Davies et al., 2010). Furthermore, the disassembly of ESCRT-III is thought to drive membrane scission and vesicle release albeit through unknown mechanisms.

The output of ESCRT and Vps4 function is the formation of MVB vesicles containing cargo proteins. Although much is known about the structure of the ESCRT proteins and individual interactions between the ESCRT complexes, the mechanisms that drive ILV formation and membrane scission have not been elucidated. Another pressing question is how Vps4 activity removes ESCRT-III from the membrane. One postulation is that ESCRT-III subunits are pulled

through the central pore of Vps4, similar to protein unfolding performed by other AAA ATPases like the proteasome (Sauer and Baker, 2010). However, this mode of action would require the refolding of recycled ESCRT-III subunits in the cytoplasm, a model that has not been tested yet.

Several *in vitro* studies of the ESCRTs have provided interesting and surprising results. Hanson, et al. reported that the overexpression of Snf7 induced the formation of spirals, filaments and invaginations on the plasma membrane of these cells (Hanson et al., 2008). SEM (scanning electron microscopy) images from these cells clearly show a variety of filaments on the surface of cells overexpressing Snf7. This observation led the hypothesis that two long oligomers of Snf7 concentrate cargoes by encircling them. The two arms of Snf7 are nucleated from the Vps25-Vps20 arms, as there are two subunits of Vsp25 capable of recruiting Vps20 (Kostelansky et al., 2006; Teo et al., 2004a). Although just a model, the ability of Snf7 to self assemble might be an important factor in MVB sorting.

Another remaining question is how the ESCRT-III complex mediates membrane scission. ESCRT-III has been shown to be necessary for the scission of several membrane budding events, although the underlying mechanism driving scission is unknown. Determination of the structural properties of the assembled ESCRT-III complex would provide useful insights into the mechanism employed by this complex to induce membrane scission. Experiments using fluorescently labeled GUVs (giant unilamellar vesicles) were performed by Wollert *et al.* to analyze the scission effects of purified ESCRT proteins on

membranes (Wollert and Hurley, 2010). Strikingly, the addition of purified ESCRT-III proteins alone induced ILV formation in GUVs, although this result has non been demonstrated *in vitro*. ESCRT-I and ESCRT-II were able to form invaginations of the GUV membranes; however, vesicles were not observed (Wollert and Hurley, 2010). From this result, the authors claimed that ESCRT-III alone is required for the scission of vesicles during MVB formation. One alternative explanation for the production of vesicles from GUVs is related to the instability of the GUVs due to their large size, rather than ESCRT induced scission. GUVs often spontaneously form vesicles both to the inside and to the outside of the GUV. The authors did not report whether or how many vesicles were released outside of the GUV upon addition of ESCRT proteins. Further experiments are required to determine the relevancy of this observation to biologically relevant context, as there is no evidence to support that ESCRT-III can mediate scission in the absence of Vps4 *in vivo*.

In the last two decades, a wealth of information regarding the ESCRTs has been amassed. One area of focus has been the structural determination of all the ESCRT complexes either by crystal or solution analysis. These results have been exceptionally useful in identifying important factors in ESCRT complex formation and ESCRT-ESCRT interactions. However, little is understood about the formation of the membrane associated ESCRT network formation or the stoichiometry between complexes in the network. The determination of ESCRT copy numbers required to facilitate the production of one ILV would be significantly improve our understanding of how the ESCRTs sort and package

cargoes into the forming ILV. These remaining questions and others are a focal point of research in the ESCRT field and will continue progress towards understanding cargo sorting and MVB biogenesis. The dynamic properties of the ESCRT network prevent the use of high-resolution structural methods, such as X-Ray crystallography and NMR (nuclear magnetic resonance). Therefore an *in vitro* system designed to study the dynamic assembly of ESCRTs on membranes would provide critical insights into ESCRT network function and structure. Clearly, there are many unknown aspects of ESCRT function and MVB biogenesis that require further investigation to tease apart the inner workings of this complicated sorting pathway.

1.7 *MVB Function In Mammalian Cells*

Up to this point, MVBs and ESCRT function have been reviewed with reference to the yeast system. However, additional MVB and ESCRT functions have been characterized in mammalian cells that, although not conserved in yeast, have provided mechanistic insights into the activity of the ESCRT machinery.

1.7.1 *The ESCRTs as Membrane Scission Machinery*

A growing body of evidence suggests that the critical components of ESCRT-dependent membrane scission are ESCRT-III and Vps4 (Figure 1.6). The ESCRTs have been implicated in the final membrane scission event during cytokinesis in both mammals and certain archaebacteria. The ESCRT-III and Vps4 bacterial orthologs are the only ESCRTs required during cytokinesis in the

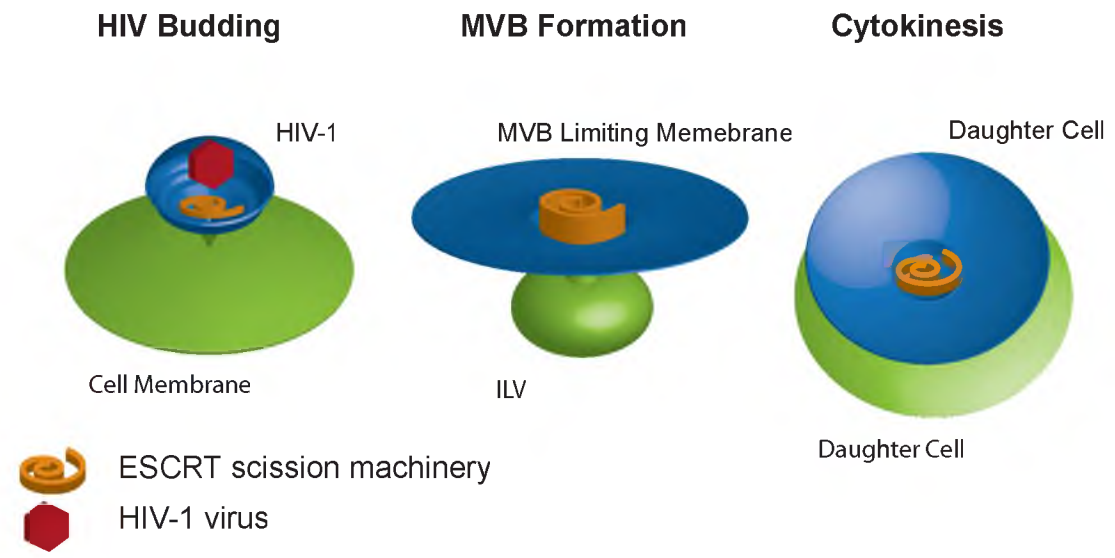

Figure 1.6. Scission Events Mediated by the ESCRTs. ESCRT-I, Alix and Ist1 are all required for HIV-1 budding from infected cells. The ESCRTs are also required for ILV formation at the MVB. Finally, the ESCRTs are also required for cytokinesis to finalize cell division by separating daughter cells.

crenarchaea archaebacteria from the genus *Sulfolobus* (Ettema and Bernander). The significance of this example is the implication that ESCRT-III-Vps4 mediated scission is evolutionarily conserved and that additional complexity found in yeast and mammalian cells likely arose as a means to temporally and spatially regulate vesicle formation and membrane scission events. Further evidence supporting ESCRT-III and Vps4 as scission machinery is demonstrated by the necessity cytokinesis to occur in mammalian cells. Inactivation of Vps4 or CHMP4 by knockdown or by the expression of dominant negative forms inhibits the scission event, arresting cytokinesis. Other factors besides the ESCRTs are required for cytokinesis. At the late stage of cytokinesis, TSG101/Vps23, an ESCRT-I subunit, and Alix/Bro1, an ESCRT-III associated protein that binds to Snf7/CHMP4, are localized to the midbody (Bouamr et al., 2007; VerPlank et al., 2001). The midbody is a narrow tube-like structure formed during cytokinesis, which connects daughter cells and must be severed to complete division. Bro1 recruitment to the midbody is followed by CHMP4 localization to the midbody. Vps4 is subsequently recruited to membrane-associated ESCRT-III, which results in the final scission event (Dukes et al., 2008). In addition, Ist1 is also recruited to the midbody and is essential for cytokinesis (Urata et al., 2007; Wirblich et al., 2006). Before scission can occur, however, a dense column of microtubules that pass through the midbody must be severed. This is achieved by through the action of the AAA ATPase spastin, which is recruited by ESCRT-III (Guizetti et al., 2011).

Additionally viruses have designed methods to recruit the ESCRT scission machinery to sites of budding on the plasma membrane. Although several viral budding systems and their requirements for the ESCRTs have been analyzed, the most well characterized example is HIV-1 (Carlton and Martin-Serrano, 2007; Chen and Lamb, 2008). The viral protein, Gag, recruits ESCRT-I and Alix to the site of budding (Garrus et al., 2001; VerPlank et al., 2001). These factors then recruit ESCRT-III components (CHMP4 and CHMP2) and Vps4, which results in the release of the virus from the cell (Morita et al., 2011; Stuchell-Brereton et al.). The E3 ligase and homolog of Rsp5, NEDD4, ubiqitnates Gag and therefore might increase the sorting efficiency of viral proteins into forming viruses (Chung et al., 2008). ESCRT-mediated viral scission differs from cytokinesis in that Ist1 is not required for viral budding.

In all three scission events, from MVB vesicle formation, to cytokinesis and virus budding, it seems that the essential step for scission is the spatial and temporal recruitment of ESCRT-III and Vps4 to the requisite membrane. It is therefore likely that ESCRT-III and Vps4 represent evolutionary conserved membrane scission machinery. However, the various membrane scission reactions differ in the mechanisms used to recruit ESCRT-III and Vps4 to the site of abscission, providing specificity to scission reactions. All ESCRT-mediated membrane scission events occur with similar topology. That is the ESCRTs assemble on the cytoplasmic side of the membrane induce membrane curvature away from the cytoplasm. This negative curvature is in contrast to other, non ESCRT-mediated membrane invagination like endocytosis. In endocytosis, the

membrane is deformed towards the cytoplasm enabling dynamin and others to bind around the neck of the vesicle forcing scission through membrane constriction mechanisms. A parallel conformation of the ESCRTs at the MVB is impossible as the outside of the vesicle neck is not ESCRT accessible. The mechanism of ESCRT-mediated scission is still largely unknown.

Finally, resolving whether Vps4 is a key component of the scission reaction or whether it is merely involved in ESCRT recycling is of great significance. However, due to the complexity of ESCRT-III and Vps4 interactions on the MVB, unraveling the key functions in scission will require the clever design of new methods and techniques. The impact of understanding the molecular details governing the regulation of ESCRT-dependent membrane scission would transcend from the regulation of MVBs in unicellular organisms to humans, as a growing number of diseases related to MVB function have been identified.

1.7.2 *The MVB Pathway and Disease*

The activity of most plasma membrane transporters, channels and receptors is in part regulated by the degradation of these cell surface proteins via the MVB pathway. The regulation of signaling receptors and ion channels are particularly important in the context of human disease. MVB trafficking defects that result in misregulation of receptors and channels has been demonstrated to induce the formation of several diseases including cancer and hypertension. In addition, the MVB pathway may also play a role in the accumulation of amyloid fibril formation, involved in the pathogenesis of Alzheimer's disease.

1.7.3 *Receptor Downregulation and Signaling Attenuation*

The degradation of plasma membrane proteins by the MVB pathway plays an essential role in the regulation of intracellular signaling events originating from signaling receptors like receptor tyrosine kinases (RTK)s (Avraham and Yarden, 2011; Eden et al., 2009; Felder et al., 1990). RTKs function in a wide variety of signaling events to control cell growth, differentiation and metabolism (Eden et al., 2009). One of the most well studied RTK is the EGFR (epidermal growth factor receptor) involved in regulating cellular growth and proliferation. The MVB pathway regulates the magnitude and duration of EGFR signaling in a process called receptor downregulation (Eden et al., 2009). Downregulation of EGFR refers to the ubiquitin-dependent endocytosis of this receptor and subsequent sorting of EGFR into the MVB pathway. The sequestration of EGFR in ILVs and the following degradation in the lysosome is essential for signal attenuation of the receptor. Continuous EGFR signaling, as observed in ESCRT mutant cells, can result in uncontrolled proliferation and tumorigenesis (Eden et al., 2009). All of the ESCRT complexes, with the exception of ESCRT-III have been implicated in oncogenesis (Wegner et al., 2011). Depletion of Hrs, Tsg101 and Vps25 all result in sustained EGFR signaling likely due to increased recycling of the activated receptor from the endosome. Interestingly, ESCRT-I components Tsg101 and Vps37A were originally identified from a tumor suppressor screen and their genes are mutated in a variety of cancer types (Li and Cohen, 1996).

The MVB pathway also mediates the regulation of ion channels at the cell surface. Misregulaton of ion transport is implicated in genetic diseases including

cystic fibrosis and Liddle's Syndrome, an inheritable form of hypertension (Stutts et al., 1995). Liddle's syndrome is caused by increased levels of the homotrimeric ENaC (epithelial Na+ channel) on the membrane of epithelial renal cells leading to increase Na+ import (Shimkets et al., 1994). ENaC is an important Na+ regulator in epithelial cells and its cell surface expression is regulated in part by the ubiquitin ligase NEDD4-2. NEDD4-2 binds to ENaC through its cytoplasmic PY (Pro, Tyr) motifs and ubiquitinates the channel resulting in downregulation and degradation (Lu et al., 2007). The degradation of ENaC is also dependent upon Hrs binding to ubiquitinated ENaC (Zhou et al., 2010). Mutation of the PY motifs, the cause of Liddel's Sydnrome, disrupts NEDD4-2 binding and ENaC degradation. The increased levels of mutant ENaC on the plasma membrane is likely caused by recycling of the mutant protein from the endosome instead of degradation through the MVB pathway. Although ESCRT complexes were not examined for their role in ENaC downregulation, it seems likely that the MVB is responsible for its degradation.

Ion transport is also import for neuronal function as membrane polarization and depolarization is crucial to synaptic function. Neurons rely heavily the MVB pathway to regulate the expression of ion channels and pumps on the plasma membrane (Winckler and Choo Yap, 2011). Defects in endosomal trafficking have been linked to neurodegenerative disorders such as Alzheimer's disease. Alzheimer's disease is caused by the accruement of β-amyloid plaques in the cytoplasm leading to neuronal cell death. Amyloid precursor protein undergoes a misfolding event inducing the misfolding of other amyloid proteins in a chain

reaction. Identification of aggregated amyloid protein in MVBs and the identification of endosomal abnormalities prior to onset of symptoms suggest the MVB pathway, might play a role in the progression of Alzheimer's disease (Almeida et al., 2006; Keating et al., 2006).

1.7.4 *Specialized MVB-Like Compartments*

In mammalian cells several endosomal compartments have been described that morphologically resemble MVBs but differ in their function from degradative MVBs. Examples of these MVB-like compartments are melanosomes found in melanocytes, MHC class II storage compartments in monocytes and dendritic cells and MVB-like endosomes that form exosomes, small vesicles released from the plasma membrane of many cell types (Piper and Katzmann, 2007).

1.7.4.1 Melanosome biogenesis. Melanosomes are large (~500 nm) MVB-related organelles found in pigment cells required for the coloration of hair, skin and eyes (for review see (Wasmeier et al., 2008)). These unique organelles contain melanosome-specific protein fibrils required for pigmentation (Katzmann, 2006; Wasmeier et al., 2008). Endosomes mature into melanosomes by accumulating specific melanosomal proteins, such as Pmel17 (Theos et al., 2006). Pmel17 is a transmembrane protein trafficked to endosomes though the biosynthetic pathway (Harper et al.). At the endosome, Pmel17 is sorted into ILVs by a mechanism that is independent of both ubiquitin and ESCRT machinery (Theos et al.). Instead of a cytoplasmic sorting signal, Pmel17 sorting is dependent upon a sequence in the lumenal domain (Theos et al., 2006).

Interestingly, Pmel17 is efficiently sorted into ILVs of MVBs when highly overexpressed in nonmelanocyte cell types, indicating that the sorting machinery required for Pmel17 are not cell-specific or limiting (Raposo and Marks, 2007; Theos et al., 2006). One model proposes that Pmel17 sorting is mediated by self-assembly of the protein with specific lipid subdomains, which might induce membrane deformation and scission (Harper et al., 2008).

Once in ILVs, Pmel17 is proteolytically cleaved releasing a soluble protein that aggregates and forms fibrils (Berson et al., 2003). The accumulation of Pmel17 fibrils in the endosome is characteristic of a distinct pre-melanosome compartment. Pigment deposition onto fibrils and delivery of additional melanosomal proteins to this intermediate are required to complete melanosome maturation (Wasmeier et al., 2008).

The insights gained from trafficking studies of melanosome have direct implications to the trafficking and sorting in MVBs. Of particular interest to MVBs is the discovery of the ESCRT-independent sorting of Pmel17 observed in melanosomes, which supports the idea that lipid composition might play an important role in MVB membrane deformation (Theos et al., 2006).

1.7.4.2 MHC class II compartments. The MVB-like compartments also play an important role in the activation of MHC class II produced by monocytes. Nascent heterodimer MHC class II proteins are assembled in the ER in a protective complex with the invariant chain (Bikoff et al., 1993; Viville et al., 1993). The CLIP domain of the invariant chain is bound to the peptide binding groove preventing premature antigenic peptide binding during transport from the ER to

the Golgi (Roche and Cresswell, 1990). The invariant chain also serves as a sorting receptor directing MHC class II trafficking from the Golgi to endosomes, either through direct delivery or through the plasma membrane (Bikoff et al., 1993; Viville et al., 1993). In the endosome, MHC class II are incorporated into ILVs within an MVB-like compartment called an MIIC (MHC class II compartment) in a ubiquitination and ESCRT-dependent mechanism (van Niel et al., 2006). MIICs are morphologically similar to MVBs in that they contain ILVs, sort cargo through a ubiquitin dependent mechanism and are acidified compartments. In this compartment, MHC class II is stored until activated by binding to the proper antigen (Reddy et al., 2008). The activation is aided by endosomal proteases that weaken CLIP binding and thus allow exchange for an antigenic peptide forming the functional MHC class II (Mosyak et al., 1998). When activated, the MHC class II containing ILVs fuse with the limiting membrane of the MIIC and the resulting compartment then fuses with the plasma membrane (Kleijmeer et al., 2001). These membrane fusion reactions result in the presentation of a large number of activated MHC class II complexes at the cell surface and the subsequent activation of the immune response (Bikoff et al., 1993; Viville et al., 1993).

1.7.4.3 Exosome formation and secretion. Exosomes are small (~100 nm) vesicles released from the plasma membrane in many, possibly all, cell types and are found in body fluids such as blood (Turchinovich et al., 2011). Well-described examples of exosome release include studies in mast cells, immune cells and tumor cells (Piper and Katzmann, 2007; Zomer et al., 2010).

Exosomes originate from ILVs that form in MVB-like compartments, which fuse with the plasma membrane. Exosomes have been shown to contain MVB related proteins including Vps36 (ESCRT-II), TSG101 (ESCRT-I), and ALIX (Bro1) (McLellan, 2009). Therefore it has been speculated that exosome formation is ESCRT dependent. However, the data from one study contradicted this conclusion suggesting that an ESCRT-independent mechanism is involved (Trajkovic et al., 2008). The physiological function of exosomes, the mechanisms required for exosome formation and secretion are poorly understood (Zomer et al., 2010).

It has become apparent that many signaling peptides, such as cytokines, produced by immune cells are released from cells in exosomes. Cytokines are required for the intracellular communication between various immune cells, including DC, B and T cells and are important for coordinating the immune response (Temme et al., 2010). IL-12 (interleukin-12) is secreted by the innate immune system following exposure to pathogens or foreign bodies and initiates the activation of T cells and B cells (Tanaka et al., 2011). Activated T cells function in the clearance and destruction of pathogens and serve as a first line of defense against infection, whereas B cells produce antibodies and function to provide immunity upon subsequent exposure to the same pathogen. Although the *in vivo* function of exosomes is unknown, it has been postulated that intercellular communication through exosomes is more efficient than protein secretion, since exosomes deliver multiple protein copies and likely contain a variety of cytokines (Camussi et al., 2010).

The analysis of exosomes secreted from several cell types revealed that they also contain miRNAs (microRNA). miRNAs are small RNAs that bind to mRNAs repressing translation, termed silencing (Gibbings et al., 2009; Zomer et al., 2010). The secretion of miRNA-containing exosomes might enable the cell producing exosomes to post-transcriptionally regulate nearby cells without making direct contact. MicroRNAs associate with RISC (RNA interfering silencing complex) to form miRISC, which binds to mRNA mediating silencing. The localization of RISC and mRNAs to MVBs suggest this organelle might be the site of miRISC formation and function (Gibbings et al., 2009). In addition, the localization miRNAs to the MVB likely facilitates the sorting of miRNAs into exosomes, although the mechanism of exosome formation is largely unknown.

Finally, HIV-1 and Epstein Barr viruses have developed ways to exploit the exosome pathway of their hosts. HIV-1 infected cells evade detection and degradation by hiding in ILVs of MVB-like structures (Alam et al.; Morita and Sundquist; Nguyen et al., 2003; Sherer et al., 2003). Subsequent secretion of HIV-1-positive exosomes spreads the infection to neighboring cells. In fact, HIV-1 was fount to be more virulent when exposed to nascent cells in exosomes than virus alone (Nguyen et al., 2003). The increase in virulence could be due to the number virions that enter the cell (Zomer et al., 2010). Epstein Barr virus initiates the release of exosomes from infected cells that contain LMP1 (latent membrane protein 1) mRNA and protein (Ceccarelli et al., 2007). LMP1 is an oncogene and is a potent activator of NF-Kb (nuclear factor-Kappa B) expression, a transcription factor important to the immune response. LMP1-induced

overexpression of NF-Kb in immune cells promotes proliferation and latency of infected cells, prolonging viral infection (Soni et al., 2007).

The role of the MVB pathway in membrane trafficking and cargo sorting is not limited to degradation, but is involved in an amazing diversity in cellular function including organelle differentiation, protein storage, membrane scission and intracellular communication as discussed in the preceding paragraphs. The presence of lumenal vesicles and the ability to sort cargoes is common to all MVB-like compartments. Insights obtained from the elucidation of the mechanisms involved in cargo sorting and ILV formation in these unique compartments will contribute to our overall understanding of ESCRT function and MVB biogenesis.

Recent studies of the ESCRT-III subunit, Snf7, show that this protein forms corkscrew-like rings at the midbody during cytokinesis, which was followed by the recruitment of Vps4, resulting in abscission (Elia et al., 2011). These data strongly implicate Snf7 in the mechanism of membrane deformation and together with Vps4, is able to induce membrane scission. One mechanism that can be drawn from these results is that Vps4, inducing membrane scission of the midbody and at the MVB, tightens the polymerized rings of ESCRT-III on membranes like a ratchet. This scission event would be akin to the function of the SNARE proteins, where membranes are forced into close proximity by protein machinery, leading to lipid mixing and fusion. In the MVB, lipid mixing between the vesicular membrane and the endosomal membrane would result in closure and release of the vesicle. Continued analysis of membrane deformation and

scission induced by the ESCRTs focused on elucidation the mechanism required for membrane manipulation will provide new insights into MVB biogenesis and all the processes involving the MVB pathway.

The following chapters report our efforts to understand ESCRT assembly on the membrane and to elucidate the regulation of the MVB pathway by starvation-response pathways.

In Chapter 2, we discuss our success in the design and optimization of a novel technique capable of analyzing the protein dynamics involved in the formation of the membrane-associated ESCRT protein network under equilibrium conditions. This *in vitro* system is also capable of determining the binding constants of the individual ESCRT complexes to the membrane, parameters that have previously been undeterminable.

In Chapter 3 we present data that demonstrates a regulatory connection between the MVB pathway and TORC1 (target of rapamycin complex 1), the central regulator of cell metabolism. In Chapter 4, we continued our analysis of the MVB pathway during starvation, which lead to the elucidation of several factors involved in the starvation response. Unexpectedly, these analyses also uncovered a novel starvation pathway activated through a TORC1-independnet mechanism. These results demonstrate an important role for the MVB pathway during the starvation response.

Together, the work presented in the subsequent chapters provide a unique method to analyze ESCRT function and also describe an essential role of the MVB pathway required for survival during starvation.

1.8 *References*

Alam, S.L., J. Sun, M. Payne, B.D. Welch, B.K. Blake, D.R. Davis, H.H. Meyer, S.D. Emr, and W.I. Sundquist. 2004. Ubiquitin interactions of NZF zinc fingers. *Embo J*. 23:1411-1421.

Almeida, C.G., R.H. Takahashi, and G.K. Gouras. 2006. Beta-amyloid accumulation impairs multivesicular body sorting by inhibiting the ubiquitin-proteasome system. *J Neurosci*. 26:4277-4288.

Angers, C.G., and A.J. Merz. 2011. New links between vesicle coats and Rab-mediated vesicle targeting. *Semin Cell Dev Biol*. 22:18-26.

Aschenbrenner, L., T. Lee, and T. Hasson. 2003. Myo6 facilitates the translocation of endocytic vesicles from cell peripheries. *Mol Biol Cell*. 14:2728-2743.

Avraham, R., and Y. Yarden. 2011. Feedback regulation of EGFR signalling: decision making by early and delayed loops. *Nat Rev Mol Cell Biol*. 12:104-117.

Azmi, I.F., B.A. Davies, J. Xiao, M. Babst, Z. Xu, and D.J. Katzmann. 2008. ESCRT-III family members stimulate Vps4 ATPase activity directly or via Vta1. *Dev Cell*. 14:50-61.

Babst, M., D.J. Katzmann, E.J. Estepa-Sabal, T. Meerloo, and S.D. Emr. 2002a. Escrt-III: an endosome-associated heterooligomeric protein complex required for mvb sorting. *Dev Cell*. 3:271-282.

Babst, M., D.J. Katzmann, E.J. Estepa-Sabal, T. Meerloo, and S.D. Emr. 2002b. Escrt-III: an endosome-associated heterooligomeric protein complex required for mvb sorting. *Dev Cell*. 3:271-282.

Babst, M., D.J. Katzmann, W.B. Snyder, B. Wendland, and S.D. Emr. 2002c. Endosome-associated complex, ESCRT-II, recruits transport machinery for protein sorting at the multivesicular body. *Dev Cell*. 3:283-289.

Babst, M., B. Wendland, E.J. Estepa, and S.D. Emr. 1998. The Vps4p AAA ATPase regulates membrane association of a Vps protein complex required for normal endosome function. *Embo J*. 17:2982-2993.

Balderhaar, H.J., H. Arlt, C. Ostrowicz, C. Brocker, F. Sundermann, R. Brandt, M. Babst, and C. Ungermann. 2010. The Rab GTPase Ypt7 is linked to retromer-mediated receptor recycling and fusion at the yeast late endosome. *J Cell Sci*. 123:4085-4094.

Bananis, E., J.W. Murray, R.J. Stockert, P. Satir, and A.W. Wolkoff. 2000. Microtubule and motor-dependent endocytic vesicle sorting in vitro. *J Cell Biol*. 151:179-186.

Berson, J.F., A.C. Theos, D.C. Harper, D. Tenza, G. Raposo, and M.S. Marks. 2003. Proprotein convertase cleavage liberates a fibrillogenic fragment of a resident glycoprotein to initiate melanosome biogenesis. *J Cell Biol*. 161:521-533.

Bikoff, E.K., L.Y. Huang, V. Episkopou, J. van Meerwijk, R.N. Germain, and E.J. Robertson. 1993. Defective major histocompatibility complex class II assembly, transport, peptide acquisition, and CD4+ T cell selection in mice lacking invariant chain expression. *J Exp Med*. 177:1699-1712.

Bilodeau, P.S., J.L. Urbanowski, S.C. Winistorfer, and R.C. Piper. 2002. The Vps27p Hse1p complex binds ubiquitin and mediates endosomal protein sorting. *Nat Cell Biol*. 4:534-539.

Bilodeau, P.S., S.C. Winistorfer, W.R. Kearney, A.D. Robertson, and R.C. Piper. 2003. Vps27-Hse1 and ESCRT-I complexes cooperate to increase efficiency of sorting ubiquitinated proteins at the endosome. *J Cell Biol*. 163:237-243.

Boettner, D.R., J.L. D'Agostino, O.T. Torres, K. Daugherty-Clarke, A. Uygur, A. Reider, B. Wendland, S.K. Lemmon, and B.L. Goode. 2009. The F-BAR protein Syp1 negatively regulates WASp-Arp2/3 complex activity during endocytic patch formation. *Curr Biol*. 19:1979-1987.

Bouamr, F., B.R. Houck-Loomis, M. De Los Santos, R.J. Casaday, M.C. Johnson, and S.P. Goff. 2007. The C-terminal portion of the Hrs protein interacts with Tsg101 and interferes with human immunodeficiency virus type 1 Gag particle production. *J Virol*. 81:2909-2922.

Burd, C.G., and S.D. Emr. 1998. Phosphatidylinositol(3)-phosphate signaling mediated by specific binding to RING FYVE domains. *Mol Cell*. 2:157-162.

Camussi, G., M.C. Deregibus, S. Bruno, V. Cantaluppi, and L. Biancone. 2010. Exosomes/microvesicles as a mechanism of cell-to-cell communication. *Kidney Int*. 78:838-848.

Carlton, J.G., and J. Martin-Serrano. 2007. Parallels between cytokinesis and retroviral budding: a role for the ESCRT machinery. *Science*. 316:1908-1912.

Ceccarelli, S., V. Visco, S. Raffa, N. Wakisaka, J.S. Pagano, and M.R. Torrisi. 2007. Epstein-Barr virus latent membrane protein 1 promotes concentration in multivesicular bodies of fibroblast growth factor 2 and its release through exosomes. *Int J Cancer*. 121:1494-1506.

Chen, B.J., and R.A. Lamb. 2008. Mechanisms for enveloped virus budding: can some viruses do without an ESCRT? *Virology*. 372:221-232.

Chen, X., A. Karnovsky, M.D. Sans, P.C. Andrews, and J.A. Williams. 2010. Molecular characterization of the endoplasmic reticulum: insights from proteomic studies. *Proteomics*. 10:4040-4052.

Chung, H.Y., E. Morita, U. von Schwedler, B. Muller, H.G. Krausslich, and W.I. Sundquist. 2008. NEDD4L overexpression rescues the release and infectivity of human immunodeficiency virus type 1 constructs lacking PTAP and YPXL late domains. *J Virol*. 82:4884-4897.

Conibear, E. 2010. Converging views of endocytosis in yeast and mammals. *Curr Opin Cell Biol*. 22:513-518.

Conner, S.D., and S.L. Schmid. 2003. Regulated portals of entry into the cell. *Nature*. 422:37-44.

Cooper, A.A., and T.H. Stevens. 1996. Vps10p cycles between the late-Golgi and prevacuolar compartments in its function as the sorting receptor for multiple yeast vacuolar hydrolases. *J Cell Biol*. 133:529-541.

Cyr, D.M., and M.G. Douglas. 1994. Differential regulation of Hsp70 subfamilies by the eukaryotic DnaJ homologue YDJ1. *J Biol Chem*. 269:9798-9804.

Cyr, D.M., T. Langer, and M.G. Douglas. 1994. DnaJ-like proteins: molecular chaperones and specific regulators of Hsp70. *Trends Biochem Sci*. 19:176-181.

Dance, A.L., M. Miller, S. Seragaki, P. Aryal, B. White, L. Aschenbrenner, and T. Hasson. 2004. Regulation of myosin-VI targeting to endocytic compartments. *Traffic*. 5:798-813.

Davies, B.A., I.F. Azmi, J. Payne, A. Shestakova, B.F. Horazdovsky, M. Babst, and D.J. Katzmann. 2010. Coordination of substrate binding and ATP hydrolysis in Vps4-mediated ESCRT-III disassembly. *Mol Biol Cell*. 21:3396-3408.

Dimaano, C., C.B. Jones, A. Hanono, M. Curtiss, and M. Babst. 2008. Ist1 regulates Vps4 localization and assembly. *Mol Biol Cell*. 19:465-474.

Dukes, J.D., J.D. Richardson, R. Simmons, and P. Whitley. 2008. A dominant-negative ESCRT-III protein perturbs cytokinesis and trafficking to lysosomes. *Biochem J*. 411:233-239.

Dunn, R., and L. Hicke. 2001a. Domains of the Rsp5 ubiquitin-protein ligase required for receptor-mediated and fluid-phase endocytosis. *Mol Biol Cell*. 12:421-435.

Dunn, R., and L. Hicke. 2001b. Multiple roles for Rsp5p-dependent ubiquitination at the internalization step of endocytosis. *J Biol Chem*. 276:25974-25981.

Eden, E.R., I.J. White, and C.E. Futter. 2009. Down-regulation of epidermal growth factor receptor signalling within multivesicular bodies. *Biochem Soc Trans*. 37:173-177.

Elia, N., R. Sougrat, T.A. Spurlin, J.H. Hurley, and J. Lippincott-Schwartz. 2011. Dynamics of endosomal sorting complex required for transport (ESCRT) machinery during cytokinesis and its role in abscission. *Proc Natl Acad Sci U S A*. 108:4846-4851.

Ettema, T.J., and R. Bernander. 2009. Cell division and the ESCRT complex: A surprise from the archaea. *Commun Integr Biol*. 2:86-88.

Feige, M.J., and L.M. Hendershot. 2011. Disulfide bonds in ER protein folding and homeostasis. *Curr Opin Cell Biol*. 23:167-175.

Felder, S., K. Miller, G. Moehren, A. Ullrich, J. Schlessinger, and C.R. Hopkins. 1990. Kinase activity controls the sorting of the epidermal growth factor receptor within the multivesicular body. *Cell*. 61:623-634.

Ferguson, S.M., A. Raimondi, S. Paradise, H. Shen, K. Mesaki, A. Ferguson, O. Destaing, G. Ko, J. Takasaki, O. Cremona, O.T. E, and P. De Camilli. 2009. Coordinated actions of actin and BAR proteins upstream of dynamin at endocytic clathrin-coated pits. *Dev Cell*. 17:811-822.

Fotin, A., Y. Cheng, N. Grigorieff, T. Walz, S.C. Harrison, and T. Kirchhausen. 2004. Structure of an auxilin-bound clathrin coat and its implications for the mechanism of uncoating. *Nature*. 432:649-653.

Fratti, R.A., and W. Wickner. 2007. Distinct targeting and fusion functions of the PX and SNARE domains of yeast vacuolar Vam7p. *J Biol Chem*. 282:13133-13138.

Galan, J.M., and R. Haguenauer-Tsapis. 1997. Ubiquitin lys63 is involved in ubiquitination of a yeast plasma membrane protein. *Embo J*. 16:5847-5854.

Gall, W.E., M.A. Higginbotham, C. Chen, M.F. Ingram, D.M. Cyr, and T.R. Graham. 2000. The auxilin-like phosphoprotein Swa2p is required for clathrin function in yeast. *Curr Biol*. 10:1349-1358.

Garrus, J.E., U.K. von Schwedler, O.W. Pornillos, S.G. Morham, K.H. Zavitz, H.E. Wang, D.A. Wettstein, K.M. Stray, M. Cote, R.L. Rich, D.G. Myszka, and W.I. Sundquist. 2001. Tsg101 and the vacuolar protein sorting pathway are essential for HIV-1 budding. *Cell*. 107:55-65.

Gaullier, J.M., A. Simonsen, A. D'Arrigo, B. Bremnes, H. Stenmark, and R. Aasland. 1998. FYVE fingers bind PtdIns(3)P. *Nature*. 394:432-433.

Geli, M.I., and H. Riezman. 1996. Role of type I myosins in receptor-mediated endocytosis in yeast. *Science*. 272:533-535.

Gibbings, D.J., C. Ciaudo, M. Erhardt, and O. Voinnet. 2009. Multivesicular bodies associate with components of miRNA effector complexes and modulate miRNA activity. *Nat Cell Biol*. 11:1143-1149.

Gill, D.J., H. Teo, J. Sun, O. Perisic, D.B. Veprintsev, S.D. Emr, and R.L. Williams. 2007. Structural insight into the ESCRT-I/-II link and its role in MVB trafficking. *Embo J*. 26:600-612.

Grosshans, B.L., H. Grotsch, D. Mukhopadhyay, I.M. Fernandez, J. Pfannstiel, F.Z. Idrissi, J. Lechner, H. Riezman, and M.I. Geli. 2006. TEDS site phosphorylation of the yeast myosins I is required for ligand-induced but not for constitutive endocytosis of the G protein-coupled receptor Ste2p. *J Biol Chem*. 281:11104-11114.

Guizetti, J., L. Schermelleh, J. Mantler, S. Maar, I. Poser, H. Leonhardt, T. Muller-Reichert, and D.W. Gerlich. 2011. Cortical constriction during abscission involves helices of ESCRT-III-dependent filaments. *Science*. 331:1616-1620.

Hanson, P.I., R. Roth, Y. Lin, and J.E. Heuser. 2008. Plasma membrane deformation by circular arrays of ESCRT-III protein filaments. *J Cell Biol*. 180:389-402.

Hanson, P.I., S. Shim, and S.A. Merrill. 2009. Cell biology of the ESCRT machinery. *Curr Opin Cell Biol*. 21:568-574.

Harper, D.C., A.C. Theos, K.E. Herman, D. Tenza, G. Raposo, and M.S. Marks. 2008. Premelanosome amyloid-like fibrils are composed of only golgi-processed forms of Pmel17 that have been proteolytically processed in endosomes. *J Biol Chem*. 283:2307-2322.

Hayer, A., M. Stoeber, C. Bissig, and A. Helenius. 2010. Biogenesis of caveolae: stepwise assembly of large caveolin and cavin complexes. *Traffic*. 11:361-382.

Hicke, L. 2001. Protein regulation by monoubiquitin. *Nat Rev Mol Cell Biol*. 2:195-201.

Hickey, C.M., and W. Wickner. 2010. HOPS initiates vacuole docking by tethering membranes before trans-SNARE complex assembly. *Mol Biol Cell*. 21:2297-2305.

Hierro, A., J. Sun, A.S. Rusnak, J. Kim, G. Prag, S.D. Emr, and J.H. Hurley. 2004. Structure of the ESCRT-II endosomal trafficking complex. *Nature*. 431:221-225.

Hirokawa, N., Y. Noda, Y. Tanaka, and S. Niwa. 2009. Kinesin superfamily motor proteins and intracellular transport. *Nat Rev Mol Cell Biol*. 10:682-696.

Hofmann, K., and L. Falquet. 2001. A ubiquitin-interacting motif conserved in components of the proteasomal and lysosomal protein degradation systems. *Trends Biochem Sci*. 26:347-350.

Holthuis, J.C., B.J. Nichols, S. Dhruvakumar, and H.R. Pelham. 1998. Two syntaxin homologues in the TGN/endosomal system of yeast. *Embo J*. 17:113-126.

Horazdovsky, B.F., G.R. Busch, and S.D. Emr. 1994. VPS21 encodes a rab5-like GTP binding protein that is required for the sorting of yeast vacuolar proteins. *Embo J*. 13:1297-1309.

Howard, J.P., J.L. Hutton, J.M. Olson, and G.S. Payne. 2002. Sla1p serves as the targeting signal recognition factor for NPFX(1,2)D-mediated endocytosis. *J Cell Biol*. 157:315-326.

Howes, M.T., S. Mayor, and R.G. Parton. 2010. Molecules, mechanisms, and cellular roles of clathrin-independent endocytosis. *Curr Opin Cell Biol*. 22:519-527.

Hughson, F.M., and K.M. Reinisch. 2010. Structure and mechanism in membrane trafficking. *Curr Opin Cell Biol*. 22:454-460.

Hurley, J.H. 2010. The ESCRT complexes. *Crit Rev Biochem Mol Biol*. 45:463-487.

Im, Y.J., and J.H. Hurley. 2008. Integrated structural model and membrane targeting mechanism of the human ESCRT-II complex. *Dev Cell*. 14:902-913.

Jonsdottir, G.A., and R. Li. 2004. Dynamics of yeast Myosin I: evidence for a possible role in scission of endocytic vesicles. *Curr Biol*. 14:1604-1609.

Katzmann, D.J. 2006. No ESCRT to the melanosome: MVB sorting without ubiquitin. *Dev Cell*. 10:278-280.

Katzmann, D.J., M. Babst, and S.D. Emr. 2001. Ubiquitin-dependent sorting into the multivesicular body pathway requires the function of a conserved endosomal protein sorting complex, ESCRT-I. *Cell*. 106:145-155.

Katzmann, D.J., C.J. Stefan, M. Babst, and S.D. Emr. 2003. Vps27 recruits ESCRT machinery to endosomes during MVB sorting. *J Cell Biol*. 162:413-423.

Kawasaki, M., T. Shiba, Y. Shiba, Y. Yamaguchi, N. Matsugaki, N. Igarashi, M. Suzuki, R. Kato, K. Kato, K. Nakayama, and S. Wakatsuki. 2005. Molecular mechanism of ubiquitin recognition by GGA3 GAT domain. *Genes Cells*. 10:639-654.

Kay, B.K., M.P. Williamson, and M. Sudol. 2000. The importance of being proline: the interaction of proline-rich motifs in signaling proteins with their cognate domains. *Faseb J*. 14:231-241.

Keating, D.J., C. Chen, and M.A. Pritchard. 2006. Alzheimer's disease and endocytic dysfunction: clues from the Down syndrome-related proteins, DSCR1 and ITSN1. *Ageing Res Rev*. 5:388-401.

Kee, Y., N. Lyon, and J.M. Huibregtse. 2005. The Rsp5 ubiquitin ligase is coupled to and antagonized by the Ubp2 deubiquitinating enzyme. *Embo J*. 24:2414-2424.

Kieffer, C., J.J. Skalicky, E. Morita, I. De Domenico, D.M. Ward, J. Kaplan, and W.I. Sundquist. 2008. Two distinct modes of ESCRT-III recognition are required for VPS4 functions in lysosomal protein targeting and HIV-1 budding. *Dev Cell*. 15:62-73.

Kihara, A., T. Noda, N. Ishihara, and Y. Ohsumi. 2001. Two distinct Vps34 phosphatidylinositol 3-kinase complexes function in autophagy and carboxypeptidase Y sorting in Saccharomyces cerevisiae. *J Cell Biol*. 152:519-530.

Kleijmeer, M., G. Ramm, D. Schuurhuis, J. Griffith, M. Rescigno, P. Ricciardi-Castagnoli, A.Y. Rudensky, F. Ossendorp, C.J. Melief, W. Stoorvogel, and H.J. Geuze. 2001. Reorganization of multivesicular bodies regulates MHC class II antigen presentation by dendritic cells. *J Cell Biol*. 155:53-63.

Kostelansky, M.S., C. Schluter, Y.Y. Tam, S. Lee, R. Ghirlando, B. Beach, E. Conibear, and J.H. Hurley. 2007. Molecular architecture and functional model of the complete yeast ESCRT-I heterotetramer. *Cell*. 129:485-498.

Kostelansky, M.S., J. Sun, S. Lee, J. Kim, R. Ghirlando, A. Hierro, S.D. Emr, and J.H. Hurley. 2006. Structural and functional organization of the ESCRT-I trafficking complex. *Cell*. 125:113-126.

Kutateladze, T.G. 2010. Translation of the phosphoinositide code by PI effectors. *Nat Chem Biol*. 6:507-513.

Leon, S., Z. Erpapazoglou, and R. Haguenauer-Tsapis. 2008. Ear1p and Ssh4p are new adaptors of the ubiquitin ligase Rsp5p for cargo ubiquitylation and sorting at multivesicular bodies. *Mol Biol Cell*. 19:2379-2388.

Li, L., and S.N. Cohen. 1996. Tsg101: a novel tumor susceptibility gene isolated by controlled homozygous functional knockout of allelic loci in mammalian cells. *Cell*. 85:319-329.

Lin, C.H., J.A. MacGurn, T. Chu, C.J. Stefan, and S.D. Emr. 2008. Arrestin-related ubiquitin-ligase adaptors regulate endocytosis and protein turnover at the cell surface. *Cell*. 135:714-725.

Lu, C., S. Pribanic, A. Debonneville, C. Jiang, and D. Rotin. 2007. The PY motif of ENaC, mutated in Liddle syndrome, regulates channel internalization, sorting and mobilization from subapical pool. *Traffic*. 8:1246-1264.

Luhtala, N., and G. Odorizzi. 2004. Bro1 coordinates deubiquitination in the multivesicular body pathway by recruiting Doa4 to endosomes. *J Cell Biol*. 166:717-729.

Madsen, K.L., V.K. Bhatia, U. Gether, and D. Stamou. 2010. BAR domains, amphipathic helices and membrane-anchored proteins use the same mechanism to sense membrane curvature. *FEBS Lett*. 584:1848-1855.

Marcusson, E.G., B.F. Horazdovsky, J.L. Cereghino, E. Gharakhanian, and S.D. Emr. 1994. The sorting receptor for yeast vacuolar carboxypeptidase Y is encoded by the VPS10 gene. *Cell*. 77:579-586.

Markgraf, D.F., F. Ahnert, H. Arlt, M. Mari, K. Peplowska, N. Epp, J. Griffith, F. Reggiori, and C. Ungermann. 2009. The CORVET subunit Vps8 cooperates with the Rab5 homolog Vps21 to induce clustering of late endosomal compartments. *Mol Biol Cell*. 20:5276-5289.

Matile, P., and A. Wiemken. 1967. The vacuole as the lysosome of the yeast cell. *Arch Mikrobiol*. 56:148-155.

McGough, I.J., and P.J. Cullen. 2011. Recent advances in retromer biology. *Traffic*.

McLellan, A.D. 2009. Exosome release by primary B cells. *Crit Rev Immunol*. 29:203-217.

McNew, J.A., F. Parlati, R. Fukuda, R.J. Johnston, K. Paz, F. Paumet, T.H. Sollner, and J.E. Rothman. 2000. Compartmental specificity of cellular membrane fusion encoded in SNARE proteins. *Nature*. 407:153-159.

Mittal, R., and H.T. McMahon. 2009. Arrestins as adaptors for ubiquitination in endocytosis and sorting. *EMBO Rep*. 10:41-43.

Morita, E., V. Sandrin, J. McCullough, A. Katsuyama, I. Baci Hamilton, and W.I. Sundquist. 2011. ESCRT-III Protein Requirements for HIV-1 Budding. *Cell Host Microbe*. 9:235-242.

Morita, E., and W.I. Sundquist. 2004. Retrovirus budding. *Annu Rev Cell Dev Biol*. 20:395-425.

Mosyak, L., D.M. Zaller, and D.C. Wiley. 1998. The structure of HLA-DM, the peptide exchange catalyst that loads antigen onto class II MHC molecules during antigen presentation. *Immunity*. 9:377-383.

Nguyen, D.G., A. Booth, S.J. Gould, and J.E. Hildreth. 2003. Evidence that HIV budding in primary macrophages occurs through the exosome release pathway. *J Biol Chem*. 278:52347-52354.

Odorizzi, G., M. Babst, and S.D. Emr. 1998. Fab1p PtdIns(3)P 5-kinase function essential for protein sorting in the multivesicular body. *Cell*. 95:847-858.

Oliveira, S., R.M. Schiffelers, J. van der Veeken, R. van der Meel, R. Vongpromek, P.M. van Bergen En Henegouwen, G. Storm, and R.C. Roovers. 2010. Downregulation of EGFR by a novel multivalent nanobody-liposome platform. *J Control Release*. 145:165-175.

Owen, D.J., and P.R. Evans. 1998. A structural explanation for the recognition of tyrosine-based endocytotic signals. *Science*. 282:1327-1332.

Parlati, F., O. Varlamov, K. Paz, J.A. McNew, D. Hurtado, T.H. Sollner, and J.E. Rothman. 2002. Distinct SNARE complexes mediating membrane fusion in Golgi transport based on combinatorial specificity. *Proc Natl Acad Sci U S A*. 99:5424-5429.

Parrish, W.R., C.J. Stefan, and S.D. Emr. 2004. Essential role for the myotubularin-related phosphatase Ymr1p and the synaptojanin-like phosphatases Sjl2p and Sjl3p in regulation of phosphatidylinositol 3-phosphate in yeast. *Mol Biol Cell*. 15:3567-3579.

Patki, V., D.C. Lawe, S. Corvera, J.V. Virbasius, and A. Chawla. 1998. A functional PtdIns(3)P-binding motif. *Nature*. 394:433-434.

Paumet, F., B. Brugger, F. Parlati, J.A. McNew, T.H. Sollner, and J.E. Rothman. 2001. A t-SNARE of the endocytic pathway must be activated for fusion. *J Cell Biol*. 155:961-968.

Paumet, F., V. Rahimian, and J.E. Rothman. 2004. The specificity of SNARE-dependent fusion is encoded in the SNARE motif. *Proc Natl Acad Sci U S A*. 101:3376-3380.

Pawlowski, N. 2010. Dynamin self-assembly and the vesicle scission mechanism: how dynamin oligomers cleave the membrane neck of clathrin-coated pits during endocytosis. *Bioessays*. 32:1033-1039.

Payne, G.S., D. Baker, E. van Tuinen, and R. Schekman. 1988. Protein transport to the vacuole and receptor-mediated endocytosis by clathrin heavy chain-deficient yeast. *J Cell Biol*. 106:1453-1461.

Piper, R.C., and D.J. Katzmann. 2007. Biogenesis and function of multivesicular bodies. *Annu Rev Cell Dev Biol*. 23:519-547.

Pitcher, C., S. Honing, A. Fingerhut, K. Bowers, and M. Marsh. 1999. Cluster of differentiation antigen 4 (CD4) endocytosis and adaptor complex binding require activation of the CD4 endocytosis signal by serine phosphorylation. *Mol Biol Cell*. 10:677-691.

Pornillos, O., S.L. Alam, R.L. Rich, D.G. Myszka, D.R. Davis, and W.I. Sundquist. 2002. Structure and functional interactions of the Tsg101 UEV domain. *Embo J*. 21:2397-2406.

Prag, G., H. Watson, Y.C. Kim, B.M. Beach, R. Ghirlando, G. Hummer, J.S. Bonifacino, and J.H. Hurley. 2007. The Vps27/Hse1 complex is a GAT domain-based scaffold for ubiquitin-dependent sorting. *Dev Cell*. 12:973-986.

Raiborg, C., and H. Stenmark. 2009. The ESCRT machinery in endosomal sorting of ubiquitylated membrane proteins. *Nature*. 458:445-452.

Raiborg, C., J. Wesche, L. Malerod, and H. Stenmark. 2006. Flat clathrin coats on endosomes mediate degradative protein sorting by scaffolding Hrs in dynamic microdomains. *J Cell Sci*. 119:2414-2424.

Ramachandran, R. 2011. Vesicle scission: dynamin. *Semin Cell Dev Biol*. 22:10-17.

Rapoport, I., W. Boll, A. Yu, T. Bocking, and T. Kirchhausen. 2008. A motif in the clathrin heavy chain required for the Hsc70/auxilin uncoating reaction. *Mol Biol Cell*. 19:405-413.

Raposo, G., and M.S. Marks. 2007. Melanosomes--dark organelles enlighten endosomal membrane transport. *Nat Rev Mol Cell Biol*. 8:786-797.

Reddy, S.K., A.S. Barbas, T.J. Gan, S.E. Hill, A.M. Roche, and B.M. Clary. 2008. Hepatic parenchymal transection with vascular staplers: a comparative analysis with the crush-clamp technique. *Am J Surg*. 196:760-767.

Reider, A., S.L. Barker, S.K. Mishra, Y.J. Im, L. Maldonado-Baez, J.H. Hurley, L.M. Traub, and B. Wendland. 2009. Syp1 is a conserved endocytic

adaptor that contains domains involved in cargo selection and membrane tubulation. *Embo J.* 28:3103-3116.

Reider, A., and B. Wendland. 2011. Endocytic adaptors - social networking at the plasma membrane. *J Cell Sci.* 124:1613-1622.

Roche, P.A., and P. Cresswell. 1990. Invariant chain association with HLA-DR molecules inhibits immunogenic peptide binding. *Nature.* 345:615-618.

Romer, W., L.L. Pontani, B. Sorre, C. Rentero, L. Berland, V. Chambon, C. Lamaze, P. Bassereau, C. Sykes, K. Gaus, and L. Johannes. 2010. Actin dynamics drive membrane reorganization and scission in clathrin-independent endocytosis. *Cell.* 140:540-553.

Rothnie, A., A.R. Clarke, P. Kuzmic, A. Cameron, and C.J. Smith. 2011. A sequential mechanism for clathrin cage disassembly by 70-kDa heat-shock cognate protein (Hsc70) and auxilin. *Proc Natl Acad Sci U S A.* 108:6927-6932.

Rue, S.M., S. Mattei, S. Saksena, and S.D. Emr. 2008. Novel Ist1-Did2 complex functions at a late step in multivesicular body sorting. *Mol Biol Cell.* 19:475-484.

Sauer, R.T., and T.A. Baker. 2010. AAA+ Proteases: ATP-Fueled Machines of Protein Destruction. *Annu Rev Biochem.*

Scales, S.J., Y.A. Chen, B.Y. Yoo, S.M. Patel, Y.C. Doung, and R.H. Scheller. 2000. SNAREs contribute to the specificity of membrane fusion. *Neuron.* 26:457-464.

Seabra, M.C., and E. Coudrier. 2004. Rab GTPases and myosin motors in organelle motility. *Traffic.* 5:393-399.

Seaman, M.N., E.G. Marcusson, J.L. Cereghino, and S.D. Emr. 1997. Endosome to Golgi retrieval of the vacuolar protein sorting receptor, Vps10p, requires the function of the VPS29, VPS30, and VPS35 gene products. *J Cell Biol.* 137:79-92.

Seaman, M.N., and H.P. Williams. 2002. Identification of the functional domains of yeast sorting nexins Vps5p and Vps17p. *Mol Biol Cell.* 13:2826-2840.

Segev, N. 2011. Coordination of intracellular transport steps by GTPases. *Semin Cell Dev Biol.* 22:33-38.

Sherer, N.M., M.J. Lehmann, L.F. Jimenez-Soto, A. Ingmundson, S.M. Horner, G. Cicchetti, P.G. Allen, M. Pypaert, J.M. Cunningham, and W. Mothes. 2003. Visualization of retroviral replication in living cells reveals budding into multivesicular bodies. *Traffic.* 4:785-801.

Shields, S.B., A.J. Oestreich, S. Winistorfer, D. Nguyen, J.A. Payne, D.J. Katzmann, and R. Piper. 2009. ESCRT ubiquitin-binding domains function cooperatively during MVB cargo sorting. *J Cell Biol*. 185:213-224.

Shim, K.W., D.S. Kim, and J.U. Choi. 2008. Simultaneous endoscopic third ventriculostomy and ventriculoperitoneal shunt for infantile hydrocephalus. *Childs Nerv Syst*. 24:443-451.

Shimkets, R.A., D.G. Warnock, C.M. Bositis, C. Nelson-Williams, J.H. Hansson, M. Schambelan, J.R. Gill, Jr., S. Ulick, R.V. Milora, J.W. Findling, and et al. 1994. Liddle's syndrome: heritable human hypertension caused by mutations in the beta subunit of the epithelial sodium channel. *Cell*. 79:407-414.

Singer-Kruger, B., Y. Nemoto, L. Daniell, S. Ferro-Novick, and P. De Camilli. 1998. Synaptojanin family members are implicated in endocytic membrane traffic in yeast. *J Cell Sci*. 111 (Pt 22):3347-3356.

Slagsvold, T., R. Aasland, S. Hirano, K.G. Bache, C. Raiborg, D. Trambaiolo, S. Wakatsuki, and H. Stenmark. 2005. Eap45 in mammalian ESCRT-II binds ubiquitin via a phosphoinositide-interacting GLUE domain. *J Biol Chem*. 280:19600-19606.

Soldati, T., A.D. Shapiro, A.B. Svejstrup, and S.R. Pfeffer. 1994. Membrane targeting of the small GTPase Rab9 is accompanied by nucleotide exchange. *Nature*. 369:76-78.

Soni, V., E. Cahir-McFarland, and E. Kieff. 2007. LMP1 TRAFficking activates growth and survival pathways. *Adv Exp Med Biol*. 597:173-187.

Stack, J.H., D.B. DeWald, K. Takegawa, and S.D. Emr. 1995. Vesicle-mediated protein transport: regulatory interactions between the Vps15 protein kinase and the Vps34 PtdIns 3-kinase essential for protein sorting to the vacuole in yeast. *J Cell Biol*. 129:321-334.

Stenmark, H. 2009. Rab GTPases as coordinators of vesicle traffic. *Nat Rev Mol Cell Biol*. 10:513-525.

Stimpson, H.E., C.P. Toret, A.T. Cheng, B.S. Pauly, and D.G. Drubin. 2009. Early-arriving Syp1p and Ede1p function in endocytic site placement and formation in budding yeast. *Mol Biol Cell*. 20:4640-4651.

Stuchell-Brereton, M.D., J.J. Skalicky, C. Kieffer, M.A. Karren, S. Ghaffarian, and W.I. Sundquist. 2007. ESCRT-III recognition by VPS4 ATPases. *Nature*. 449:740-744.

Stutts, M.J., C.M. Canessa, J.C. Olsen, M. Hamrick, J.A. Cohn, B.C. Rossier, and R.C. Boucher. 1995. CFTR as a cAMP-dependent regulator of sodium channels. *Science*. 269:847-850.

Sudhof, T.C., and J.E. Rothman. 2009. Membrane fusion: grappling with SNARE and SM proteins. *Science*. 323:474-477.

Sutton, R.B., D. Fasshauer, R. Jahn, and A.T. Brunger. 1998. Crystal structure of a SNARE complex involved in synaptic exocytosis at 2.4 A resolution. *Nature*. 395:347-353.

Sweeney, H.L., and A. Houdusse. 2010. Myosin VI rewrites the rules for myosin motors. *Cell*. 141:573-582.

Tan, P.K., J.P. Howard, and G.S. Payne. 1996. The sequence NPFXD defines a new class of endocytosis signal in Saccharomyces cerevisiae. *J Cell Biol*. 135:1789-1800.

Tanaka, S., Y. Motomura, Y. Suzuki, R. Yagi, H. Inoue, S. Miyatake, and M. Kubo. 2011. The enhancer HS2 critically regulates GATA-3-mediated Il4 transcription in T(H)2 cells. *Nat Immunol*. 12:77-85.

Teis, D., S. Saksena, B.L. Judson, and S.D. Emr. 2010. ESCRT-II coordinates the assembly of ESCRT-III filaments for cargo sorting and multivesicular body vesicle formation. *Embo J*. 29:871-883.

Temme, S., A.M. Eis-Hubinger, A.D. McLellan, and N. Koch. 2010. The herpes simplex virus-1 encoded glycoprotein B diverts HLA-DR into the exosome pathway. *J Immunol*. 184:236-243.

Teo, H., D.J. Gill, J. Sun, O. Perisic, D.B. Veprintsev, Y. Vallis, S.D. Emr, and R.L. Williams. 2006. ESCRT-I core and ESCRT-II GLUE domain structures reveal role for GLUE in linking to ESCRT-I and membranes. *Cell*. 125:99-111.

Teo, H., O. Perisic, B. Gonzalez, and R.L. Williams. 2004a. ESCRT-II, an endosome-associated complex required for protein sorting: crystal structure and interactions with ESCRT-III and membranes. *Dev Cell*. 7:559-569.

Teo, H., D.B. Veprintsev, and R.L. Williams. 2004b. Structural insights into endosomal sorting complex required for transport (ESCRT-I) recognition of ubiquitinated proteins. *J Biol Chem*. 279:28689-28696.

Theos, A.C., S.T. Truschel, D. Tenza, I. Hurbain, D.C. Harper, J.F. Berson, P.C. Thomas, G. Raposo, and M.S. Marks. 2006. A lumenal domain-dependent pathway for sorting to intralumenal vesicles of multivesicular endosomes involved in organelle morphogenesis. *Dev Cell*. 10:343-354.

Toshima, J.Y., J. Nakanishi, K. Mizuno, J. Toshima, and D.G. Drubin. 2009. Requirements for recruitment of a G protein-coupled receptor to clathrin-coated pits in budding yeast. *Mol Biol Cell*. 20:5039-5050.

Trahey, M., and J.C. Hay. 2010. Transport vesicle uncoating: it's later than you think. *F1000 Biol Rep*. 2:47.

Trajkovic, K., C. Hsu, S. Chiantia, L. Rajendran, D. Wenzel, F. Wieland, P. Schwille, B. Brugger, and M. Simons. 2008. Ceramide triggers budding of exosome vesicles into multivesicular endosomes. *Science*. 319:1244-1247.

Tsunematsu, T., E. Yamauchi, H. Shibata, M. Maki, T. Ohta, and H. Konishi. 2010. Distinct functions of human MVB12A and MVB12B in the ESCRT-I dependent on their posttranslational modifications. *Biochem Biophys Res Commun*. 399:232-237.

Turchinovich, A., L. Weiz, A. Langheinz, and B. Burwinkel. 2011. Characterization of extracellular circulating microRNA. *Nucleic Acids Res*.

Ungewickell, E., H. Ungewickell, S.E. Holstein, R. Lindner, K. Prasad, W. Barouch, B. Martin, L.E. Greene, and E. Eisenberg. 1995. Role of auxilin in uncoating clathrin-coated vesicles. *Nature*. 378:632-635.

Urata, S., T. Noda, Y. Kawaoka, S. Morikawa, H. Yokosawa, and J. Yasuda. 2007. Interaction of Tsg101 with Marburg virus VP40 depends on the PPPY motif, but not the PT/SAP motif as in the case of Ebola virus, and Tsg101 plays a critical role in the budding of Marburg virus-like particles induced by VP40, NP, and GP. *J Virol*. 81:4895-4899.

van den Bogaart, G., and R. Jahn. 2011. Counting the SNAREs needed for membrane fusion. *J Mol Cell Biol*.

van Kerkhof, P., M. Westgeest, G. Hassink, and G.J. Strous. 2011. SCF(TrCP) acts in endosomal sorting of the GH receptor. *Exp Cell Res*. 317:1071-1082.

van Niel, G., R. Wubbolts, T. Ten Broeke, S.I. Buschow, F.A. Ossendorp, C.J. Melief, G. Raposo, B.W. van Balkom, and W. Stoorvogel. 2006. Dendritic cells regulate exposure of MHC class II at their plasma membrane by oligoubiquitination. *Immunity*. 25:885-894.

VerPlank, L., F. Bouamr, T.J. LaGrassa, B. Agresta, A. Kikonyogo, J. Leis, and C.A. Carter. 2001. Tsg101, a homologue of ubiquitin-conjugating (E2) enzymes, binds the L domain in HIV type 1 Pr55(Gag). *Proc Natl Acad Sci U S A*. 98:7724-7729.

Viville, S., J. Neefjes, V. Lotteau, A. Dierich, M. Lemeur, H. Ploegh, C. Benoist, and D. Mathis. 1993. Mice lacking the MHC class II-associated invariant chain. *Cell*. 72:635-648.

von Mollard, G.F., S.F. Nothwehr, and T.H. Stevens. 1997. The yeast v-SNARE Vti1p mediates two vesicle transport pathways through interactions with the t-SNAREs Sed5p and Pep12p. *J Cell Biol*. 137:1511-1524.

Ward, D.M., M.B. Vaughn, S.L. Shiflett, P.L. White, A.L. Pollock, J. Hill, R. Schnegelberger, W.I. Sundquist, and J. Kaplan. 2005. The role of LIP5 and CHMP5 in multivesicular body formation and HIV-1 budding in mammalian cells. *J Biol Chem*. 280:10548-10555.

Warren, D.T., P.D. Andrews, C.W. Gourlay, and K.R. Ayscough. 2002. Sla1p couples the yeast endocytic machinery to proteins regulating actin dynamics. *J Cell Sci*. 115:1703-1715.

Wasmeier, C., A.N. Hume, G. Bolasco, and M.C. Seabra. 2008. Melanosomes at a glance. *J Cell Sci*. 121:3995-3999.

Wegner, C.S., L.M. Rodahl, and H. Stenmark. 2011. ESCRT Proteins and Cell Signalling. *Traffic*.

Wendland, B., K.E. Steece, and S.D. Emr. 1999. Yeast epsins contain an essential N-terminal ENTH domain, bind clathrin and are required for endocytosis. *Embo J*. 18:4383-4393.

Wickner, W. 2010. Membrane fusion: five lipids, four SNAREs, three chaperones, two nucleotides, and a Rab, all dancing in a ring on yeast vacuoles. *Annu Rev Cell Dev Biol*. 26:115-136.

Winckler, B., and C. Choo Yap. 2011. Endocytosis and Endosomes at the Crossroads of Regulating Trafficking of Axon Outgrowth-Modifying Receptors. *Traffic*.

Wirblich, C., B. Bhattacharya, and P. Roy. 2006. Nonstructural protein 3 of bluetongue virus assists virus release by recruiting ESCRT-I protein Tsg101. *J Virol*. 80:460-473.

Wollert, T., and J.H. Hurley. 2010. Molecular mechanism of multivesicular body biogenesis by ESCRT complexes. *Nature*. 464:864-869.

Wollert, T., D. Yang, X. Ren, H.H. Lee, Y.J. Im, and J.H. Hurley. 2009. The ESCRT machinery at a glance. *J Cell Sci*. 122:2163-2166.

Xing, Y., T. Bocking, M. Wolf, N. Grigorieff, T. Kirchhausen, and S.C. Harrison. 2010. Structure of clathrin coat with bound Hsc70 and auxilin: mechanism of Hsc70-facilitated disassembly. *Embo J*. 29:655-665.

Yamamoto, A., D.B. DeWald, I.V. Boronenkov, R.A. Anderson, S.D. Emr, and D. Koshland. 1995. Novel PI(4)P 5-kinase homologue, Fab1p, essential for normal vacuole function and morphology in yeast. *Mol Biol Cell*. 6:525-539.

Yu, I.M., and F.M. Hughson. 2010. Tethering factors as organizers of intracellular vesicular traffic. *Annu Rev Cell Dev Biol*. 26:137-156.

Zhou, X., Y. Ren, L. Moore, M. Mei, Y. You, P. Xu, B. Wang, G. Wang, Z. Jia, P. Pu, W. Zhang, and C. Kang. 2010. Downregulation of miR-21 inhibits EGFR pathway and suppresses the growth of human glioblastoma cells independent of PTEN status. *Lab Invest*. 90:144-155.

Zomer, A., T. Vendrig, E.S. Hopmans, M. van Eijndhoven, J.M. Middeldorp, and D.M. Pegtel. 2010. Exosomes: Fit to deliver small RNA. *Commun Integr Biol*. 3:447-450.

CHAPTER 2

IN VITRO ANALYSIS OF ESCRT-II USING PLANAR SUPPORTED LIPID BILAYERS

2.1 Abstract

The ESCRT protein complexes assemble on endosomes where they function in the sorting transmembrane proteins into vesicles that bud towards the lumen of the compartment. Much is known about the structure of the ESCRTs and the interactions that occur between these protein complexes. However, little is understood about the membrane-associated ESCRT network. NMR and X-ray crystallography are not suited to analyze large dynamic membrane-associated networks. In addition, fluorescence microscopy lacks the spatial resolution to analyze protein complexes *in vivo*.

We describe here the development of an *in vitro* planar lipid bilayer system to reconstitute the ESCRT machinery and study its function. This *in vitro* system is capable of closely mimicking the *in vivo* conditions while allowing a high degree of control over the composition of the membrane and the protein machinery. Protein binding to the bilayer can be analyzed by fluorescence microscopy and the surface-specific spectroscopic techniques of ultraviolet-visible sum-frequency generation (UV-Vis SFG) for the label-free detection of ESCRT assembly in collaboration with the Conboy group (Department of Chemistry, University of Utah). This novel approach has the potential to determine the binding constants of the ESCRT protein complexes to membranes, which would provide critical insights into the dynamics within the formation of the ESCRT network, an aspect of the ESCRT system which, is currently uncharacterized.

2.2 *Background*

2.1.1 *The ESCRT Machinery*

Sorting of cargoes into ILVs and vesicle formation within the MVB are dependent upon the serial recruitment of the soluble ESCRT protein complexes, ESCRT-0, -I, -II, -III and Vps4, an AAA-ATPase, to the endosomal membrane (Wollert et al., 2009) (Figure 1.4). The three-dimensional structure of ESCRT-0, ESCRT-I and ESCRT-II has revealed detailed information about inter-ESCRT interactions and interactions with ubiquitinated cargoes and PI(3)P on MVBs (Alam et al., 2004; Gill et al., 2007; Hierro et al., 2004; Im et al., 2009; Kostelansky et al., 2007; Misra and Hurley, 1999; Prag et al., 2007; Teo et al., 2006; Teo et al., 2004a; Teo et al., 2004b). A brief overview of the ESCRTs, with particular focus on ESCRT-II is necessary to understand the results of this chapter. ESCRT-0 recruits ESCRT-I by binding to the UEV domain in Vps23 (Teo et al., 2004b). ESCRT-II localizes to endosomal membranes independent of the other ESCRT complexes (Babst et al., 2002b). At the membrane, the GLUE domain of ESCRT-II and makes contacts with ubiquitin (Alam et al., 2004; Slagsvold et al., 2005), PI(3)P (Hirano et al., 2006), ESCRT-I (Gill et al., 2007) and ESCRT-III (Teo et al., 2004a). Both the GLUE domain and the UEV domain are attached to the rest of the protein complex by flexible linkers, which are likely important to optimize binding interactions with PI3P (Hirano et al., 2006) and ubiquitin (Teo et al., 2004b) during the formation of the ESCRT network. The C-terminal domain of the ESCRT-II subunit Vps25 recruits the ESCRT-III subunit Vps20 to the membrane, initiating the assembly of the ESCRT-III complex (Teo

et al., 2004a). Finally, ESCRT-III recruits the Vps4 complex, which uses the energy from ATP hydrolysis to disassemble the bound ESCRT-III complex (Babst et al., 1998). It has been speculated that the disassembly of ESCRT-III (Babst et al., 2002a), might be responsible for cargo concentration and membrane deformation. However, the mechanism driving vesicle formation is not well understood. Part of the ESCRT machinery is also recruited to other sites of membrane fission within mammalian cells, including sites of viral budding from the plasma membrane and to the midbody of cells undergoing cytokinesis (Carlton and Martin-Serrano, 2007; Elia et al., 2011). This observation suggests the ESCRTs are a fundamental component of the machinery required for scission of membrane necks and tubes (Figure 1.5).

However, the composition of the membrane-associated ESCRT network and the dynamics of the formation and dissociation of the network are not understood, despite structural characterization of individual ESCRT complexes. Study of the ESCRT network has been thwarted by the lack of techniques capable of analyzing a large dynamic network on the surface of bilayers. One of the most basic parameters necessary to understand the dynamics of the ESCRT system is the affinity of these protein complexes with the membrane and how this affinity is affected by the lipid composition and the presence of cargo. *In vitro* techniques used to determine the binding constants of membrane binding proteins like the ESCRTs, have historically employed liposome-based analysis (Burd et al., 1998; Im and Hurley, 2008; Kostelansky et al., 2007). There are several caveats to this technique, some of which occlude the results from these

studies. Protein entrapment is the largest source of error and can dramatically diminish the sensitivity and accuracy of the experiment. Furthermore, liposome analyses can not detect binding constants in equilibrium because wash steps are necessary to remove unbound protein from the liposome solution prior to analysis. Perturbations to the equilibrium caused by the wash steps are likely to disrupt weak membrane binding events, making the results a poor representation of protein dynamics *in vivo*. In collaboration with the Conboy group (Department of Chemistry, University of Utah) we sought to develop an *in vitro* method using PSLBs (planar supported lipid bilayers) to detect membrane association and dissociation of many proteins simultaneously under equilibrium conditions.

2.1.2 *Planar Supported Lipid Bilayers and Sum-Frequency Generation*

PSLBs are highly dynamic lipid bilayers produced on the surface of glass and can be created from a specific lipid mixture. A layer of one-to-two water molecules thick separates the membrane from the glass, ensuring normal lipid fluidity in the membrane. Lipid dynamics and bilayer formation of PSLBs can be easily analyzed by fluorescence microscopy, specifically FRAP (fluorescence recovery after photobleaching). PSLBs have also been used in conjunction with a surface-specific spectroscopy technique called UV-Vis SFG (ultraviolet-visible sum-frequency generation), to detect protein association to lipid membranes without the use of fluorescent labels (Nguyen et al., 2009). All proteins contain highly polarizable π systems, in the form of the amino acids tryptophan, tryrosine and phenylalanine, in addition to the amide bonds comprising the polypeptide

backbone, that strongly resonate in the UV. These intrinsic components can be used as spectroscopic probes in UV-Vis SFG to measure the surface association of a protein to a lipid bilayer (Zhao, 1993). SFG is a coherent second order nonlinear spectroscopic method that involves simultaneously focusing two laser beams, one in the visible spectrum and one in the UV, overlapping on the surface of the PSLB. The laser beams mix at the surface to produce a resultant beam equal to the sum of the two incident frequencies (Nguyen et al., 2009). An increase in UV-Vis-SFG signal is produced when the sum frequency resonates with the transition state of proteins stabilized at the surface of the sample. By scanning the UV laser through the UV spectrum, different transition states of the protein are detected resulting in an protein-specific SFG plot (Shen, 1984). One advantage of this surface-specific technique is the ability to conduct experiments in protein equilibrium, as proteins in solution are not detected and therefore the sample does not require a wash step. Additionally, in some cases proteins have unique UV spectra discernible from other proteins present in the sample, enabling the detection of several proteins simultaneously. Finally, proteins are detected directly, without the requiring the addition of a fluorescent tag through recombinant techniques or chemical modification. SGF is a coherent scattering technique, thus no direct electronic excitation is produced, as is the case with fluorescence, reducing or eliminating adverse photochemical reactions. UV-Vis-SFG has been used previously to study protein interaction with bilayers, however, to our knowledge these techniques have never been used for the analysis of large membrane-associated protein systems.

In collaboration with the Conboy group, we sought to develop an *in vitro* technique exploiting the advantages of PSLBs to study the dynamic properties of the assembly of the 2.1.3 ESCRT network on bilayers by UV-Vis-SFG. Two methods were used to form PSLBs: the Langmuir-Blodgette (LB) method (Montal and Mueller, 1972) and liposome fusion. The LB method controls the lipid packing and produces high quality bilayers that are uniform across the substrate (see Materials and Methods)(Liu and Conboy, 2005a). Furthermore, the LB method can produce bilayer leaflets composed of separate lipid mixtures, whereas bilayers produced by liposome fusion are symmetric (Montal and Mueller, 1972). The largest drawback to the LB method is the time-consuming procedure. In contrast, the liposome fusion technique is fast (30 minutes) and does not require expensive, specialized equipment. However, one disadvantage to this technique is the decrease of bilayer coverage across the glass, as lipid packing is not controlled. Because of simplicity for most of our microscopy-based studies we used liposome-fusion, whereas more sensitive SFG experiments were performed on bilayers created by the LB method.

2.2 *Results and Discussion*

2.2.1 *Chamber Construction*

To expedite and simplify preliminary optimization experiments, two PSLB analysis chambers were created. Both chambers were constructed from Teflon, glass and Viton gaskets, all resistant to stringent acid bath cleansing protocol necessary for PSLB stability (see materials and methods). The first chamber contained 10 wells and ensured easy and reproducible experimental conditions

and was named the Binding Chamber. Lipid bilayers were formed on the glass surface of the binding chambers by the liposome-fusion method (Figure 2.1A) (see Appendix A for more detail). For fluorescence microscopy analysis of the *in vitro* system we constructed the second chamber, a temperature-controlled Flow Cell that is mounted onto the stage of an inverted microscope (DeltaVision deconvoluting microscope) (Figure 2.1B). The Flow Cell was designed to analyze lipid dynamics by FRAP, thus allowing us to analyze the effect of lipid composition and protein binding on the lateral lipid diffusion rate. Bilayers are created on a glass coverslip, which also seals the bottom of the Flow Cell. The Flow Cell contains ports enabling protein addition without disturbing the assembly (see Appendix B for more detail). Most importantly, the Flow Cell was designed to analyze the dynamics of bilayers under conditions where membrane binding proteins are in equilibrium.

2.2.2 *Analysis of Membranes with Lipid Composition Similar to that of Endosomes*

The lipid composition of membranes plays an important role in the association of the ESCRTs to membranes, as ESCRT-0 and ESCRT-II bind directly to a lipid enriched in the endosomal membrane, PI(3)P. We used a lipid mixture designed to mimic endosomal membranes. This mixture contained phophatidylcholine (PC), phosphatidylethanolamine (PE), phophatidylinositol (PI) and cholesterol in a molar ratio of 56:23:11:10 and was based on the lipid analysis of purified endosomal membranes (12). PI(3)P or P(I)4P were added to 1%, a physiologically relevant concentration (Kobayashi et al., 2002). The length

Figure 2.1 Binding Chamber and Flow Cell Design. (A) The 10 well of the Binding Chamber allow for multiple experiments to be conducted simultaneously. Bilayers are created on the glass slide, which seals the bottom of the chamber when assembled. The vacuum system eliminates error and ensures enough liquid is maintained to stabilize the bilayer. (B) The flow cell is compatible with an inverted microscope for FRAP analysis of protein binding to bilayer. The temperature control chamber allows for water heated or cooled to the desired temperature to flow through the chamber adjacent to the bilayer. The lipid chamber also has access for protein or buffer injection in to the bilayer chamber.

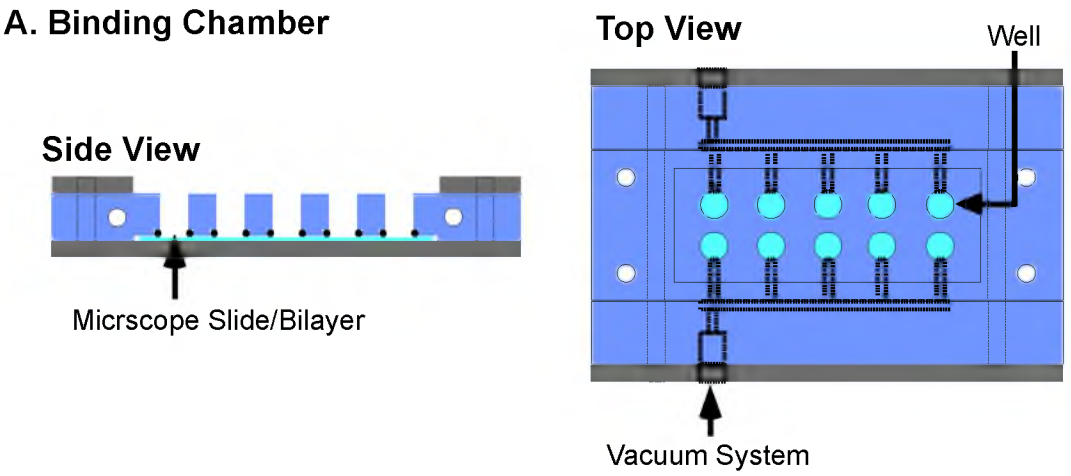
A. Binding Chamber
Top View
Well
Side View
Micrscope Slide/Bilayer
Vacuum System

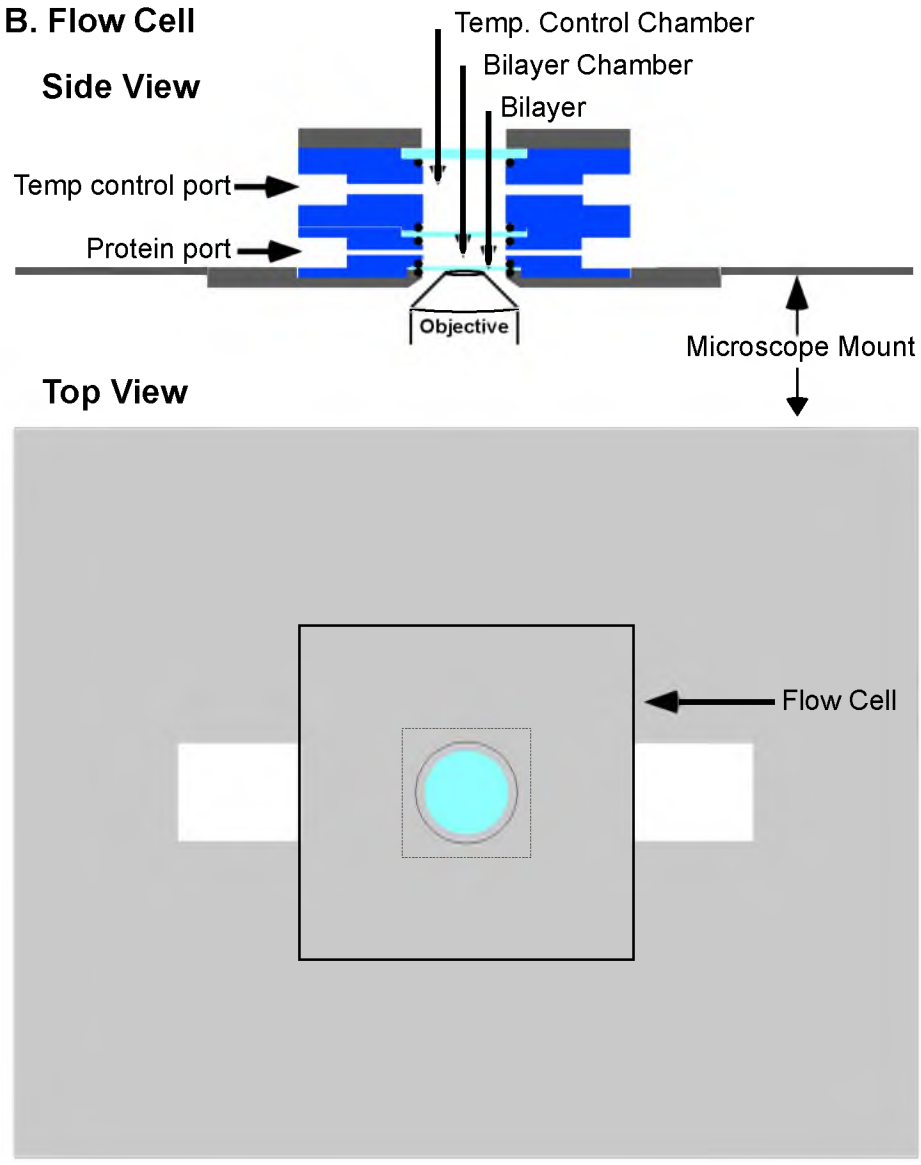
B. Flow Cell
Temp. Control Chamber
Bilayer Chamber
Bilayer
Side View
Temp control port
Protein port
Objective
Microscope Mount
Top View
Flow Cell

Table 2.1. Protein Expression Plasmids

Plasmids	Descriptive Name	Genotype or Description	Reference or Source
E. coli			
XL1-Blue		recA1 endA1 gyrA96 thi-1 hsdR17 supE44 relA1 lac [F' proAB lacIqZDM15 Tn10(tetr)]	Stratagene (La Jolla, CA)
pEO23	GST-GFP-$FYVE_{EEA1}$	Ap^rKan^r (pGEX-KG(Kan))	This Study
pEO42	ESCRT-II	*URA3* Kan^r (pET28a+) *VPS22,Vps25,Vps36*	This Study

crenarchaea archaebacteria from the genus *Sulfolobus* (Ettema and Bernander). The significance of this example is the implication that ESCRT-III-Vps4 mediated scission is evolutionarily conserved and that additional complexity found in yeast and mammalian cells likely arose as a means to temporally and spatially regulate of the fatty acids tails ranged from 16-18 and the saturated to unsaturated fatty acid ratio was ~0.8. The PSLBs formed from this lipid mixture by liposome fusion were visualized by the addition of 0.5-1% Rhodamine-labeled PE (Rhodamine-PE). Fluorescence microscopy (Figure 2.2 A) and FRAP analysis (Figure 2.2 B) of these PSLBs in the Flow Chamber at 30˚C indicated a fluid, homogeneous bilayer that is suitable for further *in vitro* experiments. Membranes lacking cholesterol contained regions where Rhodamine-PE was excluded creating a poke-a-dot pattern by fluorescence microscopy. These analyses further demonstrate the necessity of cholesterol in the membrane to maintain fluidity and lipid homogeneity at 25-30 ˚C and were therefore included in all bilayers.

2.2.3 *Analysis of PI(3)P PSLBs*

PI(3)P is required for the localization of ESCRTs to the endosomal membrane and therefore must be incorporated into PSLBs (Wollert et al., 2009). To test if incorporation of PI(3)P into the PSLBs was successful, we employed the Binding Chamber to determine whether the FYVE domain of EEA1 purified from *E. coli* bound to PSLBs created from a liposome emulsion containing PI(3)P (Figure 2.3). We used the FYVE domain, a 70 amino acid sequence conserved domain present in many PI3P interacting proteins (Burd and Emr, 1998; Stenmark et al., 1996), from EEA1 due to its high affinity and specificity for

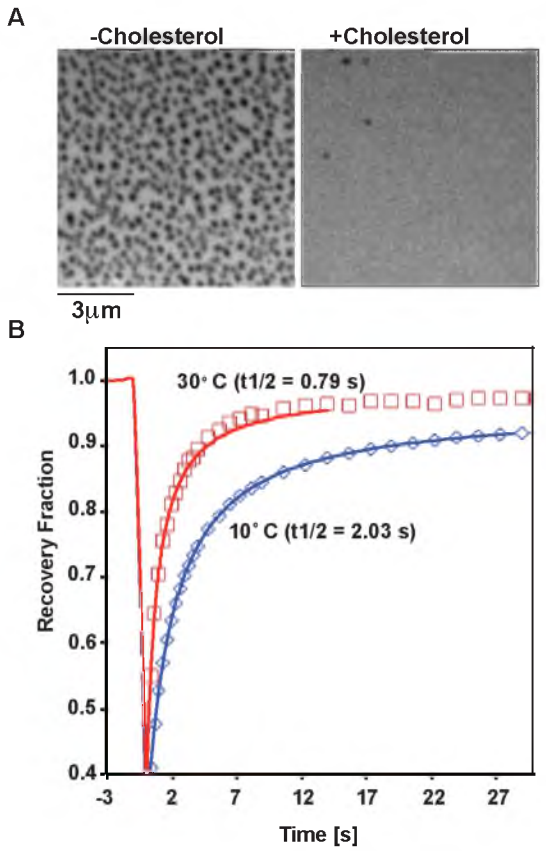

Figure 2.2. Cholesterol is Required to Maintain Fluid Bilayers Created with an Endosomal-like Lipid Composition. (A) FRAP analysis of PSLBs made by liposome fusion in the Flow Cell. PLSBs contained a mixture of PC, PE, PI with or without cholesterol. The addition of cholesterol was essential to promote membrane homogeneity and fluidity. (B) PSLBs were made with the control mix (PI:PE:PC:cholesterol = 11:23:56:10) containing cholesterol and 1% Rhodamine-PE, were analyzed by FRAP. We demonstrate here that the lipids used and the liposome fusion method produce fluid PSBLs as they recover readily from bleaching. In addition, the temperature dependency of diffusion indicates that these membranes are dynamic and responsive to environmental conditions. Solid lines are the predicted recovery of fluorescence by the 2D diffusion model.

PI(3)P (K_d=50 nM) (Gaullier et al., 1998). GST-GFP-$FYVE_{EEA1}$ was expressed in *E. coli* cells and purified by GST (glutathione S transferase) affinity chromatography on GSH resin (see Materials and Methods for more details). Figure 2.3 A shows the result of a membrane-binding assay conducted on bilayers formed by liposome fusion containing or lacking 1% PI(3)P. Purified GST-GFP-$FYVE_{EEA1}$ was added to the binding chamber at a concentration of 0.5 μM in a buffer solution (see materials and methods). The SDS-PAGE analysis of the membrane-bound proteins revealed that the presence of PI(3)P significantly increased the membrane association of GST-GFP-$FYVE_{EEA1}$, indicated by the stronger SDS-PAGE signal for the PI(3)P lane. This result demonstrated the successful incorporation of PI(3)P into the bilayer. We also used UV-Vis-SFG to analyze the binding of purified GST-GFP-$FYVE_{EEA1}$ to bilayers (PI:PE:PC:cholesterol = 11:23:56:10) containing either no additional lipid or 1% PI(3)P (Figure 2.3 B). We observed a binding constant for GST-GFP-$FYVE_{EEA1}$ to PI(3)P containing membranes of K_d=5.5 nM, which is 10-fold lower than previously published results determined by liposome analysis (K_d=50 nM) (Gaullier et al., 1998). The binding constant determined for GFP-GFP- $FYVE_{EEA1}$ binding to control lipids was on the order of 10-fold lower (K_d=13.8 nM) than PI(3)P-containing bilayers. The binding curve obtained by UV-Vis-SFG indicates that the bilayer containing PI(3)P is almost saturated at the lowest concentration whereas the control membrane illustrated increased binding capacity after the addition of more protein. This could be the source of discrepancy between our results and previously published results (Gaullier et al., 1998). However, this

Figure 2.3. Analysis of PI(3)P Incorporation into PSLBs. (A) Binding assay of purified GST-GFP-$FYVE_{EEA1}$ on PSLBs formed with or without PI(3)P by liposome fusion in the Binding Chamber. Control membranes contained PI:PE:PC:cholesterol = 11:23:56:10) . PI(3)P was added to make PI(3)P bilayers. 0.5mM of purified protein was added to each well. Samples were analyzed by SDS-PAGE followed by silver staining to visualize bound protein. (B) SFG analysis of GST-GFP-$FYVE_{EEA1}$ binding to PSLBs made by the LB method. (C). Fluoresce microcopy of BoDipy-PI(3)P in PSLBs made with PI:PE:PC:cholesterol = 11:23:56:10 and 1% Rhodamine-PE. PI(3)P was added to 1%. Bilayers were created by liposome fusion.

A

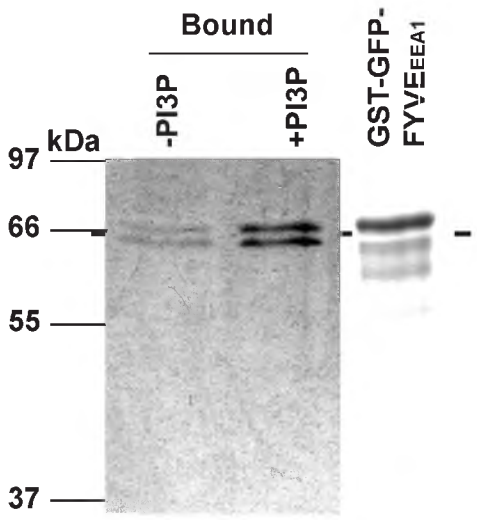
Bound
-PI3P
+PI3P
GST-GFP-FYVE$_{EEA1}$
kDa
97
66
55
37

B

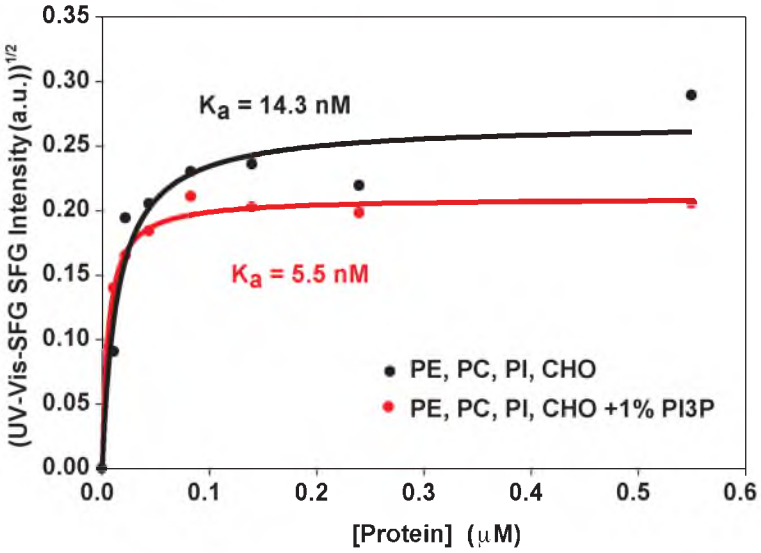
(UV-Vis-SFG SFG Intensity (a.u.))$^{1/2}$
0.35
0.30
0.25
0.20
0.15
0.10
0.05
0.00
K_a = 14.3 nM
K_a = 5.5 nM
PE, PC, PI, CHO
PE, PC, PI, CHO +1% PI3P
0.0
0.1
0.2
0.3
0.4
0.5
0.6
[Protein] (μM)

C

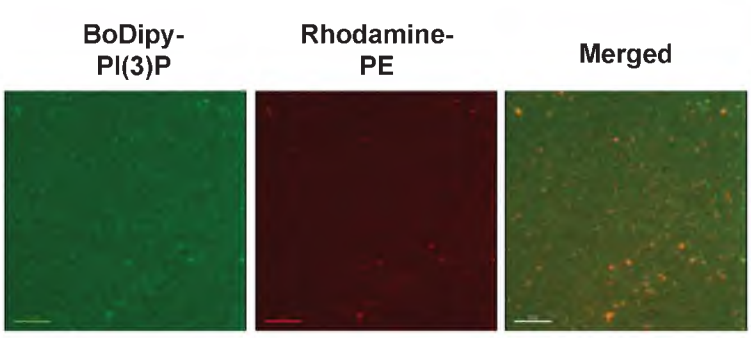
BoDipy-PI(3)P
Rhodamine-PE
Merged

result strongly indicates the incorporation of PI(3)P into the bilayer. We next analyzed a PSLB containing BoDipy-PI(3)P (1%), a fluorescently-tagged PI(3)P and Rhodamine-PE (0.5%) by fluorescence microscopy (Figure 2.3 C) and FRAP analysis (not shown).

The results of this analysis indicated the presence of membrane regions with high concentration of PI(3)P that did not exchange lipids with the surrounding membrane. The rate of diffusion of Rhadamine-PE in these bilayers was also negligible (not shown). Despite several solvent modifications of the lipid mixture, we were unsuccessful in creating a fluid bilayer with BoDipy-PI(3)P. These results suggested that the BoDipy modification of PI(3)P prevented bilayer formation possibly by inhibiting proper mixing with the other lipids.

We demonstrate here that PSLBs produced by liposomes fusion from an endosomal-like PI(3)P-containing lipid emulsion formed homogeneous and dynamic bilayers. We further demonstrated PI(3)P incorporation by the preferential binding of GST-GFP-FYVE$_{EEA1}$ to bilayers created with PI(3)P over the control through binding and SFG analyses. Together, these data strongly suggest that PI(3)P is incorporated into PSLBs produced by liposome fusion. These results validate the use of PSLBs as an alternative to liposome-based *in vitro* analyses to study endosomal membrane specific protein-membrane interactions by UV-Vis-SFG.

2.2.4 *Analysis of Membrane-Associated ESCRT-II*

The GLUE domain of ESCRT-II has been shown to bind to PI(3)P and studies have indicated that ESCRT-II can localize to the endosomal membrane

independently of other ESCRTs (Babst et al., 2002b) making this protein complex an ideal candidate for PI(3)P-binding studies. Figure 2.4 shows the result of an ESCRT-II binding experiment using bilayers containing either no additional lipid, 1% PI(4) or 1% PI(3)P. Purified ESCRT-II complex was added to the Binding Chamber at a concentration of 0.2 μM in a buffer solution (see materials and methods). The SDS-PAGE and analysis of the membrane-bound proteins revealed similar amounts of ESCRT-II bound to the bilayer formed by the basic lipid mixture or the mixture containing PI(4)P. However, the increase in the amount of ESCRT-II in the lane corresponding to PI(3)P demonstrates specificity of the interaction between ESCRT-II and PI(3)P. These results furthermore indicate that the purified ESCRT-II complex is functional.

We next used FRAP analysis to examine the dynamics of PSLBs before and after the addition of purified ESCRT-II to the bilayer (Figure 2.4 B). PSLBs were created by liposome fusion either in presence or absence of 1% PI(3)P. Rhodamine-PE was added to both the control and PI(3)P lipid mixture to visualize the membrane. The Flow Cell was assembled and mounted onto the microscope. The rate of lipid diffusion before the addition of ESCRT-II was $D=5.01x10^{-2}$ μm^2 ($t_{1/2}=1.39$) and after protein addition the rate was similar, $D=5.01x10^{-2}$ μm^2 ($t_{1/2}=1.38$). The rate of diffusion on the PI(3)P containing membrane prior to ESCRT addition was lower that the control membrane and was $D=4.78x10^{-2}$ μm^2 ($t_{1/2}=1.61$). After the addition of ESCRT-II to the PI(3)P containing membrane, the diffusion rate decreased to $D=4.78x10^{-2}$ μm^2 ($t_{1/2}=1.91$), although the change in diffusion was not significantly different. The

Figure 2.4 ESCRT-II Binding to PSLBs. (A) ESCRT-II was purified from *E. coli* His(6)-tag affinity purification. Bilayers were created in the Binding Chamber by liposome fusion with no lipid or PI(3)P or PI(4)P added to the PI:PE:PC:cholesterol = 11:23:56:10 lipid composition. Samples were analyzed by SDS-PAGE followed by silver staining to visualize protein. (B) Bilayers were made using a similar lipid mixture as described in A, however Rhodamine-PE was added (1%) to visualize the bilayers. The rate of diffusion was measured before and after the addition of 0.2 μM ESCRT-II following 10 minutes of incubation and were not significantly different. Solid lines represent the predicted rate of recovery based on the 2D diffusion recovery model. (C) SFG was also used to analyze ESCRT-II binding to PSLBs (see Methods and Materials). PSLBs were crated using the LB method with similar lipid composition as described in A. The binding constant of ESCRT-II for the control membrane was not obtainable.

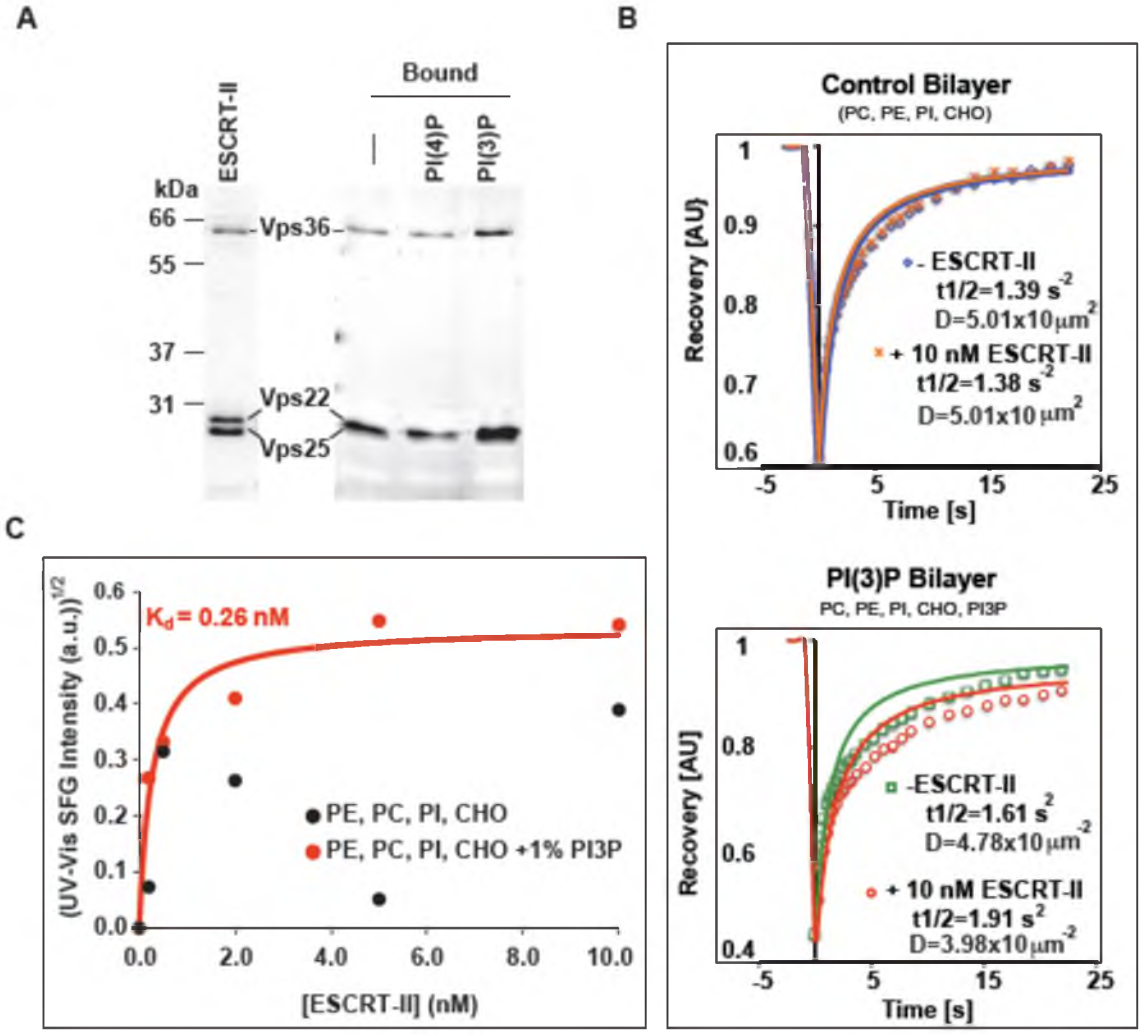
A
Bound
ESCRT-II
—
PI(4)P
PI(3)P
kDa
66
55
37
31
Vps36
Vps22
Vps25
B
Control Bilayer
(PC, PE, PI, CHO)
Recovery [AU]
1
0.9
0.8
0.7
0.6
- ESCRT-II
t1/2=1.39 s-2
D=5.01x10 μm2
+ 10 nM ESCRT-II
t1/2=1.38 s-2
D=5.01x10 μm2
-5
5
15
25
Time [s]
PI(3)P Bilayer
PC, PE, PI, CHO, PI3P
Recovery [AU]
1
0.8
0.6
0.4
-ESCRT-II
t1/2=1.61 s-2
D=4.78x10 μm-2
+ 10 nM ESCRT-II
t1/2=1.91 s-2
D=3.98x10 μm-2
-5
5
15
25
Time [s]
C
(UV-Vis SFG Intensity (a.u.))1/2
Kd = 0.26 nM
PE, PC, PI, CHO
PE, PC, PI, CHO +1% PI3P
0.0
0.1
0.2
0.3
0.4
0.5
0.6
0.0
2.0
4.0
6.0
8.0
10.0
[ESCRT-II] (nM)

absence of a decrease in the rate of diffusion was surprising based on the results from the binding assay which clearly demonstrated ESCRT-II binding to bilayers containing PI(3)P. This result suggested that binding of ESCRT-II to 1% PI(3)P in the bilayer does not affect the rate of diffusion of Rhodamine-PE. However, due to the size of the ESCRT-II complex, it is likely that ESCRT-II binding to PI(3)P would decrease the rate of diffusion of PI(3)P through the membrane.

Another surprising result was the consistent variance of bilayer fluorescence recovery values of Rhodamine-PE from the theoretical 2-D diffusion recovery model predicted for a fluid bilayer. The 2-D diffusion recovery model is the fastest theoretical rate at which a bilayer can diffuse and is based on the initial intensity, the size of the bleach spot and the percent of lipid bleached within the spot. The disagreement between the predicted recovery model and the measured values suggest that there are at least two, possibly more, different lipid kinetics occurring in the bilayer. UV-Vis-SFG experiments were conducted to confirm our result that purified ESCRT-II showed enhanced binding to PI(3)P-containing bilayers (Figure 2.4 C) and to determine the binding constant of ESCRT-II to these bilayers. UV-Vis-SFG was performed on PSLBs created by the LB method using a standard lipid mixture in presence of 1% PI(3)P (Figure 2.4 C). These experiments indicated a binding constant of ESCRT-II to PI(3)P-containing PSLBs of K_d=0.26 nM. This unexpectedly high affinity of ESCRT-II to PI(3)P-containing PSLBs is roughly 200-fold greater than that of $FYVE_{EEA1}$. However, this SFG experiment will have to be repeated and additional controls will be necessary to validate the findings.

2.3 *Conclusions*

We have demonstrated the successful development an *in vitro* system capable of detecting the dynamic recruitment of large protein complexes, like ESCRT-II, to PSLBs under protein equilibrium conditions using the UV-Vis-SFG method. We tested our system with purified GST-GFP_FYVE$_{EEA1}$ and ESCRT-II, two proteins known to bind to PI(3)P and determined that our Binding Chamber and UV-Vis-SFG produced results that were consistent. The value of this *in vitro* system is realized by its potential to study the dynamic assembly of the entire ESCRT network using purified protein complexes and determine individual binding constants under equilibrium conditions. Currently, there is not a similar technique available, thus this *in vitro* system is highly desirable and can be used to study other protein-membrane interaction networks such as those involved in cell signaling, vesicle trafficking and organelle remodeling. In addition, we designed a temperature-controlled Flow Cell that is compatible with FRAP analysis and can be used to study the affects of proteins or other molecules on lipid dynamics.

However, we encountered several problems during testing of the *in vitro* system that will have to be addressed. Specifically, we were unable to determine the source causing the observed deviation from the theoretical lipid-diffusion model. The deviance of the measured recovery from the theoretical recovery model could be caused by partial separation of lipids into micro-domains or other perturbation in membrane homogeneity. However, our initial characterization of PSLBs did not exhibit this effect (compare Figure 2.2 B to Figure 2.4 B). We also

observed day-to-day variances in the diffusion rates of bilayers large enough to obscure possible changes induced by ESCRT-II binding. The inconsistency in measurement could have been caused by fluctuations in lipid preparation, humidity, and surface preparation of the glass substrate. Therefore only experiments that analyzed ESCRT-II membrane binding on the same day and using the same PSLB are comparable. It would be most beneficial to repeat the above experiments in the Flow Chamber using PSLBs created by the LB method, as this method is able to control for lipid packing and might be able to resolve the deviations from the predicted 2-D diffusion recovery model. After optimizing the experimental conditions the binding constants of all the ESCRT complexes including ESCRT-0, ESCRT-I and ESCRT-III should be determined. These data would provide extremely useful insight into the assembly of the ESCRT network.

IR-Vis-SFG, a technique similar to UV-Vis-SFG, capable of detecting membrane perturbations induced by protein associations by analyzing the IR resonance patterns of the C-H bonds in lipids. IR-Vis-SFG analysis might be used to directly determine whether PI(3)P is efficiently incorporated into the membrane and whether ESCRT binding directly effects the bilayer (Liu and Conboy, 2005a; Liu, 2007). It has been hypothesized that the association of the ESCRT machinery to the membrane induces structural reorganization in the membrane leading to membrane budding (Piper and Katzmann, 2007). Analysis by IR-Vis-SFG could provide insight into how and if the ESCRTs induce physical changes in the bilayer. IR-Vis SFG has been shown by the Conboy group to be a powerful tool for the study of membrane structure, asymmetry and dynamics

(Anglin et al., 2007; Liu and Conboy, 2004; Liu and Conboy, 2005b). The analysis of the ESCRTs by IR-Vis-SFG is a logical second step following optimization of UV-Vis-SFG.

2.4 *Materials and Methods*

2.4.1 *Materials*

Phosphatidylinositol (Sodium Salt, Bovine, Liver), L-a Phosphatidylethanolamine (Egg, Chicken), L-a Phosphatidylcholine (Egg, Chicken) and 1,2-Dimyristoyl-*sn*-Glycerol-3-Phosphaoethanolamine-N-(Lissamine Rhodamine B Sulfonly) were obtained from (Avanti Polar Lipids). D-*myo*-Phosphatidylinositol 3-phosphate (14:0) and BODIPY®-FL PIP (505/513), C_{16} were obtained from Eschelon Inc. (Salt Lake City, UT). D-*myo*-Phosphatidylinositol 4-phosphate (14:0) was ag gift from Eschelon. Cholesterol was purchased from Sigma (St Louis, MO). The PI, PE, PC, cholesterol was used as the control bilayer and used at 1mg/ML. Lipids were stored in a piranha-cleaned glass vials at -80 C. and cholesterol (Fischer).

2.4.2 *Methods*

2.4.2.1 ESCRT-II protein purification. A 100 mL culture of Arctic Express (yellow) cells transformed with pEO42, was grown overnight in Kanamycin and Gentamyicn and were used to inoculate 2 L of autoinduction medium. The inoculum was incubated at 30 °C for 4 hours before transfer to a 15 °C water bath for 36 hours. Cells were spun in a GS3 rotor for 10 minutes at 5,500 RPM. The pellet was resuspended in Wash Buffer and spun again and were then

resuspended in Lysis Buffer. 0.5 mL E.Coli protease inhibitors were added and 0.4 mg/mL Lysozyme. Cells were Incubated on RT rocker for 10 minutes and then cooled on ice for 10 minutes. Cells were sonnicated 3-5 times for 30 second intervals with large blunt end probe and the sonnicator was set to # 8. Lysate was spun in an SS34 rotor for 15 minutes at 15,000 RMP. Supernatant was collected and Tween-20 to 0.5%, imidizole to 5 mM were added. The lysate was desiccated on ice to remove air bubbles before being loading onto the column. The GSH column was pre-equilibrate with His-Binding buffer and loaded onto Ni-chelating column at 3 mL/min. The flow through was loaded again. The column was washed 2x with 2x the sample volume. The protein was eluted in HIS-Elution buffer containing 100 mM imidazole. Purified ESCRT-II was then loaded onto a G25 Sephadex desalting column to remove imidazole. The running buffer was 100 mM NaCl, 20 mM Tris pH 8 and 1 mM NaN_3. From the desalting column, ESCRT-II was loaded onto a 1 mL Resource Q (Pharmacia Biotech) and fractions pooled. The His(6)-tag was removed by thrombin cleavage for 2 hours at room temperature. ESCRT-II was then re-run over the HPLC column, resulting in purified ESCRT-II.

2.4.2.2 GST-GFP-FYVE$_{EEA1}$ purification. A 60 mL starter culture of transformed ArcticExress (blue) was grown overnight and used to inoculate 2 L of Super Broth medium (1:50). Cells were incubated for 2 hours at 30 ^{o}C prior to the addition of 0.5 mM $ZnSO_4$ and 0.5 mM IPTG (Sigma). Cells were incubated for 25 hours at 10.5 ^{o}C. Harvested cells were resuspended in Lysis Buffer (10 mM Tris pH8, 1 mM EDTA). 20 μL of protease inhibitors and lysozyme was

added to the cells and incubated at room temperature for 15 minutes. Cells were then cooled in ice for 10 minutes. Cells were then sonnicated with 5 pulses for 20 seconds each, cooling on ice inbetween pulses. The cells were spun in an Ultra Centrifuge (Sigma) @ 40,000 x g for 15 minutes at 4 ^{o}C. 150 mM NaCl and 0.5 % were added to the supernatant. The lysate was flowed over a GSH-sepharose column twice. The column was equilibrated with a GST-Wash buffer (150 mM NaCl, 20 mM Tris pH8). After protein loading the column was washed with same buffer twice. Protein was eluted by pumping 20 mM Trish pH8, 50 mM NaCl and 10 mM GSH (Glutathione-S Transferase)

2.4.2.3 Piranha acid bath. 70%HNO_3SO_4, 30%H_2O_2. All Teflon and glass components were incubated overnight and washed thoroughly with purified water. Glass components used to support bilayers were dried in a drying oven. All other components remained in water until use.

2.4.2.4 Liposome fusion. Lipids were solubilized per manufacture's recommendation. Lipids were mixed in a molar ratio of PI:PE:PC:Cholestol, 11:23:56:10. PI(3)P was solubilized in chloroform: methanol: water 1:2:0.8. If added, PI(3)P was first transferred to a cleaned class vile with a glass syringe and dried for one hour in a vacuum desiccator and resuspended in 400 μL 1:1 chloroform, methanol. Control lipids were diluted in half with 1:1 methanol:chloroform prior to transfer to the PI(3)P vial. The lipid mixture was then dried again. The lipids were suspended in 200 mM Tris, pH 8, 250 mM NaCl or 20 mM HEPES pH 7.4, 150 mM KAc and sonnicated for about 2-3 minutes until clear. A drop of roughly 100 μL was placed on the glass substrate and

incubated for 10 minutes to allow formation of the bilayer. Glass substrates were cleaned in an acid bath, washed with water and dried in a drying oven. Finally substrates were cleaned in a Argon plasma cleaner for 1.5 minutes.

2.4.2.5 Langmuir-Blodgette method. The LB method was conducted as described (Liu and Conboy, 2005a). Briefly, a 1 mg/mL lipid solution was spread on the water surface of a Langmuir-Blodgette trough (KSV Instruments). The first bilayer is deposited on the glass substrate via a vertical pull through the lipid monolayer. The second layer is applied by lowering the flat surface of the substrate onto the monoloayer. Lipid transfers were carried out at a surface tension pressure of 30 mN/m at 22 C.

2.4.2.6 UV-Vis-sum frequency vibrational spectroscopy. Experiments were conducted as described previously, (Nguyen et al., 2009) A UV-Vis SFG flow cell was used with a voume of 0.5 mL. The bilayer was assembled in a Teflon block and sealed by pressure against Viton o-rings. To access ports enable influx and efflux of protein and buffer solutions into the binding chamber. The 532 nm (2^{nd} harmonic) and 355 (3^{rd} harmonic) beams from an Nd-YAG laser (Continuum Surelite II 20 Hz) at 12 and 14 mJ/pulse were used. The beams of light were overlapping at the surface of the bilayer and were counter propagating. They were aimed at the surface just greater than the critical angle, ~70^{o} .UV and Vis light filters were placed between the photomultiplier detector to prevent measurement of scattered light. A boxcar integrator was used to process the signal.

2.4.2.7 Binding Chamber assay. The Binding Chamber and microscope slide were submerged in piranha solution overnight and washed thoroughly with purified water and dried completely prior to assembly. Viton O-rings were cleaned with both isopropanol and methanol. forty μL of liposome emulsion were placed on the glass slide and incubated for 10 minutes. ESCRT-II Binding. Purified ESCRT-II complex was added to the binding chamber at a concentration of 0.2 μM in 20 mM HEPES pH 7.4, 150 mM KAc. Membranes were washed 2x with 500 μL with buffer solution. Solutions were removed using the vacuum system. Protein solution was added and incubated for 10 minutes. Membranes were washed as previously described. Two μL of 10% SDS (sodium dodecyl sulfate (BioRad)) were added to each well to solubilize the membrane. The liquid in each well was transferred to clean glass vial and dried in a heated RotoVac for 1 hour. 10 μL of sample buffer (0.1 M Tris, pH 6.8, 10% glycerol, 0.01% bromophenol blue, 5% β-mercaptoethanol) was added and the sample was loaded onto an SDS gel.

2.4.2.8 Flow Cell assay. A 100 μL drop was placed on a clean glass coverslip and inverted suspended by two glass supports. The hanging drop was incubated at room-temp for 10 minutes. The cover glass was submerged in clean water and assembled into the flow cell. The bilayers were washed 2x with 500 μL each. GST-GFP-FYVE$_{EEA1}$ and ESCRT-II was added to the bilayer compartment in the flow cell.

2.4.2.9 SDS-PAGE. GST-GFP-FYVEEEA1 was loaded onto a 12 % acrylamide gel. ESCRT-II was loaded onto a 10 % acrylamide gel.

2.4.2.10 Silver staining. Following SDS-PAGE, the gel was exposed to a silver nitrate process. The gels were fixed for 20 minutes in a solution of that contained 50 mL of MeOH, 10 mM glacial acedic acid, 10 mL fixative concentrate (BioRad (hurleles, CA)) and 30 mLs of water. The gels were rinsed for 20 minutes accompanied by one wash step. The first baker contained the staining solution: 25 mL water, 1.25g Accelerator (BioRad). The second beaker contained 17.5 mL water, 2.5 mL SolI, 2.5 mL of Sol2 and 2.5 mLs of solIII (Biorad). Adding a 5 % glacial acidic acid to the gels stopped the reaction.

2.5 *Appendix*

2.5.1 *Binding Chamber*

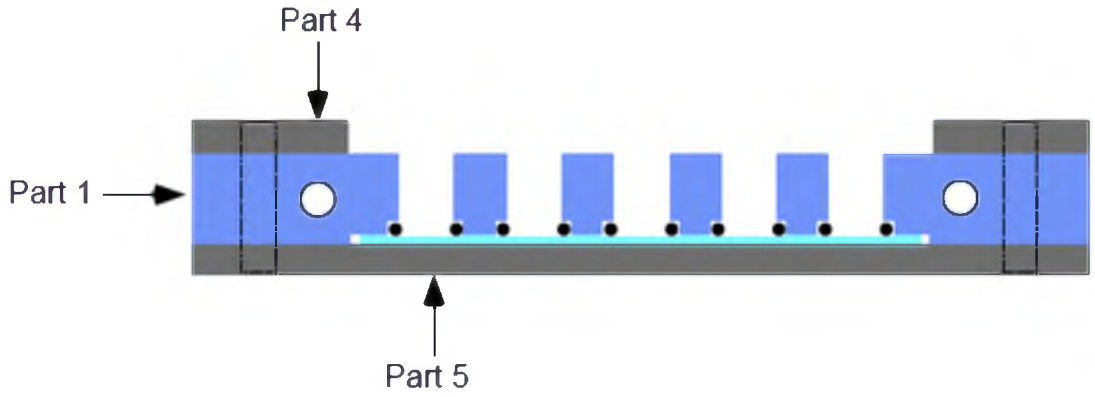

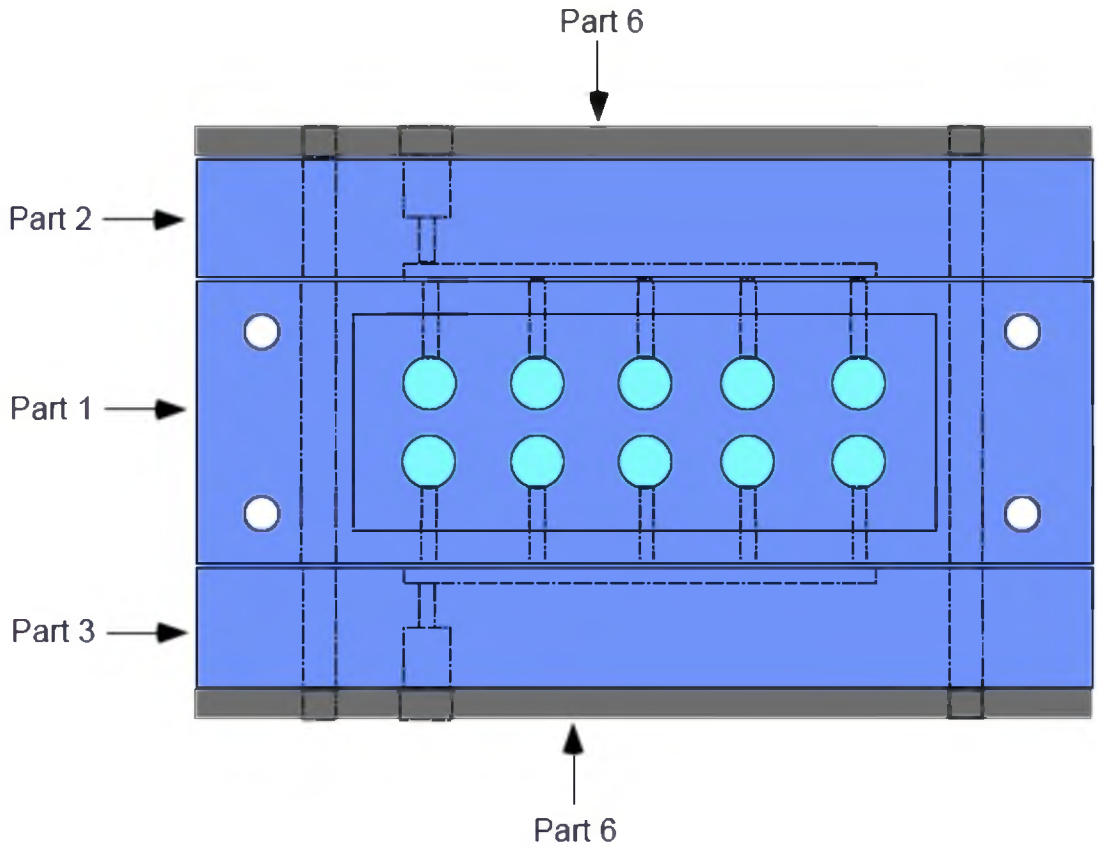

Part 1
Material: Teflon
Measurements in inch

Top View

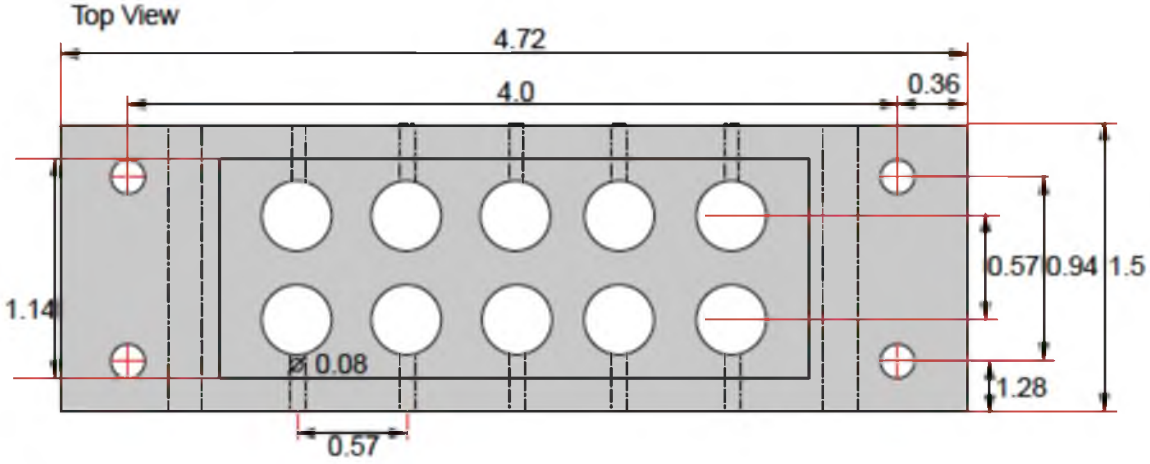

Side View

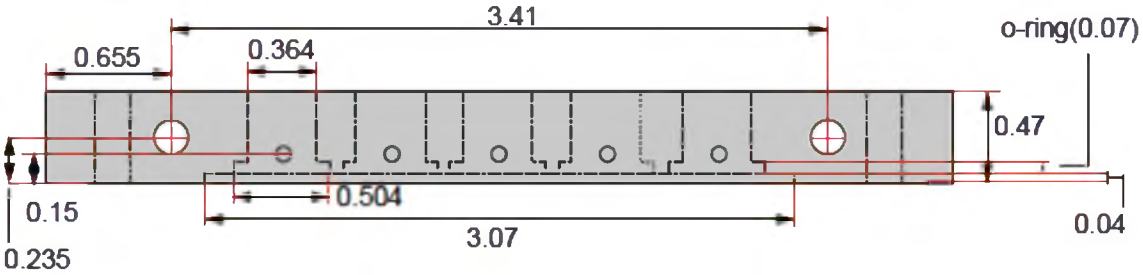

Part 2/3

Material: Teflon

Measurements in inch

Part 2

Top View

Part 3

Top View

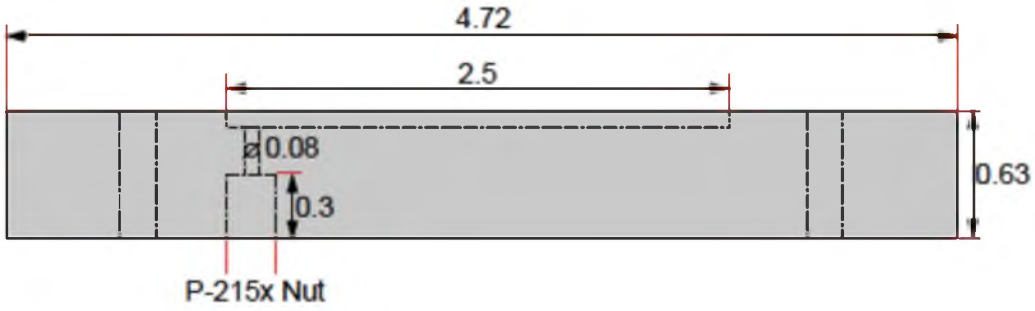

Part 2/3

Side View

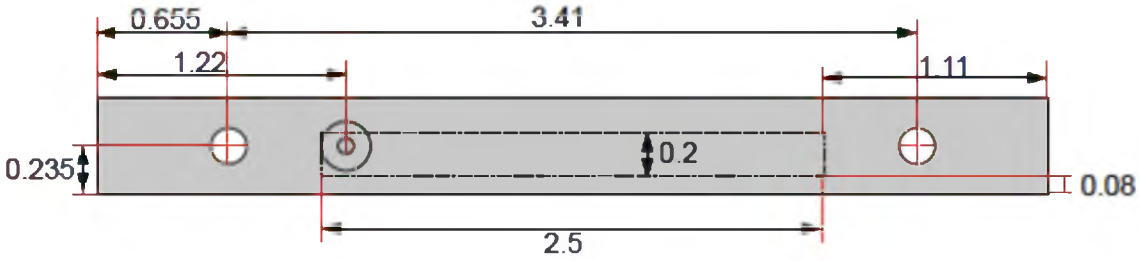

Part 4
Material: Aluminum
Measurements in inch

Top View

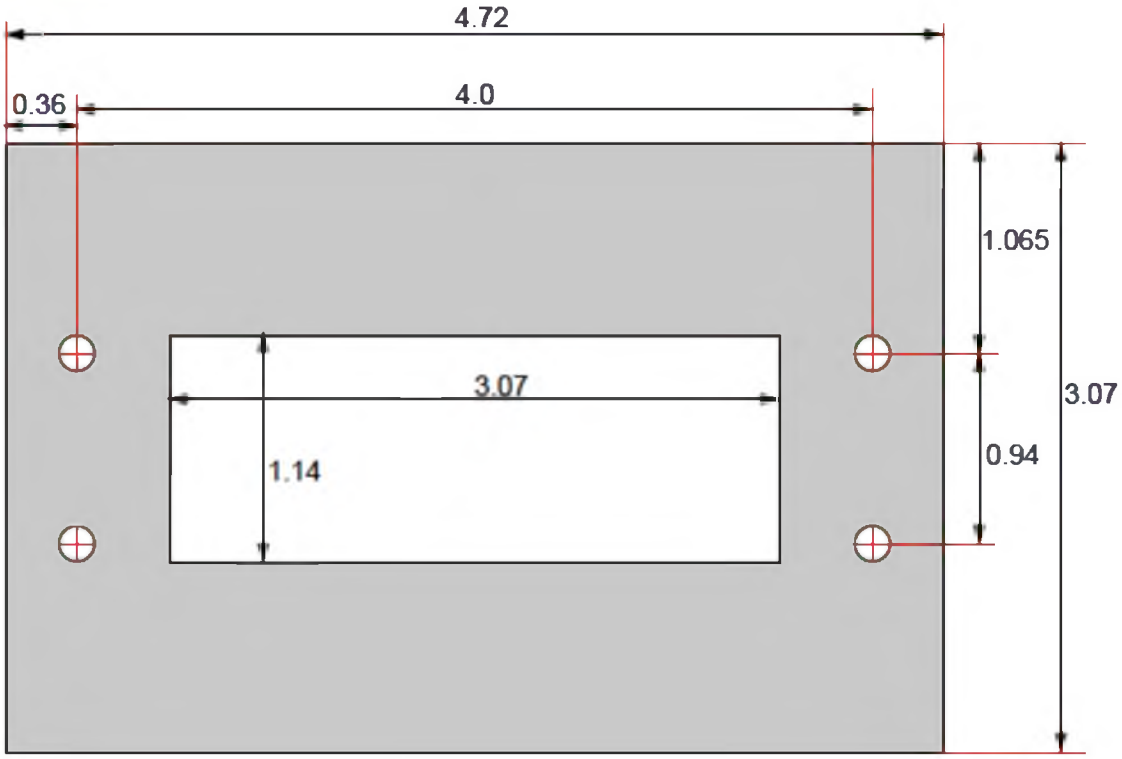

Side View

Part 5
Material: Aluminum
Measurements in inch

Top View

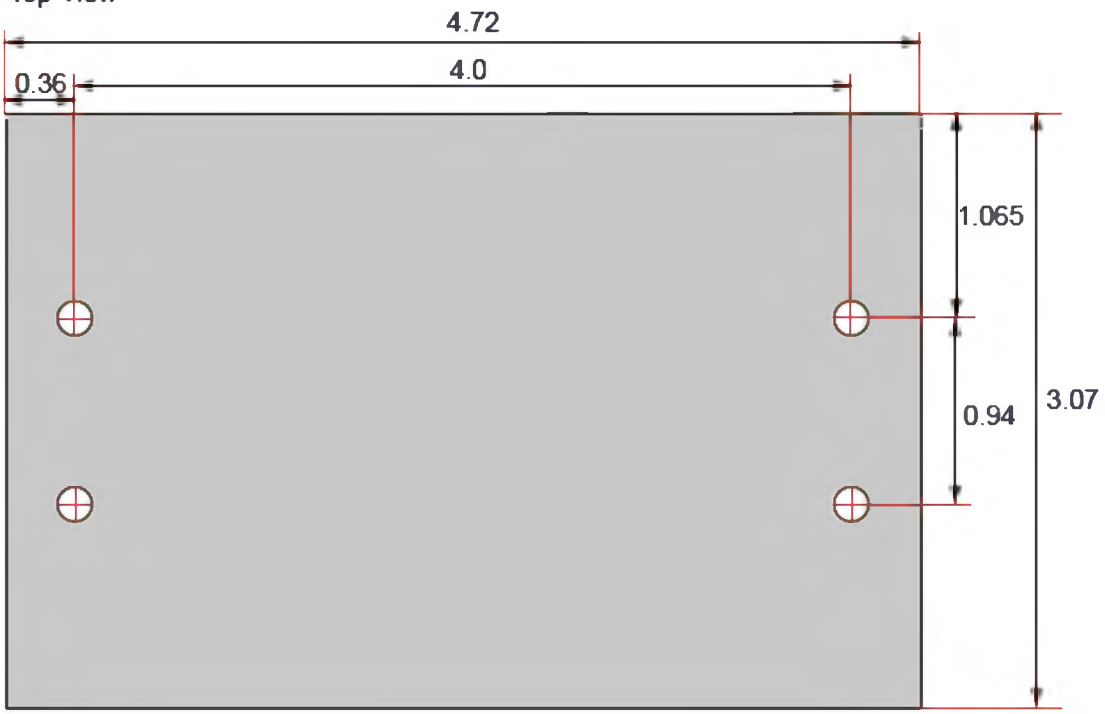

Side View

Part 6 (2 identical parts)
Material: Aluminum
Measurements in inch

Top View

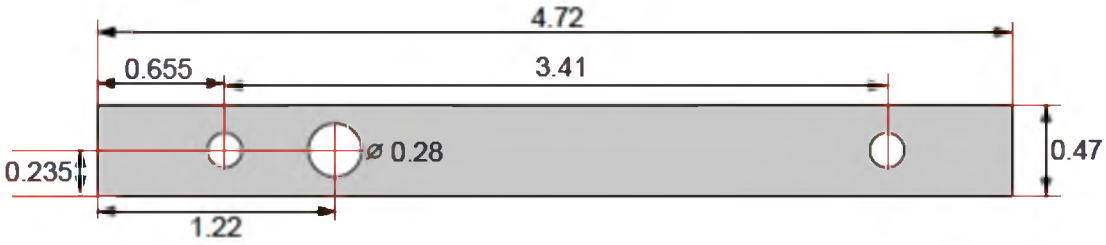

Side View

2.5.2 *Flow Cell*

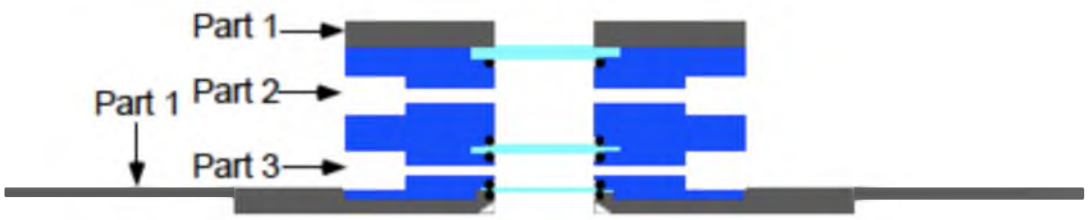

Part 1

Material: Aluminum Measurements in inch

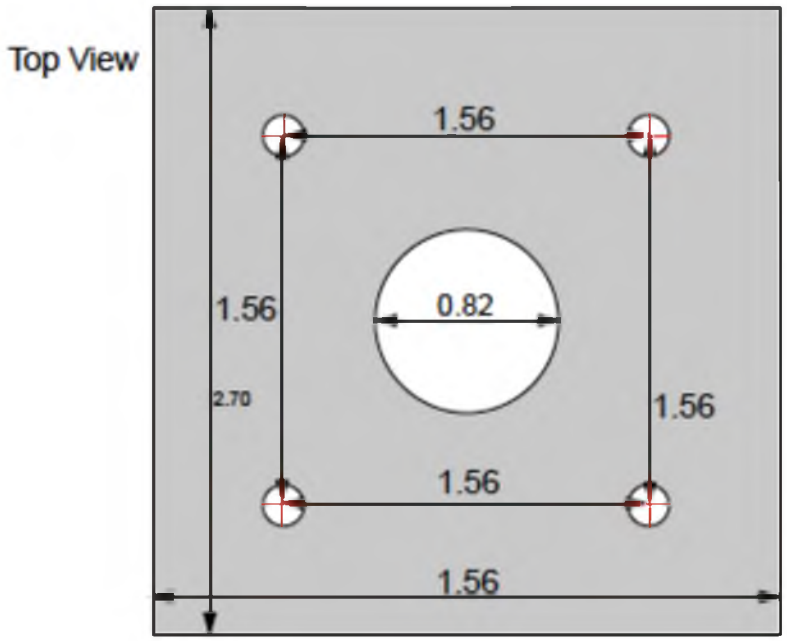

Material: Teflon Measurements in inch

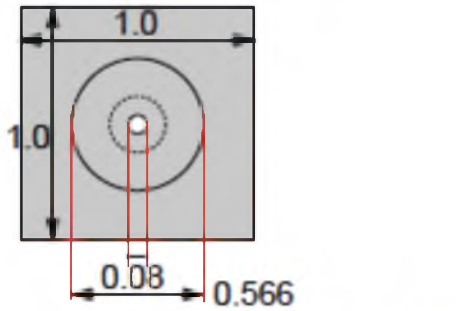

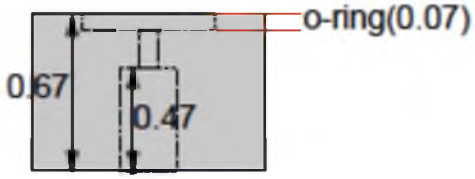

P-215x Nut

Part 2 Material: Teflon

Measurements in inch

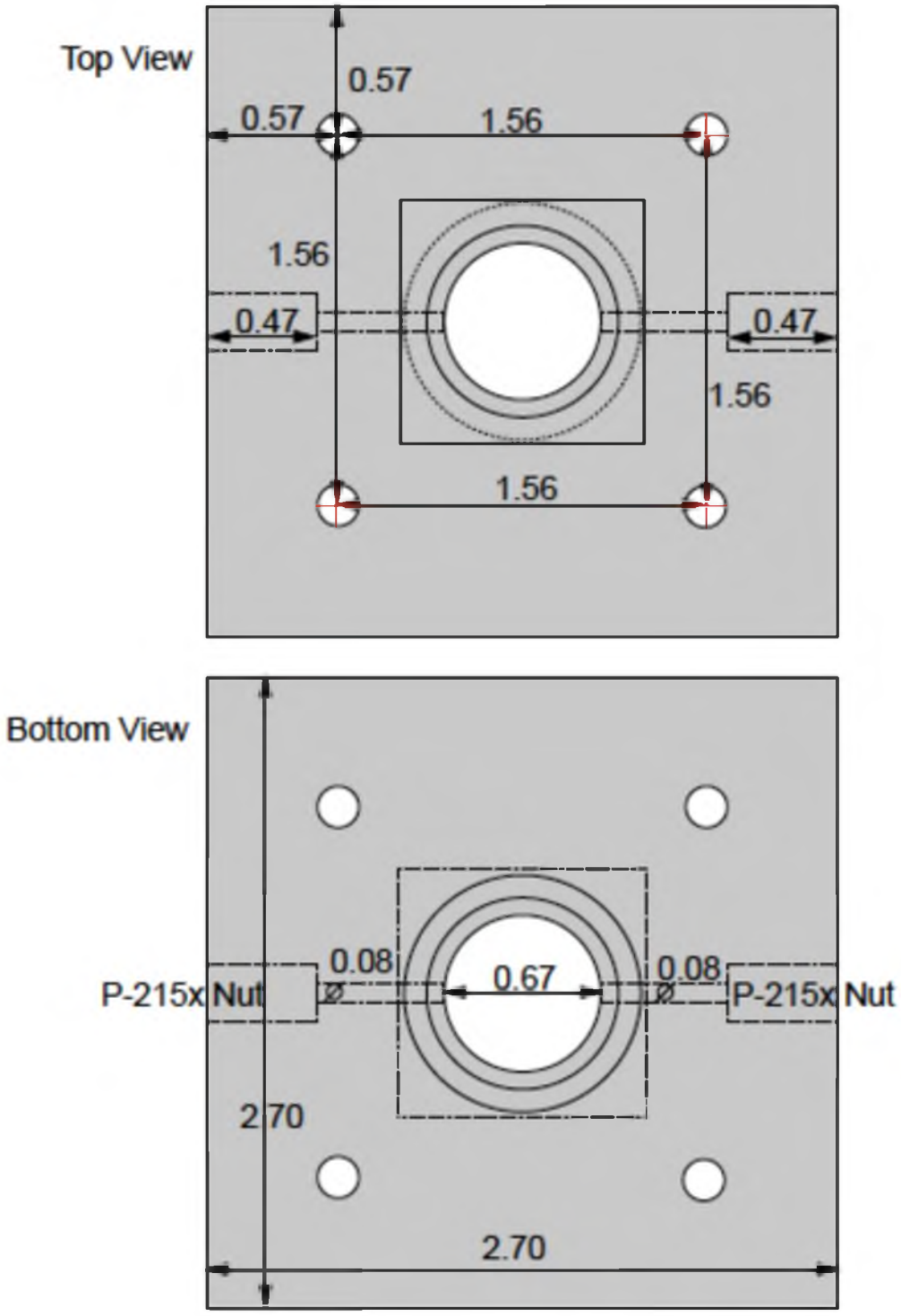

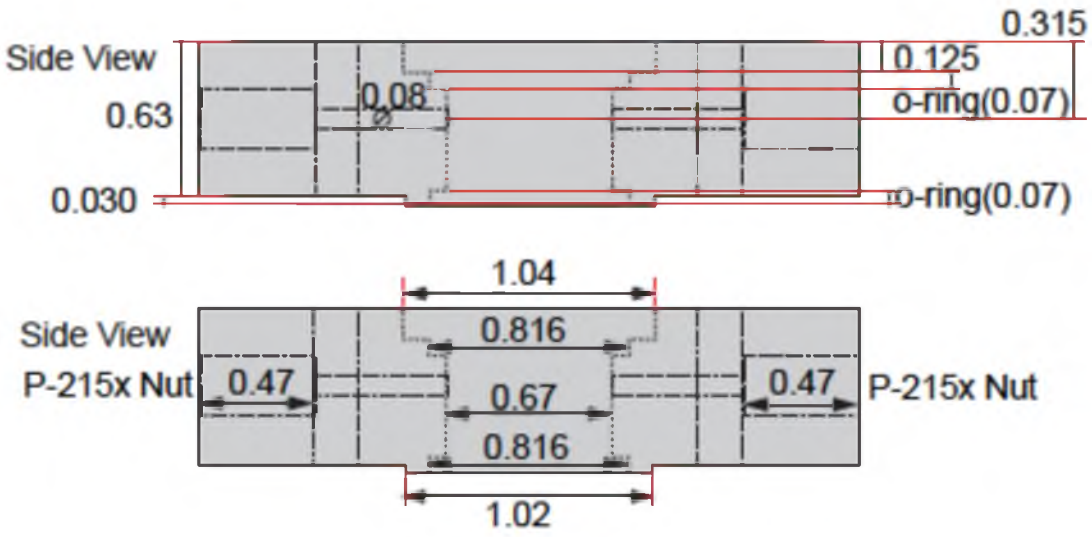
Side View
0.63
0.030
0.08
0.315
0.125
o-ring(0.07)
o-ring(0.07)
Side View
P-215x Nut
1.04
0.816
0.47
0.67
0.47
P-215x Nut
0.816
1.02

Part 3 Material: Teflon

Measurements in inch

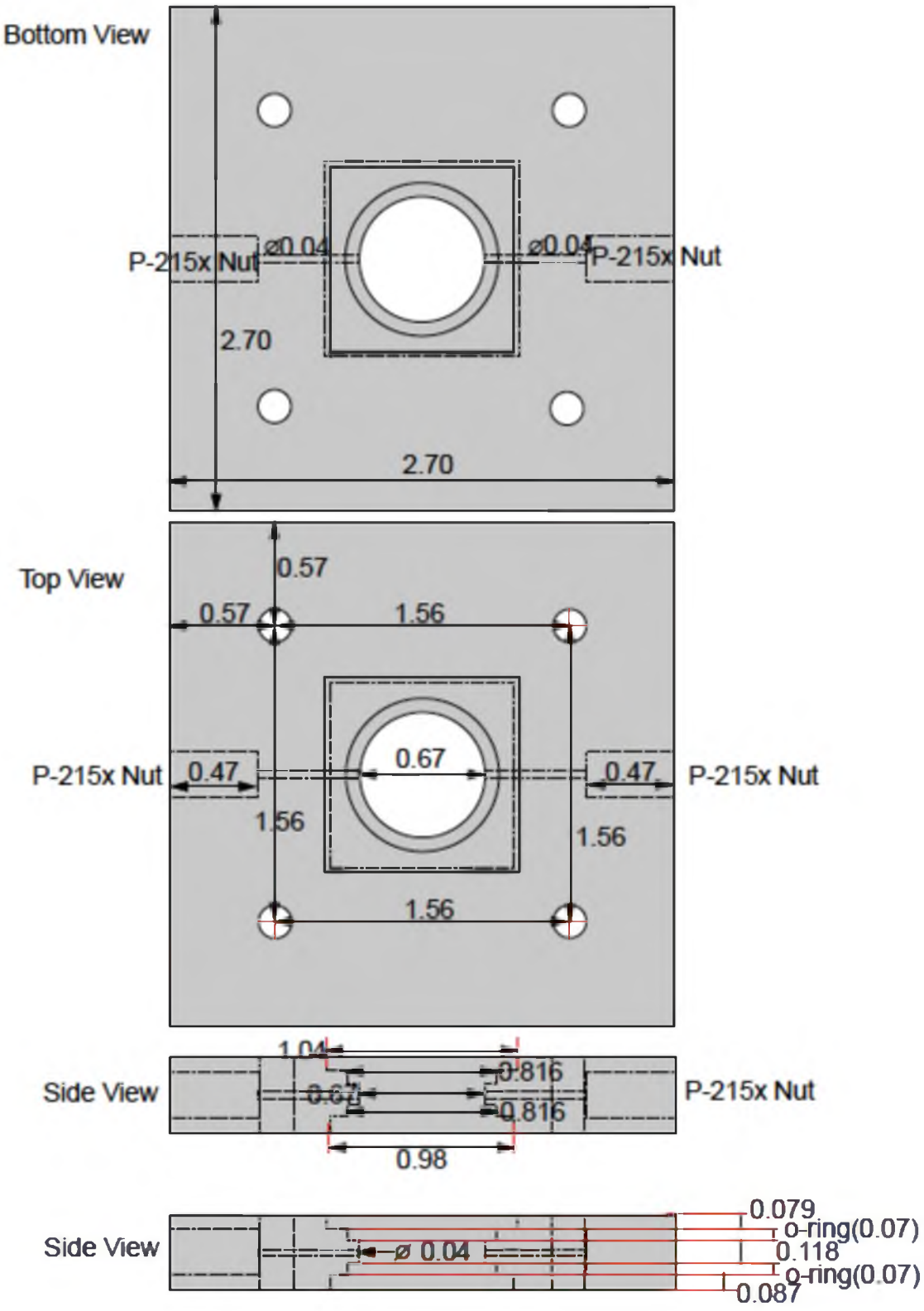

Part 4

Material: Aluminum

Measurments in inches

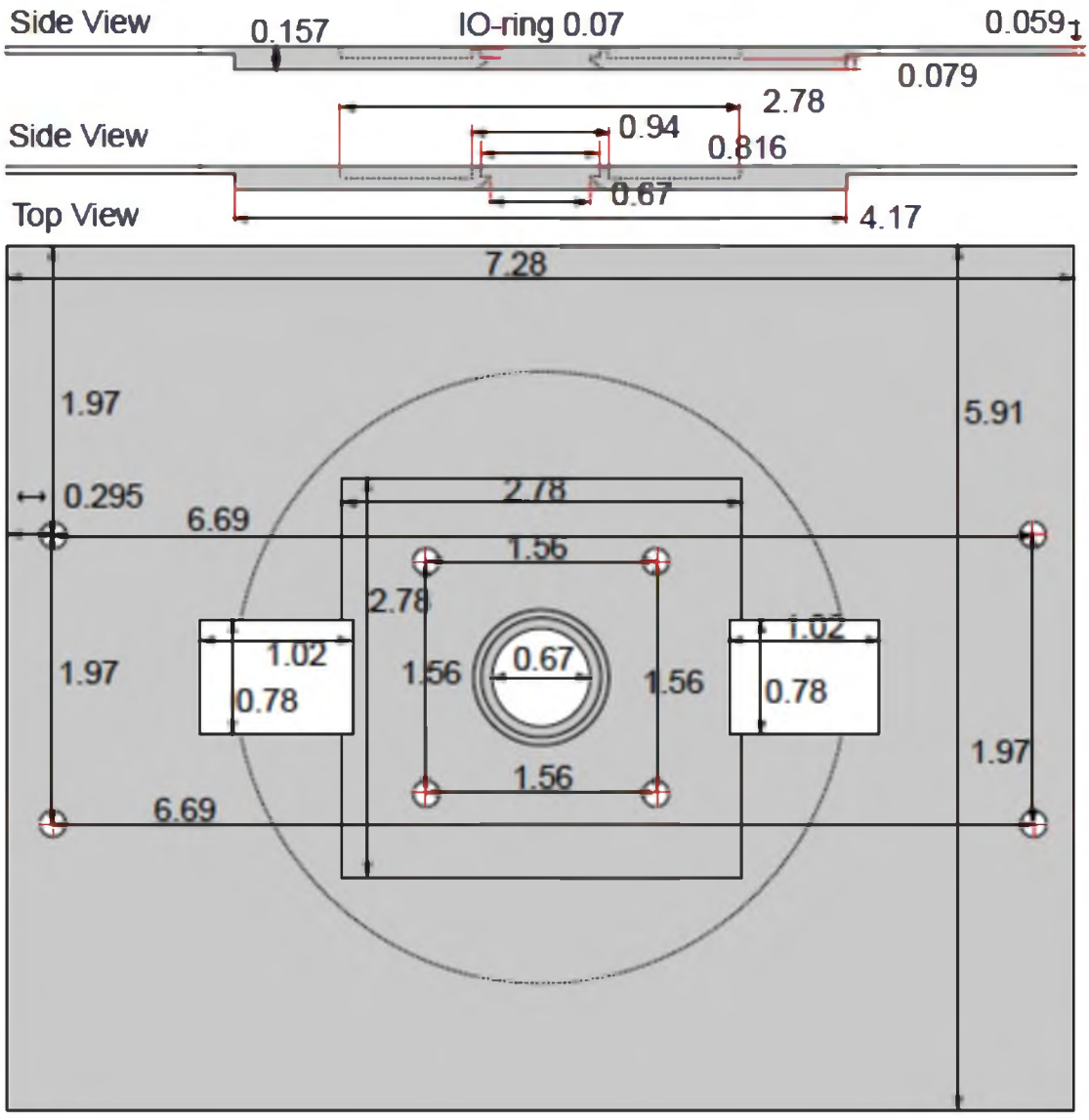

2.6 *References*

Alam, S.L., J. Sun, M. Payne, B.D. Welch, B.K. Blake, D.R. Davis, H.H. Meyer, S.D. Emr, and W.I. Sundquist. 2004. Ubiquitin interactions of NZF zinc fingers. *Embo J.* 23:1411-1421.

Anglin, T.C., J. Liu, and J.C. Conboy. 2007. Facile lipid flip-flop in a phospholipid bilayer induced by gramicidin A measured by sum-frequency vibrational spectroscopy. *Biophys J.* 92:L01-03.

Babst, M., D.J. Katzmann, E.J. Estepa-Sabal, T. Meerloo, and S.D. Emr. 2002a. Escrt-III: an endosome-associated heterooligomeric protein complex required for mvb sorting. *Dev Cell.* 3:271-282.

Babst, M., D.J. Katzmann, W.B. Snyder, B. Wendland, and S.D. Emr. 2002b. Endosome-associated complex, ESCRT-II, recruits transport machinery for protein sorting at the multivesicular body. *Dev Cell.* 3:283-289.

Babst, M., B. Wendland, E.J. Estepa, and S.D. Emr. 1998. The Vps4p AAA ATPase regulates membrane association of a Vps protein complex required for normal endosome function. *Embo J.* 17:2982-2993.

Burd, C.G., M. Babst, and S.D. Emr. 1998. Novel pathways, membrane coats and PI kinase regulation in yeast lysosomal trafficking. *Semin Cell Dev Biol.* 9:527-533.

Burd, C.G., and S.D. Emr. 1998. Phosphatidylinositol(3)-phosphate signaling mediated by specific binding to RING FYVE domains. *Mol Cell.* 2:157-162.

Carlton, J.G., and J. Martin-Serrano. 2007. Parallels between cytokinesis and retroviral budding: a role for the ESCRT machinery. *Science.* 316:1908-1912.

Elia, N., R. Sougrat, T.A. Spurlin, J.H. Hurley, and J. Lippincott-Schwartz. 2011. Dynamics of endosomal sorting complex required for transport (ESCRT) machinery during cytokinesis and its role in abscission. *Proc Natl Acad Sci U S A.* 108:4846-4851.

Gaullier, J.M., A. Simonsen, A. D'Arrigo, B. Bremnes, H. Stenmark, and R. Aasland. 1998. FYVE fingers bind PtdIns(3)P. *Nature.* 394:432-433.

Gill, D.J., H. Teo, J. Sun, O. Perisic, D.B. Veprintsev, S.D. Emr, and R.L. Williams. 2007. Structural insight into the ESCRT-I/-II link and its role in MVB trafficking. *Embo J.* 26:600-612.

Hierro, A., J. Sun, A.S. Rusnak, J. Kim, G. Prag, S.D. Emr, and J.H. Hurley. 2004. Structure of the ESCRT-II endosomal trafficking complex. *Nature.* 431:221-225.

Hirano, S., N. Suzuki, T. Slagsvold, M. Kawasaki, D. Trambaiolo, R. Kato, H. Stenmark, and S. Wakatsuki. 2006. Structural basis of ubiquitin recognition by mammalian Eap45 GLUE domain. *Nat Struct Mol Biol*. 13:1031-1032.

Im, Y.J., and J.H. Hurley. 2008. Integrated structural model and membrane targeting mechanism of the human ESCRT-II complex. *Dev Cell*. 14:902-913.

Im, Y.J., T. Wollert, E. Boura, and J.H. Hurley. 2009. Structure and function of the ESCRT-II-III interface in multivesicular body biogenesis. *Dev Cell*. 17:234-243.

Kobayashi, T., M.H. Beuchat, J. Chevallier, A. Makino, N. Mayran, J.M. Escola, C. Lebrand, P. Cosson, and J. Gruenberg. 2002. Separation and characterization of late endosomal membrane domains. *J Biol Chem*. 277:32157-32164.

Kostelansky, M.S., C. Schluter, Y.Y. Tam, S. Lee, R. Ghirlando, B. Beach, E. Conibear, and J.H. Hurley. 2007. Molecular architecture and functional model of the complete yeast ESCRT-I heterotetramer. *Cell*. 129:485-498.

Liu, J., and J.C. Conboy. 2004. Direct measurement of the transbilayer movement of phospholipids by sum-frequency vibrational spectroscopy. *J Am Chem Soc*. 126:8376-8377.

Liu, J., and J.C. Conboy. 2005a. Structure of a gel phase lipid bilayer prepared by the Langmuir-Blodgett/Langmuir-Schaefer method characterized by sum-frequency vibrational spectroscopy. *Langmuir*. 21:9091-9097.

Liu, J., and J.C. Conboy. 2005b. Structure of a gel phase lipid bilayer prepared by the Langmuir-Blodgett/Langmuir-Schaefer method characterized by sum-frequency vibrational spectroscopy. *Langmuir*. 21:9091-9097.

Liu, J.C., J.C. 2007. Asymmetric Distribution of Lipids in a Phase Segregated Phospholipid Bilayer Observed by Sum-Frequency Vibrational Spectroscopy. *Journal of Pysical Chemistry*. 111:8988-8999.

Misra, S., and J.H. Hurley. 1999. Crystal structure of a phosphatidylinositol 3-phosphate-specific membrane-targeting motif, the FYVE domain of Vps27p. *Cell*. 97:657-666.

Montal, M., and P. Mueller. 1972. Formation of bimolecular membranes from lipid monolayers and a study of their electrical properties. *Proc Natl Acad Sci U S A*. 69:3561-3566.

Nguyen, T.T., K. Rembert, and J.C. Conboy. 2009. Label-free detection of drug-membrane association using ultraviolet-visible sum-frequency generation. *J Am Chem Soc*. 131:1401-1403.

Piper, R.C., and D.J. Katzmann. 2007. Biogenesis and function of multivesicular bodies. *Annu Rev Cell Dev Biol*. 23:519-547.

Prag, G., H. Watson, Y.C. Kim, B.M. Beach, R. Ghirlando, G. Hummer, J.S. Bonifacino, and J.H. Hurley. 2007. The Vps27/Hse1 complex is a GAT domain-based scaffold for ubiquitin-dependent sorting. *Dev Cell*. 12:973-986.

Shen, Y.R. 1984. The Principles of Nonlinear Optics. Wiley, New York.

Slagsvold, T., R. Aasland, S. Hirano, K.G. Bache, C. Raiborg, D. Trambaiolo, S. Wakatsuki, and H. Stenmark. 2005. Eap45 in mammalian ESCRT-II binds ubiquitin via a phosphoinositide-interacting GLUE domain. *J Biol Chem*. 280:19600-19606.

Stenmark, H., R. Aasland, B.H. Toh, and A. D'Arrigo. 1996. Endosomal localization of the autoantigen EEA1 is mediated by a zinc-binding FYVE finger. *J Biol Chem*. 271:24048-24054.

Teo, H., D.J. Gill, J. Sun, O. Perisic, D.B. Veprintsev, Y. Vallis, S.D. Emr, and R.L. Williams. 2006. ESCRT-I core and ESCRT-II GLUE domain structures reveal role for GLUE in linking to ESCRT-I and membranes. *Cell*. 125:99-111.

Teo, H., O. Perisic, B. Gonzalez, and R.L. Williams. 2004a. ESCRT-II, an endosome-associated complex required for protein sorting: crystal structure and interactions with ESCRT-III and membranes. *Dev Cell*. 7:559-569.

Teo, H., D.B. Veprintsev, and R.L. Williams. 2004b. Structural insights into endosomal sorting complex required for transport (ESCRT-I) recognition of ubiquitinated proteins. *J Biol Chem*. 279:28689-28696.

Wollert, T., D. Yang, X. Ren, H.H. Lee, Y.J. Im, and J.H. Hurley. 2009. The ESCRT machinery at a glance. *J Cell Sci*. 122:2163-2166.

Zhao, S., Walker D.S: Reichert, W.M. 1993. Cooperativity in the binding of avidin to biotin-lipid-doped Langmuir-Blodgett films. *Langmuir*. 9:3166-3173.

CHAPTER 3

REGULATION OF MEMBRANE PROTEIN DEGRADATION BY STARVATION-RESPONSE PATHWAYS

3.1 *Abstract*

The multivesicular body (MVB) pathway represents a major protein-turnover system in eukaryotic cells. Concurrent with its well-established role in moderating the protein composition of the plasma membrane, the MVB pathway also serves to sustain cells' free amino acid pools through lysosomal/vacuolar protein degradation. This function is essential for survival during periods of starvation. Starvation conditions cause increased cargo flux through the MVB pathway through the upregulation of both endocytosis and ESCRT-mediated sorting of plasma membrane proteins. This regulation of the MVB pathway is controlled by cellular nutrient-sensing systems including TORC1 and Gcn2, which regulate the ubiquitination of cargo proteins and control the expression levels of the ESCRT- regulatory factor Ist1. Starvation conditions cause a rapid drop in Ist1 levels due to a general translational shutdown. Low Ist1 levels promote ESCRT sorting and increase MVB-mediated protein turnover, thereby bolstering amino acid pools to facilitate conditional adaptation.

3.2 *Background*

All eukaryotic organisms are able to respond rapidly to changing nutrient conditions through a complex array of cellular signaling pathways. Eukaryotic cells rely on these pathways to maintain homeostasis, as they are incapable of substantial nutrient storage. Fluctuations in extracellular nutrient availability are mitigated by physiological responses, including limitation of nonessential protein synthesis, biosynthetic generation of deficient nutrients (e.g., amino acids), and

conservation and reutilization of existing resources (reviewed in (Sonenberg and Hinnebusch, 2009).

Central to eukaryotic nutrient sensing systems is the highly conserved target of rapamycin (TOR) kinase (mTOR in mammals) (reviewed in (Wang and Proud, 2009). This Ser/Thr kinase exists in two structurally and functionally distinct multiprotein complexes in the cell, termed TORC1 (TOR complex 1) and TORC2. Studies of TORC1 have revealed its role as a central regulator of several cellular processes, including translation, nutrient transport, ribosome biogenesis, cellular proliferation, and autophagy. The function of TORC2, whose activity is insensitive to rapamycin, is less understood and is involved in regulation of the actin cytoskeleton, endocytosis, and lipid biogenesis.

Amino acids stimulate TORC1 signaling, though the mechanisms remain unclear. Nutrient deprivation, or treatment with rapamycin, results in rapid TORC1 inactivation and the instigation of cellular starvation-response mechanisms (Figure 3.1). These include a block of general translation initiation, transcriptional upregulation of stress-response genes, and derepression of autophagy (Wullschleger et al., 2006). A key step in inhibiting general translation is the phosphorylation and inactivation of translation initiation factor eIF2 by the kinase Gcn2. TORC1 inactivation induces Gcn2 activity, though Gcn2 can also be activated by the presence of uncharged t-RNAs (Staschke et al., 2010).

In addition to transcriptional and translational alterations, starving cells degrade organelles and portions of cytoplasm to recycle existing resources. This

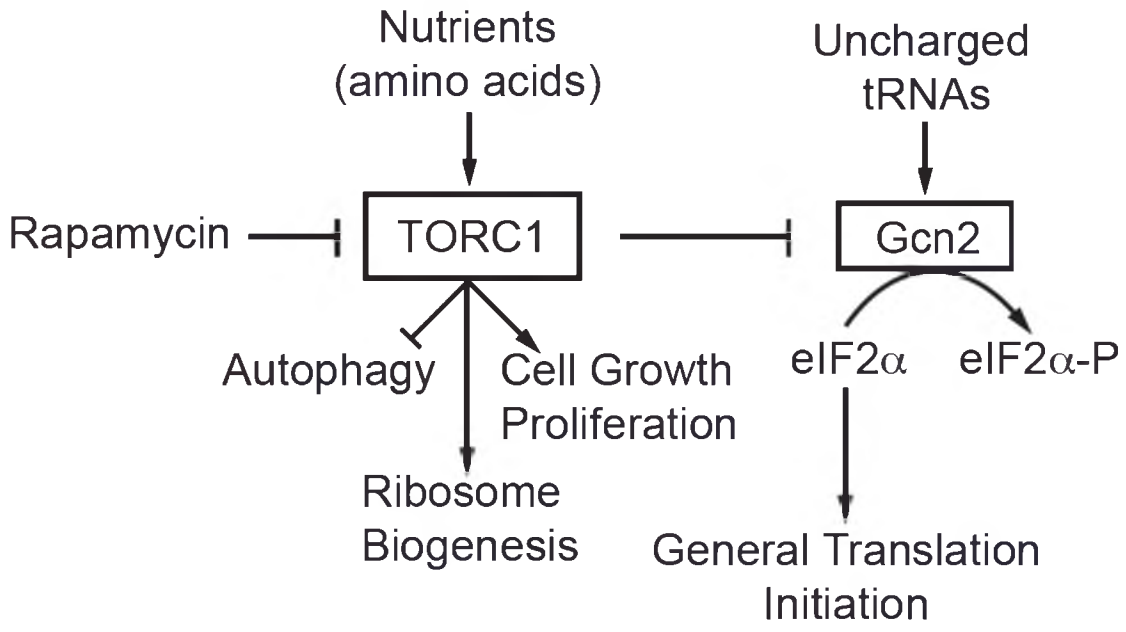

Figure 3.1. TORC1 Signaling During Starvation. The Tor1 kinase in TORC1 is activated by nutrients like amino acids and positively regulates anabolic activities while repressing autophagy, a long-term starvation response pathway. The activation of TORC1 represses the activity of the downstream kinase, Gcn2. The activation of Gcn2 following TORC1 inactivation, results in the phosphorylation of the general transcription factor, eIF2A, which, subsequently represses general transcription. Gcn2 is also activated by the presence of uncharged tRNAs. Kinases are enclosed in a black box.

process, known as autophagy, is highly conserved in eukaryotes and is necessary for survival during prolonged starvation (Chang et al., 2009).

The multivesicular body (MVB) pathway is the primary means of degrading transmembrane proteins in a cell, linking its function to processes such as nutrient uptake and signaling downregulation (Piper and Katzmann, 2007). MVB protein sorting results in the formation of late endosomes containing cargo-laden intralumenal vesicles. These MVBs fuse with the lysosome / vacuole and release the cargo to the compartment's interior for degradation. The minimum signal for MVB sorting is the covalent attachment of a single ubiquitin molecule to the cytoplasmic portion of a target protein by ubiquitin ligase machinery, often Rsp5 in yeast and Nedd4-related ligases in mammalian cells (Belgareh-Touze et al., 2008). Ubiquitinated cargo is sorted at the MVB by a set of protein complexes collectively termed ESCRTs (Endosomal Sorting Complex Required for Transport). The four ESCRT complexes, ESCRT-0, -I, -II, and -III are recruited sequentially from the cytosol to the endosomal membrane where these complexes are thought to recognize, concentrate, and sequester transmembrane cargoes for packaging into vesicles that bud into the lumen of the compartment (Piper and Katzmann, 2007). Additionally, the ESCRT machinery is utilized throughout the cell in other membrane fission events such as cytokinesis and retroviral budding (Carlton and Martin-Serrano, 2007).

MVB formation requires that the ESCRT machinery be released from the endosomal membrane in a reaction catalyzed by the ATPase Vps4. This energy-requiring step is regulated in part by Ist1, which has been shown to physically

interact with the N-terminal substrate-recognition motif of Vps4 (Agromayor et al., 2009; Bajorek et al., 2009a; Dimaano et al., 2008; Shestakova et al., 2010). Regulation of Vps4 by Ist1 seems to be two fold. Genetic data suggest that Ist1 is involved in the recruitment of Vps4 to the endosomal membrane and, as such, is supportive of Vps4 function. Conversely, *in vitro* data shows Ist1 as having a potent negative effect on Vps4 by inhibiting its assembly and ATPase activity (Dimaano et al., 2008). These observations suggest that Ist1 fills a unique regulatory niche within the framework of the MVB pathway

This work presents evidence for a regulatory link connecting canonical cellular starvation-response/nutrient-sensing systems (TORC1- and Gcn2-mediated processes) with the MVB sorting and degradation pathway. This link centers on the MVB factor Ist1, whose protein levels vary dramatically in response to changing nutrient conditions. Cellular levels of Ist1 protein dictate its action and, by extension, its regulation of the MVB pathway. This provides the basis for a system in which protein degradation via the MVB pathway is inversely regulated with respect to general protein synthesis and thereby helps to maintain homeostasis through conditions of variable nutrient availability.

3.3 *Results*

3.3.1 *Recycling of Amino Acids Through the MVB Pathway Is Important for Survival During Starvation*

Previous studies have shown that diploid strains carrying mutations in the ESCRT machinery exhibited sporulation defects (Enyenihi and Saunders, 2003). During our work with ESCRT mutants, we observed that these strains rapidly lost

viability when kept in stationary phase on agar plates. These observations suggested that a block in the MVB pathway might affect starvation- response pathways. To further test this idea, we examined the survival rate of wild-type and ESCRT-mutant strains under starvation conditions. Note that the yeast strain SEY6210, referred to as 'wild type', contains several mutations that render the strain auxotrophic for leucine, tryptophan, histidine, lysine and uracil (Table 3.1). For most of our experiments, we used leucine-free medium to induce starvation conditions. Leucine is the most common amino acid found in proteins, and leucine synthesis is dependent on *LEU2*, which is mutated in SEY6210. The data shown in Figure 3.2 A demonstrated that lack of either Vps4 or Vps24, two proteins essential for a functional MVB pathway, dramatically decreased the survival rate during leucine-starvation conditions. Half of the ESCRT mutant cells died within the first two days. In contrast, wild-type cells exhibited no loss of viability in the same time period, but instead showed a ~20 percent increase in cell number, likely due to the completion of cytokinesis by cells in later stages of mitosis. This increase in cell number was not observed with cells deleted for *IST1*, a gene encoding an ESCRT factor that is not essential for MVB formation (Dimaano et al., 2008; Rue et al., 2008). These data demonstrated a strong correlation between MVB pathway activity and the survival of yeast cells under starvation conditions.

The MVB pathway delivers membrane proteins into the lumen of the vacuole for degradation. The resulting amino acids are pumped into the cytoplasm by vacuolar transporters where they are reused for protein synthesis

Table 3.1. List of Plasmids and Strains

Strain or Plasmid	Descriptive Name	Genotype or Description	Reference or Source
Yeast Strains			
SEY6210	WT	MATα leu2-3,112 ura3-52 his3-Δ200 trp1-Δ901 lys2-801 suc2-Δ9	(Robinson et al., 1988)
MBY3	*vps4Δ*	SEY6210, *VPS4::TRP1*	(Babst et al., 1997)
MBY63	*ist1Δ*	SEY6210, *IST1::HIS3*	(Dimaano et al., 2008)
BWY102	*vps24Δ*	SEY6210, *VPS24::HIS3*	(Babst et al., 2002b)
CJY13	*IST1-HA*	SEY6210, *IST1-HA::KanMX6*	This study
GOY23	*pep4Δ prb1Δ*	SEY6210; *prb1Δ::LEU2 pep4 Δ::LEU2*	(Luhtala and Odorizzi, 2004)
MCY52	*npr1Δ*	SEY6210, *NPR1::KanMX6*	This study
CBY118	*FTR1-GFP*	SEY6210.1, *FTR1-GFP::HISMX*	C. Burd, unpublished
MCY51	*FTR1-GFP ist1Δ*	CBY118, *IST1::URA3*	This study
EOY14	*CAN1-GFP*	SEY6210, *CAN1-GFP::TRP1*	This study
JKY4	*CAN1-GFP ist1Δ*	EOY14, *IST1::HIS3*	This study
TSY183	*FTR1-GFP rsp5Δ*	SEY6210, *RSP5::HIS3* + *pDsRED415-rsp5^{L733S}*, *FTR1-GFP::URA3*	(Strochlic et al., 2008)
MCY54	*FTR1-GFP npr1Δ*	CBY118, *NPR1::KanMX6*	This study
EOY9	*FTR1-HA*	SEY6210, *FTR1-HA::HIS5*	This study
EOY21	*FTR1-HA*	MBY63, *FTR1-HA::KanMX6*	This study
MCY29	*pdr5Δ*	SEY6210, *PDR5::HIS3*	This study
MCY30	*pdr5Δ vps4Δ*	MBY3 (SEY6210, *VPS4::TRP1), PDR5::HIS3*	This study

Table 3.1. Cont.

Strain or Plasmid	Descriptive Name	Genotype or Description	Reference or Source
EOY77	*FTR1-GFP npr1Δ bit61Δ*	MCY54 (SEY6210.1, *FTR1-GFP::HISMX*, *NPR1::KanMX6*), *BIT61::TRP1*	This study
EOY78	*FTR1-GFP avo2Δ*	CBY118 (6210.1, *Ftr1-GFP::HISMX*), *AVO2::TRP1*	This study
EOY79	*FTR1-GFP npr1Δ avo2Δ*	MCY54 (SEY6210.1, *FTR1-GFP::HISMX*, *NPR1::KanMX6*), *AVO2::TRP1*	This study
EOY80	*FTR1-GFP bit61Δ*	EOY75 (SEY6210, *BIT61::HIS3*), *FTR1GFP::KanMX*	This study
E. coli			
XL1-Blue		recA1 endA1 gyrA96 thi-1 hsdR17 supE44 relA1 lac [F' proAB laclqZDM15 Tn10(tetr)]	Stratagene (La Jolla, CA)
Plasmids			
pMB241	*IST1-HA*	*URA3* Ap^r (pRS416) *IST1-HA*	(Dimaano et al., 2008)
pMB243	*IST1-GFP*	*URA3* Ap^r (pRS416) *IST1-GFP*	(Dimaano et al., 2008)
pMB409	P*(SNF7)-IST1-HA*	*URA3* Ap^r (pRS416) P*(SNF7)-IST1-HA*	This study
pMB327	P*(CPS1)-IST1-HA*	*URA3* Ap^r (pRS416) P*(CPS1)-IST1-HA*	This study
pJK12	P*(SNF7)-FUR4-GFP*	*TRP1* Ap^r (pRS414) P*(SNF7)-FUR4-GFP*	This study
pJK6	P*(CPS)-FUR4-GFP*	*LEU2* Ap^r (pRS415) P*(CPS1)-FUR4-GFP*	This study

Table 3.1. Cont.

Strain or Plasmid	Descriptive Name	Genotype or Description	Reference or Source
pMB277	P*(GAL)-IST1-HA*	*URA3* Ap^r (pRS416) P(*GAL1*)-*IST1-HA*	(Dimaano et al., 2008)
pCJ50	*DID2-HA*	*HIS3* Ap^r (pRS423) *DID2-HA*	This study
pCD2	*GST-IST1*	Ap^r Kan^r (pGEX-KG) *GST-IST1*	(Dimaano et al., 2008)
pAH32	*GST-DID2(CT)*	Ap^r (pGEX-KG) *GST-DID2(113-204)*	(Shestakova et al., 2010)
pMB63	*GST-VPS4^{E233Q}*	Ap^r (pGEX-KG) GST-*vps4(E233Q)*	(Babst et al., 1998)
pCJ51	*VPS4*	*HIS3* Ap^r (pRS423) *VPS4*	This study
pRS316GFP-Aut7	*GFP-ATG8*	*URA3* Ap^r (pRS316) GFP-ATG8	(Reggiori et al., 2004)
pJV40U	*CRH2-GFP (internal in-frame fusion)*	*URA3* Ap^r (pRS416) CRH2-GFP	(Rodriguez-Pena et al., 2000)
pMC47	*ist1(S244A)-HA*	*URA3* Ap^r (pRS416) *ist1(S244A)-HA*	This study
pMB66	*vps4(E233Q)*	*HIS3* Ap^r (pRS413) *vps4(E233Q)*	(Babst et al., 1998)

Figure 3.2. The MVB Pathway is Instrumental in Maintaining Cellular Viability and Amino Acid Levels During Starvation. (A) Survival of leucine auxotrophic wild-type and mutant strains in YNB (-Leu) over five days. The data show the average of three parallel experiments (+/- standard deviation). (B) Analysis of free cellular amino acid content in leucine auxotrophic wild-type (*leu2Δ*) and *vps4*Δ (*vps4Δleu2Δ*) cells following a shift from YNB Complete Synthetic Medium (CSM) to YNB (-Leu). Charts indicate changes in cellular amino acid content relative to starting conditions. (C) Graphical representation of changes in cellular leucine levels relative to starting point in wild-type and *vps4*Δ cells as shown in (B).

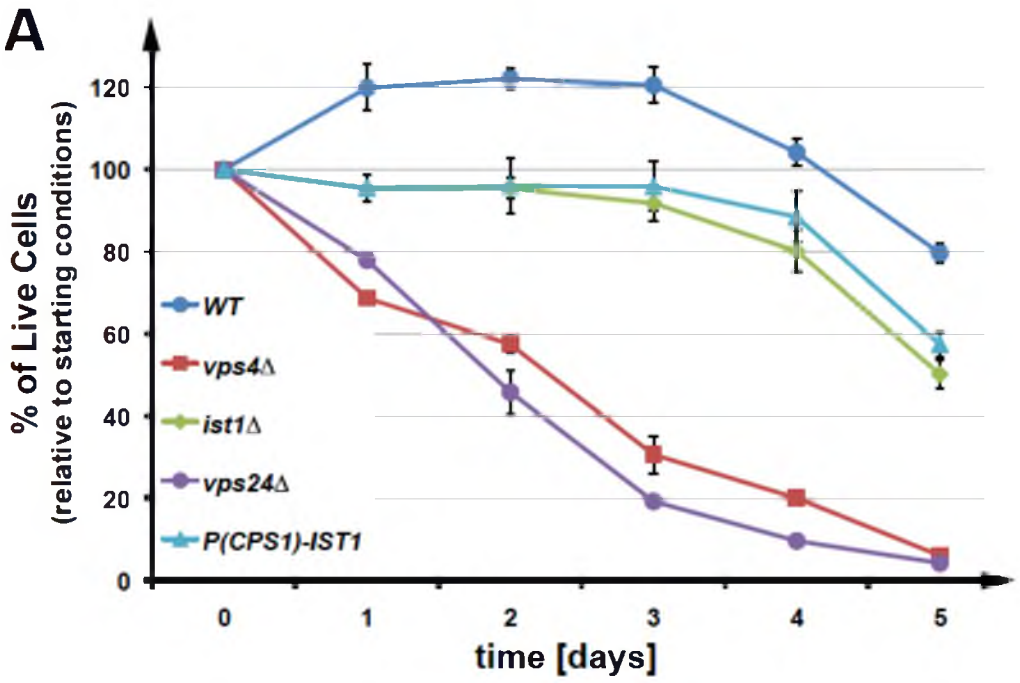
A
% of Live Cells
(relative to starting conditions)
120
100
80
60
40
20
0
WT
vps4Δ
ist1Δ
vps24Δ
P(CPS1)-IST1
0
1
2
3
4
5
time [days]

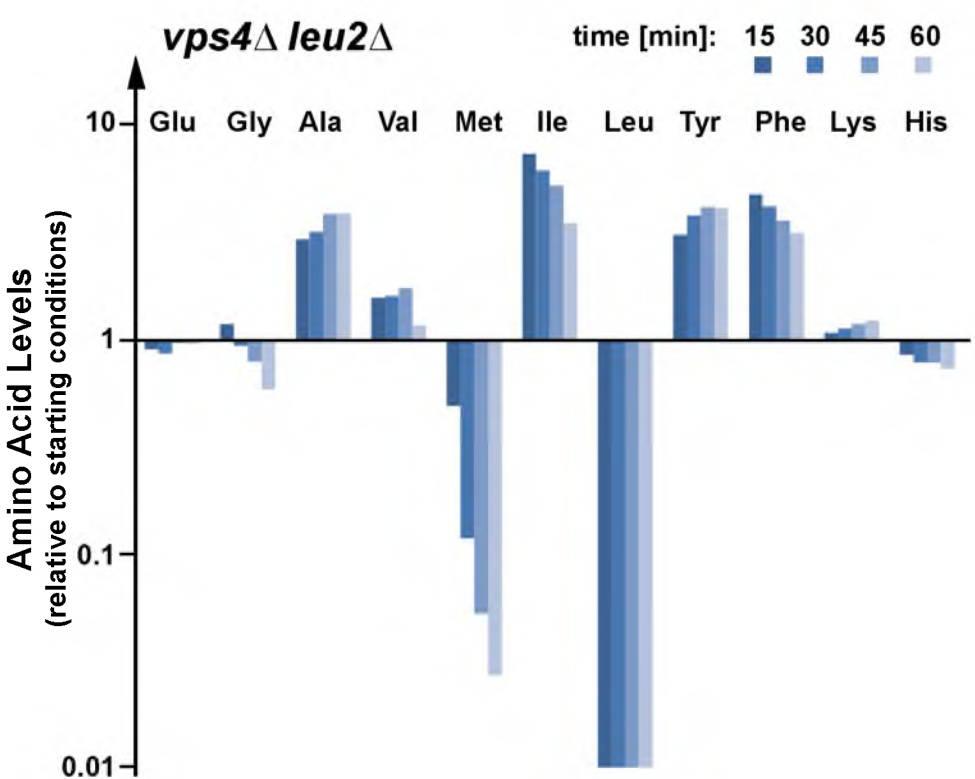

Figure 3.2 Cont.

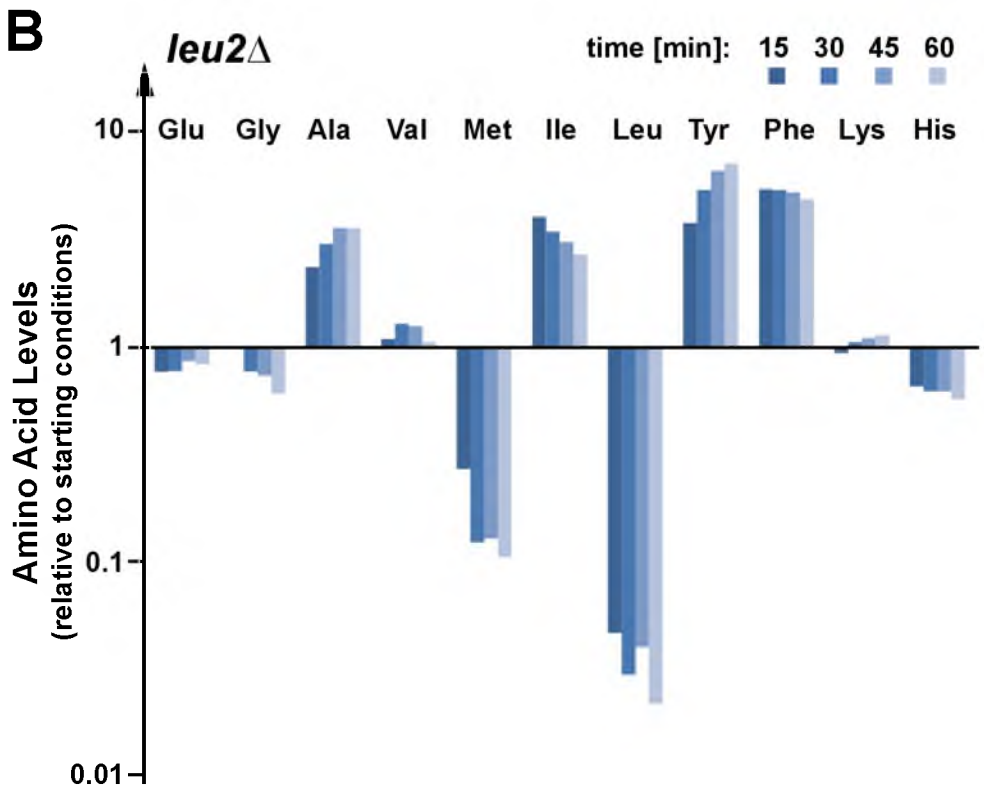
B
leu2Δ
time [min]: 15 30 45 60
Glu Gly Ala Val Met Ile Leu Tyr Phe Lys His
10
1
0.1
0.01
Amino Acid Levels
(relative to starting conditions)

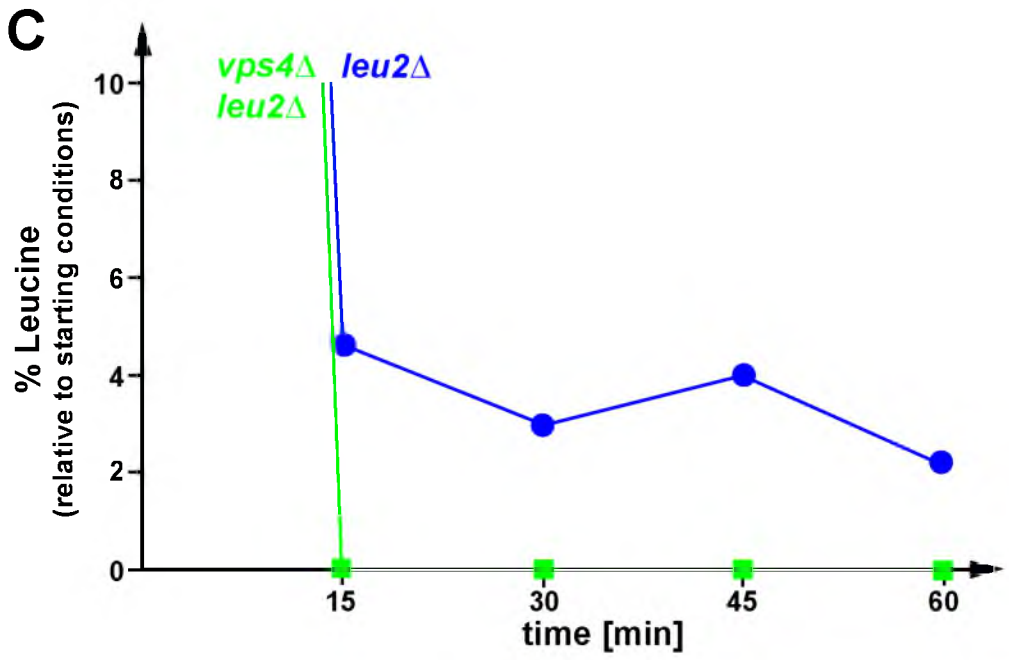

Figure 3.2 Cont.

(Sekito et al., 2008).

This amino acid recycling pathway might play an important role during starvation conditions. To test this hypothesis, wild-type (for ESCRT function) or *vps4*Δ strains, both leucine auxotrophs (*leu2*Δ), were transferred into growth medium lacking leucine, and the cellular concentrations of various free amino acids were determined at different time points. Overall, the starting amino acid levels and the response to leucine starvation was very similar between wild-type and the MVB mutant strain *vps4*Δ (Figure 3.2 B, Table S3.1). The levels of alanine, isoleucine, tyrosine and phenylalanine rapidly increased following leucine starvation, which is likely caused by a broad translational shutdown combined with a continued uptake of these amino acids from the medium. The major difference between the two strains was the extent to which the leucine levels dropped. Wild-type cells maintained 3-5% of the initial leucine concentration, while that of *vps4*Δ cells decreased to not detectable amounts of leucine (Figure 3.2 C), a result that was consistently observed in other independent experiments (Figure S3.2 A). These data indicated that the MVB pathway plays a role in maintaining minimal levels of amino acids during starvation conditions. Interestingly, we observed a dramatic decrease in methionine levels in both strains, though methionine was not limited in the growth medium. Similar decreases in methionine levels were observed in cells starved for lysine (Figure 3.2 A) or histidine (data not shown), suggesting that this drop in free methionine might be part of the starvation response and connected to a block in general translation initiation.

3.3.2 *Ist1 Protein Levels Regulate the MVB Pathway.*

Ist1 has been shown to function in the recruitment of Vps4 to ESCRT-III, suggesting a supportive role for Ist1 in MVB trafficking (Dimaano et al., 2008; Shestakova et al., 2010). However, overexpression of Ist1 results in reduced recruitment of Vps4 to ESCRT-III and a defect in MVB trafficking (Dimaano et al., 2008), suggesting that Ist1 can have both a positive and negative effect on Vps4 activity, depending on Ist1 protein levels. To test this idea, we preformed an *in vitro* 'GST-pull-down' experiment using purified recombinant proteins. Did2 is an important factor in the recruitment of Vps4 due to its interactions with Ist1, Vps4 and ESCRT-III (Shestakova et al., 2010). Therefore, we used the binding of Vps4 to Did2 as readout for recruitment efficiency. For the assay, the C-terminal half of Did2 (GST-Did2(CT), amino acids 113-204), which contains the Vps4 and Ist1 interaction regions, was immobilized on glutathione-sepharose beads. These beads were then incubated with an equal amount of the ATP-locked form of Vps4 ($Vps4^{E233Q}$) in the presence of various concentrations of Ist1. The results indicated that, consistent with previously published data (Shestakova et al., 2010), the addition of an approximate equimolar amount of Ist1 increased the recruitment of Vps4 to Did2 (Figure 3.3 A), likely through the formation of a trimeric Vps4-Ist1-Did2 complex. In contrast, increasing amounts of Ist1 caused a reduction of Did2-associated Vps4 (Figure 3.3 A) suggesting that at higher concentrations, Ist1 might bind to Did2 and Vps4 independently, resulting in the

Figure 3.3. Regulation of Vps4 by Ist1. (A) *In vitro* binding studies using recombinant Vps4(E233Q), Ist1 and GST-Did2(CT) (amino acids 113-204). GST-Did2(CT) was immobilized on GSH-sepharose and an approximately equimolar amount of Vps4(E233Q) was added in the presence of ATP. The Ist1 concentrations were varied from zero to approximately four times the molar amount of Vps4(E233Q). Bound and unbound fractions were analyzed by SDS-PAGE and coomassie staining, and the amount of bound Vps4(E233Q) was determined by densitometric scanning. The obtained values were normalized according to the amount of bound GST-Did2(CT), then plotted relative to the negative control (no GST-Did2(CT) = 0) and the maximum signal (1xIst1 = 1). (B) Survival of wild-type yeast, yeast expressing a dominant-negative version of Vps4 (*vps4E233Q,* pMB66), and yeast with *GAL1*-driven overexpression of Ist1 over a period of 5 days. The data show the average of three parallel experiments (+/- standard deviation). (C) Steady state localization of three permeases, Ftr1-GFP (iron), Fur4-GFP (uracil), and Can1-GFP (arginine) after extended exponential phase growth in WT and *ist1Δ* cells. Images were inverted for better visualization (brightest GFP signal appears black).

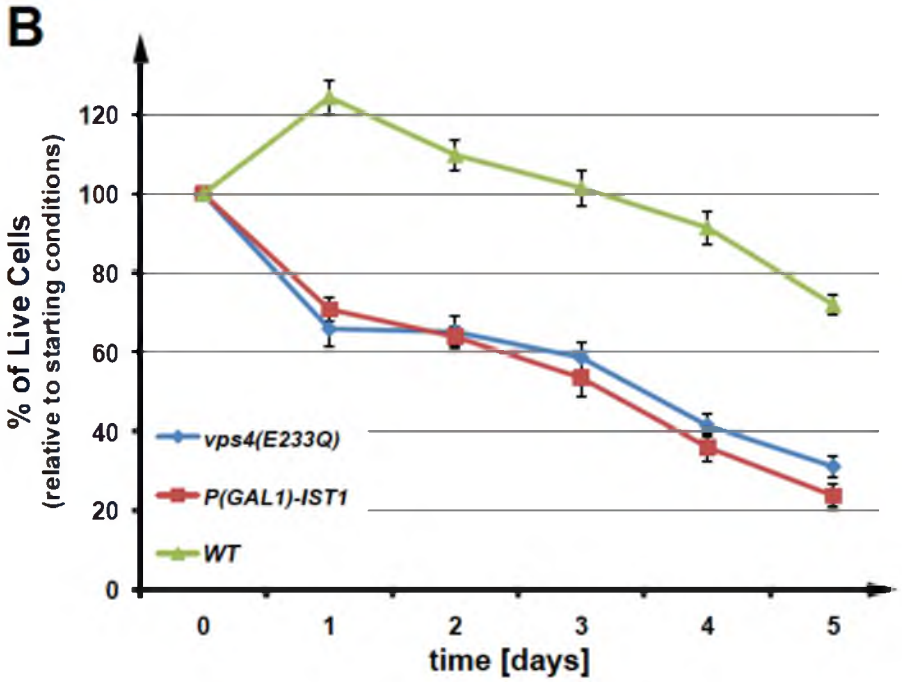
B
% of Live Cells
(relative to starting conditions)
120
100
80
60
40
20
0
vps4(E233Q)
P(GAL1)-IST1
WT
0
1
2
3
4
5
time [days]

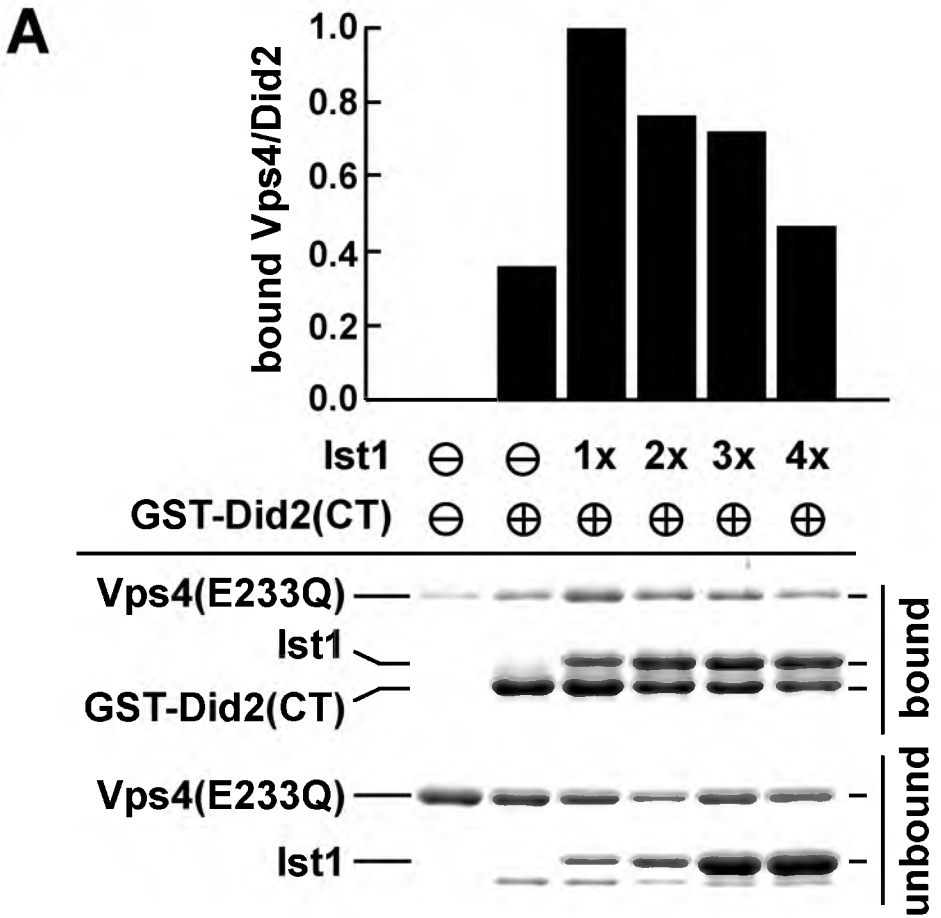
A
bound Vps4/Did2
1.0
0.8
0.6
0.4
0.2
0.0
Ist1 ⊖ ⊖ 1x 2x 3x 4x
GST-Did2(CT) ⊖ ⊕ ⊕ ⊕ ⊕ ⊕
Vps4(E233Q)
Ist1
GST-Did2(CT)
bound
Vps4(E233Q)
Ist1
unbound

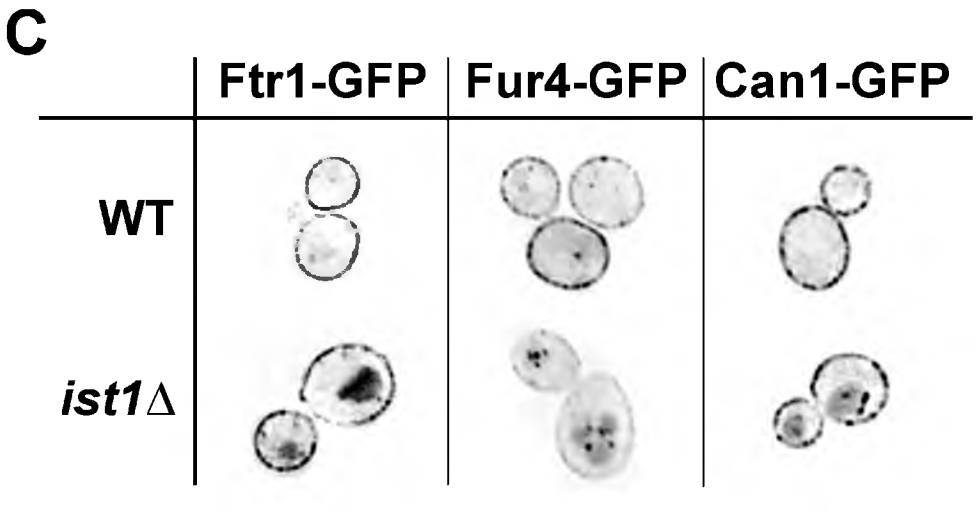

Figure 3.3 Cont.

formation of Did2-Ist1 and Ist1-Vps4 complexes that inhibit the formation of the trimeric complex. This effect of Ist1 on Vps4 recruitment to GST-Did2 was consistently observed in other independent pulldown assays, although the Ist1 concentration necessary to affect the Vps4-Did2 interaction varied (Figure S3.2 B). These variations are likely due to the tendency of Ist1 to oligomerize/aggregate (Bajorek et al., 2009b), thereby changing the concentration of soluble Ist1 protein in the *in vitro* assay. These *in vitro* observations are consistent with the altered endosomal recruitment of Vps4 when Ist1 protein levels are elevated *in vivo* (Dimaano et al., 2008).

Additional support for this regulatory model comes from the observation that artificially high cellular levels of Ist1 induced by using a *GAL1* promoter (p*GAL1*-Ist1-HA), resulted in loss of viability during leucine starvation (Figure. 3.3 B). This drop in viability was similar to the drop observed in cells expressing the dominant-negative mutant *vps4(E233Q)*, which renders the MVB pathway nonfunctional (Babst et al., 1998). In comparison to the data shown in 3.1 A, this viability assay was performed using a different yeast strain (W303) and a different carbon source (galactose).

Analysis of cell-surface protein trafficking indicated that Ist1 protein levels in exponentially growing cells have a negative regulatory effect on the MVB pathway. GFP-tagged versions of the plasma membrane proteins Ftr1 (iron transporter), Fur4 (uracil transporter) and Can1 (arginine transporter) showed obvious vacuolar staining when expressed in cells deleted for *IST1*, whereas no vacuolar signal was observed in wild-type cells (Figure 3.3 C). These

observations suggested that loss of Ist1 caused increased downregulation of plasma membrane proteins, likely due to increased MVB pathway activity in these mutant cells.

We analyzed Ist1 protein levels in growing cells by Western blot using a functional HA-tagged version of Ist1. The data showed that Ist1-HA levels change dramatically with growth conditions (Figure 3.4 A). Ist1 levels increased at low cell densities, peaked during exponential growth and then fell to barely detectable levels as cells entered stationary phase. In contrast, the concentration of the control protein Snf7 (ESCRT-III subunit), showed only minor changes during the different growth phases of the cells. The drop in Ist1 levels coincided with the end of the growth phase and an increase in phosphorylated translation-initiation factor eIF2 (time = 6h, Figure 3.4 A). Phosphorylation of eIF2 at the α-subunit has been shown to block general protein translation in response to amino acid starvation (Sonenberg and Hinnebusch, 2009), suggesting that starvation might have caused the decrease in Ist1 levels. Consistent with this idea, free amino acid analysis of the same samples revealed a sharp drop in cellular lysine levels after 6 hours of growth, which occurred concurrently with a marked decline in Ist1 levels (red-marked time point in Figure 3.4 A). The yeast strain used for the experiment is a lysine-auxotroph, and after approximately 6 hours of growth, the lysine provided by the medium was depleted (Figure 3.4 A, bottom panel), causing the induction of starvation response pathways. The resulting changes in the levels of other tested amino acids were similar to those observed during leucine starvation (Figure 3.2 B).

Figure 3.4. Ist1 Protein Levels Mirror the Translational Activity of the Cell. (A) Time-course samples analyzed by Western blot to detect HA-tagged Ist1 protein levels (expressed from pMB241) and levels of phospho-eIF2α in MBY63 grown in YNB (-Ura) medium. Snf7 is a loading control. The same samples were analyzed for free amino acid content to track changes relative to starting conditions throughout growth. Red bar indicates the transitional point at hour six, wherein cellular free lysine levels drop dramatically, Ist1 protein levels begin to decline, and phosphorylation of eIF2α increases. (B) Western blot analysis and quantitative RT-PCR performed on samples collected over a 10 hour period encompassing the entire yeast growth curve (black trendline shows OD_{600} of culture). The strain contains a genomically integrated *HA*-tag downstream of the native *IST1* locus. Snf7 is a loading control. Blue trendline shows *IST1* mRNA levels relative to actin. Red line represents densitometric quantitation of Ist1-HA protein levels from the blot shown (relative to Snf7, an ESCRT-III subunit) showed only minor changes during the different growth phases of the cells.

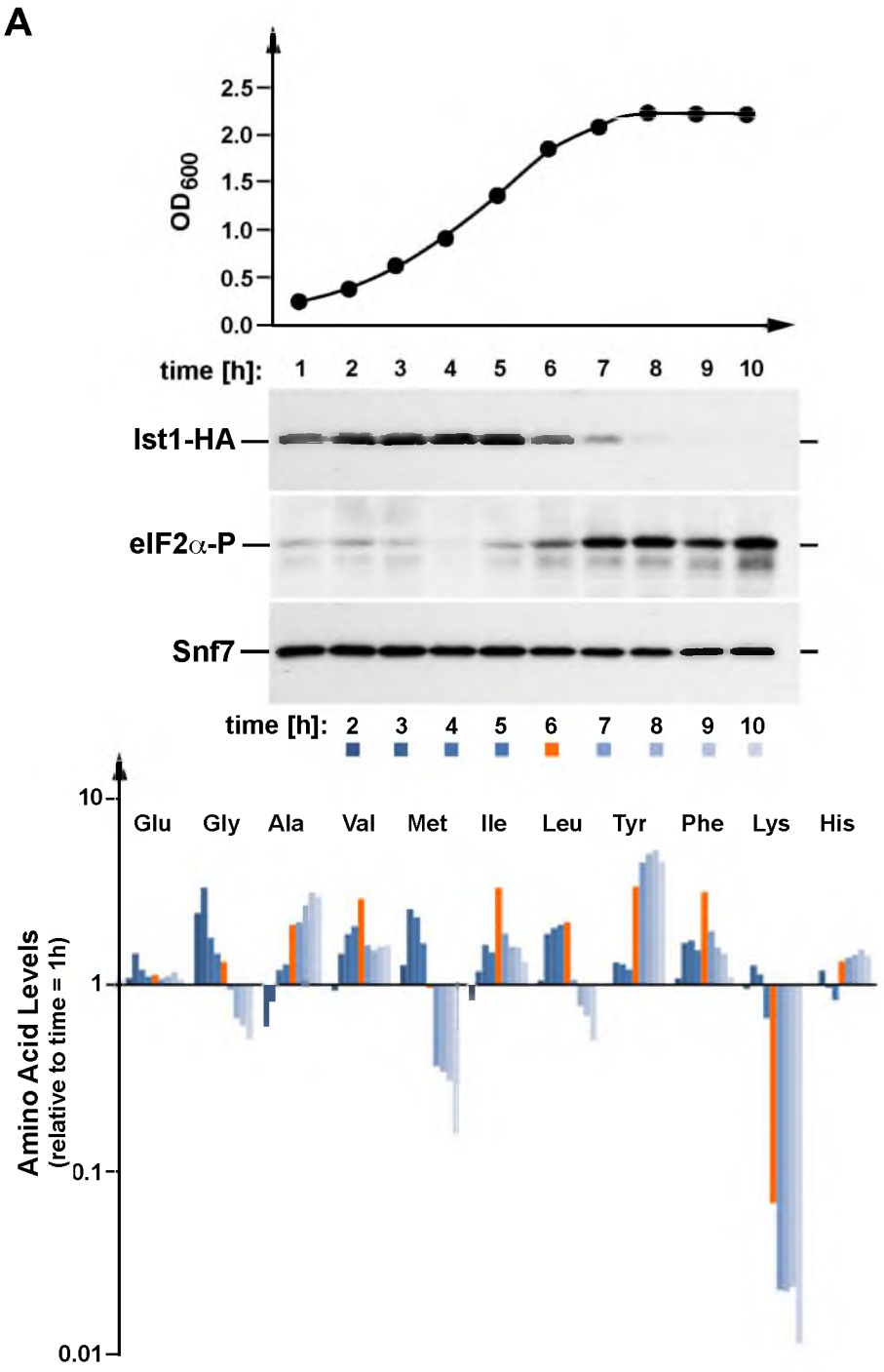
A
2.5
2.0
1.5
1.0
0.5
0.0
OD600
time [h]: 1 2 3 4 5 6 7 8 9 10
Ist1-HA
eIF2α-P
Snf7
time [h]: 2 3 4 5 6 7 8 9 10
10
1
0.1
0.01
Amino Acid Levels
(relative to time = 1h)
Glu Gly Ala Val Met Ile Leu Tyr Phe Lys His

Figure 3.4 Cont.

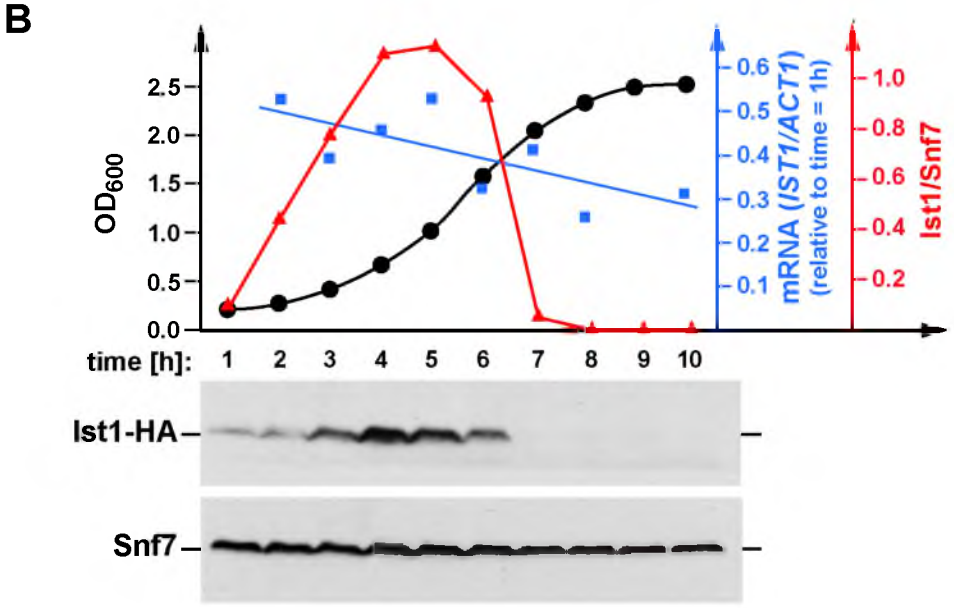
B
OD600
2.5
2.0
1.5
1.0
0.5
0.0
mRNA (IST1/ACT1)
(relative to time = 1h)
0.6
0.5
0.4
0.3
0.2
0.1
Ist1/Snf7
1.0
0.8
0.6
0.4
0.2
time [h]: 1 2 3 4 5 6 7 8 9 10
Ist1-HA
Snf7

To identify the mechanism responsible for regulating Ist1 protein levels, the growth-dependent Ist1 expression analysis was repeated using a strain containing a genomically integrated *HA*-tag immediately downstream from the *IST1* locus. This strain was grown in YNB Complete Synthetic Medium (CSM). Samples were taken every hour and analyzed by Western blot for the presence of Ist1-HA, phospho-eIF2α and Snf7. Furthermore, quantitative RT-PCR was performed to determine the amount of *IST1-HA* mRNA relative to the control mRNA of the actin gene *ACT1* (Figure 3.4 B). The results showed growth-dependent levels of Ist1-HA, eIF2α-P and Snf7 similar to the patterns observed in the experiment of Figure 3.2 A, which used plasmid-encoded *IST1-HA*. In contrast to the Ist1 protein levels, the relative amount of *IST1-HA* mRNA exhibited only minor changes during growth of the yeast culture, indicating that Ist1 levels are not transcriptionally controlled; rather, they are likely regulated at the level of protein translation and/or degradation.

The rate of Ist1 degradation was determined by adding the translational inhibitor cycloheximide to cells and monitoring Ist1 levels over time by Western blot. The strains used for these experiments were deleted for the multidrug transporter Pdr5 to enhance the effect of the proteasomal inhibitor MG132. The results showed that in cells treated with cycloheximide, Ist1-HA was almost completely degraded within two hours; whereas, the control protein Snf7 (ESCRT-III subunit) remained stable during the same time period (Figure 3.5 A, lanes 1-3). The addition of the proteasomal inhibitor MG132 partially stabilized Ist1-HA (Figure 3.5 A, lanes 4-6). In contrast, no change in Ist1-HA turnover was

Figure 3.5. Ist1 is Degraded by the Proteasome, and its Levels Drop Dramatically During Starvation Conditions. (A) Ist1-HA protein levels (expressed from pMB241) of exponentially growing cells (OD_{600} = 0.7) were analyzed at intervals following cycloheximide addition in *pdr5Δ*, *pdr5Δvps4Δ*, and *pep4Δprb1Δ* cells in the presence or absence of the proteasomal inhibitor MG132. Snf7 is a loading control. (B) Subcellular fractionation of wild-type cells overexpressing Ist1 (pMB277) into soluble [S] and membrane-associated pellet [P] fractions and detection via Western Blot. (C) Western blot detection of Ist1 protein degradation of under different conditions. All treatments and collections were performed on exponentially growing cells. Individual sets (1-4) were obtained with parallel sample collection, preparation, and film exposure to ensure comparability. Snf7 serves as a loading control. P*(SNF7)-IST1-HA* and P*(CPS1)-IST1-HA* refer to non-endogenous promoters driving *IST1-HA* expression. *2μ VPS4* and *2μ DID2* indicate strains overexpressing the corresponding proteins Vps4 and Did2, respectively, using a high-copy vector.

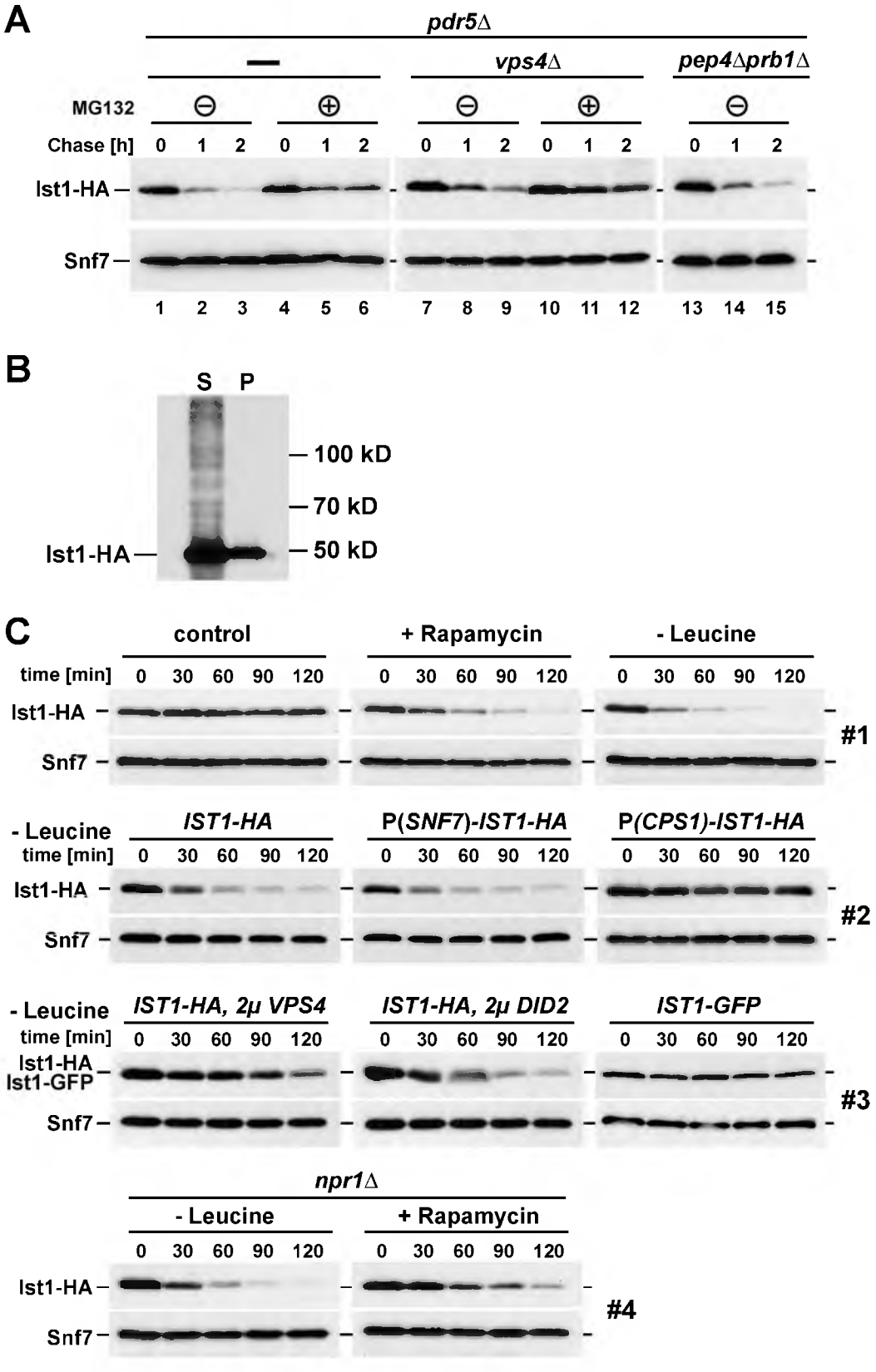
A
pdr5Δ
—
vps4Δ
pep4Δprb1Δ
MG132
⊖
⊕
Chase [h]
0 1 2 0 1 2 0 1 2 0 1 2 0 1 2
Ist1-HA
Snf7
1 2 3 4 5 6 7 8 9 10 11 12 13 14 15
B
S P
100 kD
70 kD
50 kD
Ist1-HA
C
control
+ Rapamycin
- Leucine
time [min]
0 30 60 90 120
Ist1-HA
Snf7
#1
- Leucine
IST1-HA
P(SNF7)-IST1-HA
P(CPS1)-IST1-HA
#2
- Leucine
IST1-HA, 2μ VPS4
IST1-HA, 2μ DID2
IST1-GFP
Ist1-HA
Ist1-GFP
#3
npr1Δ
- Leucine
+ Rapamycin
#4

observed in cells lacking Pep4 and Prb1, two proteases that play a key role in vacuolar protein degradation (Figure 3.5 A, lanes 13-15). These results indicated that Ist1-HA is rapidly degraded, and the proteasome rather than the MVB pathway mediates that turnover.

We observed a decreased rate of Ist1-HA degradation in cells deleted for *VPS4* (Figure 3.5 A, lanes 7-9), a mutation that causes the accumulation of Ist1 at the endosome with ESCRT-III (Dimaano et al., 2008). This stabilization effect was even more pronounced in *vps4Δ* cells that were treated with MG132 (Figure 3.5 A, lanes 10-12). These results suggested that predominantly the soluble pool of Ist1, not the membrane associated pool, is targeted for degradation by the proteasome. This is further supported by fractionation studies in cells overexpressing Ist1-HA with a *GAL1* promoter. Western blot analysis of these fractions showed a banding pattern of soluble (S) Ist1-HA reminiscent of polyubiquitination, whereas Ist1-HA modification was not observed in the membrane-associated pellet fraction (P, Figure 3.5 B).

The observed drop in Ist1 levels as cells enter stationary phase (Figure 3.5) suggested that starvation conditions might result in the loss of Ist1 protein. To test this idea, we followed yeast Ist1-HA levels by Western blot during acute starvation. Starvation conditions were induced by either transferring cells to growth medium lacking leucine or by adding rapamycin, a drug that blocks the kinase activity of the TORC1 complex. In contrast to the non-treated control samples, both leucine starvation and rapamycin addition resulted in the rapid disappearance of Ist1 (Figure 3.5 C, set 1). This rapid drop in Ist1-HA levels was

also observed when Ist1-HA was expressed from the constitutive *SNF7* promoter (the promoter driving expression of the control protein Snf7), further support that Ist1 levels are not transcriptionally regulated (Figure 3.5 C, set 2). In contrast, a fusion of *IST1-HA* to the 5' UTR region of *CPS1* resulted in stable Ist1-HA protein levels during leucine-starvation (Figure 3.5 C, set 2). The expression of the vacuolar hydrolase Cps1 is upregulated during starvation conditions, indicating that Cps1 belongs to a set of proteins that is efficiently translated during these stress conditions (Bordallo and Suarez-Rendueles, 1993). Together, the results suggested that the observed drop in Ist1 levels during starvation is mainly caused by general translational repression in combination with the intrinsically rapid turnover rate of the protein, despite the lack of a degradation sequence like the PEST sequence. We predicted that the starvation-induced drop in Ist1 levels increases the efficiency of the MVB pathway and thus increases the recycling of amino acids required for the stress-response pathways. Consistent with this idea, we observed diminished fitness in starving cells that maintain artificially high levels of Ist1 due to the *CPS1* promoter fusion (P(*CPS1*)-*IST1*, Figure 3.2 A).

C-terminally GFP-tagged Ist1 (Ist1-GFP) did not exhibit a starvation-induced drop in protein levels (Figure 3.5 C, set 3). This result suggested that the large, C-terminal GFP domain might interfere with the degradation of Ist1. Interestingly, the C-terminal region of Ist1 contains a cluster of lysine residues that could be targeted for ubiquitination. Rsp5 is the principle ubiquitin ligase acting in endocytosis and the MVB pathway. However, starvation-induced degradation of Ist1 was found to be independent of Rsp5 function (Figure S3.1

A). Similarly, mutation of a reported Ist1 C-terminal phosphorylation site (Gruhler et al., 2005), showed no effect on the rapid degradation of the protein during starvation (Ist1(S244A), Figure S3.1 A). Finally, microscopy of Ist1-GFP-expressing cells showed no obvious change in Ist1 localization during acute starvation (Figure S3.1 B). Therefore we found that neither Rsp5, nor some unidentified kinase mediates the degradation of Ist1. Also, the degradation is not attributable to a change in Ist1 localization following starvation.

Because the lysine-rich C-terminus of Ist1 contains the Vps4-interaction domain, we tested whether high levels of Vps4 would also stabilize the Ist1 protein. The experiment demonstrated that overexpression of Vps4 (expressed from a 2μ high copy vector) was indeed able to inhibit the starvation-induced degradation of Ist1-HA. In contrast, overexpression of Did2, which binds to the N-terminal region of Ist1, had only a minor effect on the Ist1 degradation rate (Figure 3.5 C, set 3). In summary, our analysis suggested that soluble, non-Vps4-associated Ist1 was targeted for proteasomal degradation through ubiquitination of the C-terminal domain. This degradation, together with decreased translation, resulted in the observed rapid loss of Ist1 following the induction of starvation-response pathways.

3.3.3 *Starvation Induces Downregulation of Plasma Membrane Proteins*

We investigated the effect of starvation on Ftr1-GFP trafficking using fluorescence microscopy. Within 45 minutes of either leucine starvation or rapamycin addition, we observed the relocalization of Ftr1-GFP from the plasma

membrane to vacuole-proximal compartments, likely late endosomes, and to the vacuolar lumen (Figure 3.6 A). A similar Ftr1-GFP relocalization was observed when cells were treated with high concentrations of iron, which causes substrate-dependent downregulation and has been described previously (Felice et al., 2005; Strochlic et al., 2008). Consistent with the microscopy data, Western blot analysis showed the emergence of a smaller GFP protein band (~25 kD) following starvation, which is likely an intermediate in the vacuolar degradation of Ftr1-GFP (Figure 3.6 B). Quantitative analysis of the Western blot data indicated a loss of 10-30 percent of Ftr1-GFP within two hours of starvation (data not shown). These results suggested that starvation induced the rapid endocytosis of Ftr1-GFP and its delivery to the vacuole for degradation. Cells deleted for *IST1* still showed increased Ftr1-GFP turnover with starvation (Figure 3.6 B), suggesting that the starvation-response not only upregulates the MVB pathway via Ist1 degradation, but also increases the efficiency of endocytosis through an unknown mechanism.

The starvation-induced internalization was not limited to Ftr1 but was also observed with the arginine transporter Can1 (Figure S3.2 A). Furthermore, previous studies have shown starvation-induced downregulation of Fur4 (uracil transporter, (Galan et al., 1994), Tat2 (tryptophane transporter, (Beck et al., 1999), Mal61 (maltose transporter, (Penalver et al., 1998), Bap2 (amino acid transporter, (Omura et al., 2001) and Hxt17 (glucose transporter, (Krampe and Boles, 2002). These data suggested that amino acid starvation might cause a broad endocytic response that results in rapid internalization and degradation of

Figure 3.6. Starvation Conditions Cause Downregulation of Ftr1. (A) Localization of Ftr1-GFP in exponentially growing cells with no treatment (con.) or after 45 minutes of rapamycin treatment (+Rap.), leucine starvation (-Leu), or iron treatment (+Fe^{2+}, 0.5 mM) in wild-type cells, cells expressing an *rsp5* mutant allele (*rsp5-1*), or *npr1Δ cells*. 'Minus' (-) designates minimal internalization of Ftr1, 'plus' (+) designates heightened internalization and accompanying late endosomal/vacuolar staining. (B) Time-course Western blot analysis of Ftr1-GFP stability with amino acid starvation (-Leu, -Trp) or rapamycin treatment (+Rap.) in WT, *ist1Δ*, cells expressing defective Rsp5 (*rsp5-1*, this strain is a leucine-autotroph and thus tryptophan-depletion is used for starvation), or *npr1Δ* cells. Blots show full length Ftr1-GFP, free GFP (cleaved from chimera in vacuole), and Snf7 as a loading control. (C) Western blot analysis of eIF2α phosphorylation upon rapamycin-treatment of wild-type and *npr1Δ* cells using a phospho-specific antibody.

A

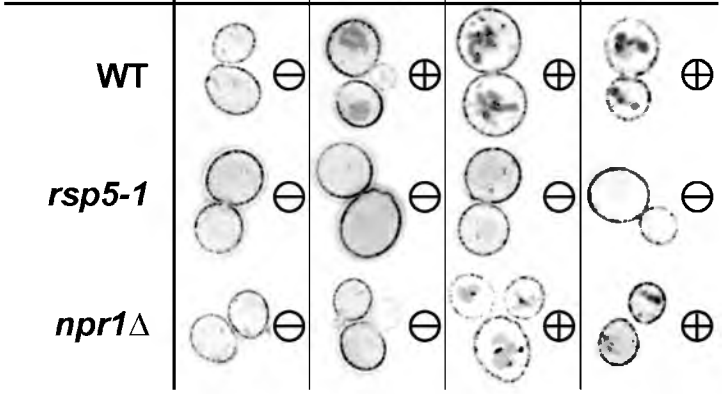

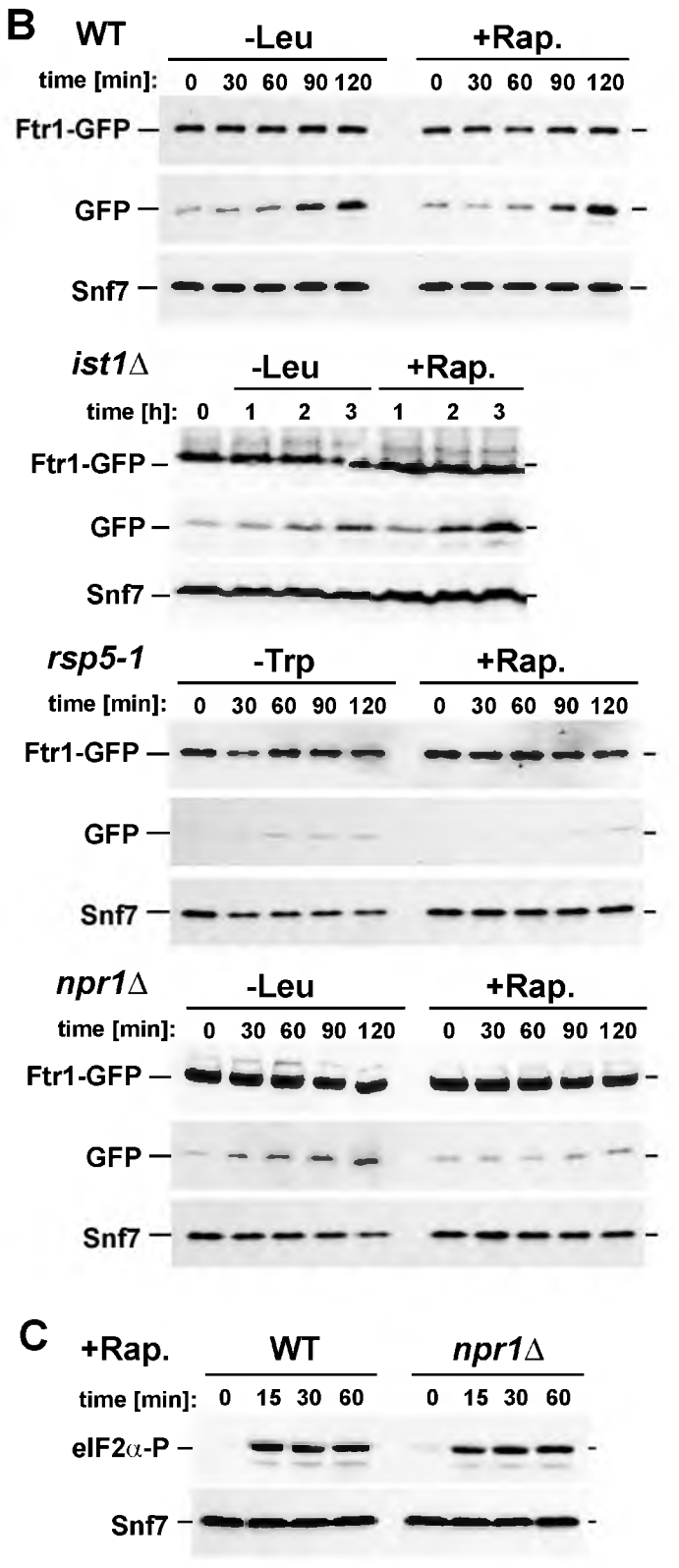

Figure 3.6 Cont.

multiple plasma membrane proteins. However, starvation does not induce non-specific, bulk-flow endocytosis, as rapamycin treatment did not increase the internalization of the GPI-anchored protein Crh2-GFP (Figure S3.2 B).

Rapid degradation of Ftr1 under starvation conditions was dependent on the function of Rsp5, the same ubiquitin-ligase associated with downregulation of Ftr1 in high iron concentrations (Strochlic et al., 2008). Both microscopy and Western blot analysis indicated that cells expressing the *rsp5-1* mutant allele (defective in ubiquitin conjugation) are deficient in the starvation-induced degradation of Ftr1-GFP, irrespective of the type of starvation (Figure 3.6 A and B). This Rsp5-dependence suggested that starvation conditions might simply upregulate the same machinery that normally regulates Ftr1 endocytosis.

Addition of rapamycin or depletion of leucine resulted in similarly increased protein internalization (Figure 3.6 A and B), suggesting that TORC1 might be the key regulator for the endocytic effects observed during both treatments. The TORC1 downstream kinase Npr1 has been implicated in the regulation of membrane protein trafficking (De Craene et al., 2001; Kamura et al., 2001). Therefore, we tested whether Npr1 was required for Ftr1 internalization during acute starvation by analyzing Ftr1-GFP trafficking in a *NPR1* deletion strain. The result showed that rapamycin-induced endocytosis of Ftr1 was delayed in *npr1*Δ cells. However, leucine-starved *npr1*Δ cells showed Ftr1 internalization similar to wild-type cells (Figure 3.6 A and B). Similar results were obtained with Can1-GFP expressed in *npr1*Δ (Figure S3.2 A).

These findings indicated the presence of at least two systems that regulate the nutrient-dependent degradation of Ftr1 and Can1. One system is regulated by TORC1 and its downstream kinase Npr1. A second system is induced by amino acid deficiency and causes downregulation in a TORC1-independent manner. Deletion of *NPR1* had no effect on rapamycin-induced phosphorylation of eIF2α (Figure 3.6 C) and showed only a slight delay in the starvation-induced drop in Ist1 levels (Figure 3.5 C, set 4), suggesting that Ist1 does not have a primary role in Npr1-dependent regulation of protein trafficking. We also analyzed Ftr1-GFP internalization following treatment with cycloheximide in wild-type and Δ*npr1* cells (Figure S3.3). The results showed Ftr1-GFP internalization in *Δnpr1* cells was similar to wild-type cells following cyclohexamide treatment. Cycloheximide stalls ribosomes during translation, simulating tRNA depletion or amino acid depletion. The internalization of Ftr1-GFP following cycloheximide treatment in the *Δnpr1* result is in agreement with our conclusion that a TORC1-indepenent pathway causes the downregulation of Ftr1-GFP following both leucine starvation or cycloheximide treatment in *Δnpr1* cells.

An obvious candidate for the TORC1-independent regulation of the endocytic pathway is the rapamycin-insensitive TORC2 complex. Because deletion of the Tor2 kinase is lethal, we analyzed the starvation response in cells lacking the nonessential TORC2 subunits Avo2 or Bit61. Deletion of either *AVO2* or *BIT61* increased Ftr1 downregulation even under rich medium conditions, a phenotype that was lost when combined with a deletion of *NPR1* (*npr1*Δ*avo2*Δ,

*npr1*Δ*bit61*Δ; Figure 3.7 A). Furthermore, leucine-starvation increased Ftr1 downregulation in both single- and double-mutant strains (*avo2*Δ, *bit61*Δ, *npr1*Δ*avo2*Δ, *npr1*Δ*bit61*Δ; Figure 3.7 A). These data suggested that TORC2 mutations likely impact downregulation of plasma membrane proteins via TORC1 and Npr1, and that TORC2 does not represent the TORC1-independent system regulating endocytosis.

3.3.4 *Autophagy Is Not Blocked in Yeast ESCRT Mutants*

Recent studies in mammalian cells showed that loss of ESCRT function impairs fusion of autophagosomes with lysosomes, thereby impeding degradation of autophagic cargo (Lee et al., 2007; Rusten et al., 2007). To test if the observed starvation-response defect in yeast ESCRT mutant strains (Figure 3.2 A) is caused by a block in autophagy, we analyzed both the starvation-induced and starvation-recovery expression and degradation of GFP-tagged Atg8 and in wild-type and *vps4*Δ cells. Atg8 is highly expressed under starvation conditions, where it functions in the formation of autophagosomes and is subsequently degraded in the lysosome. Therefore GFP-Atg8 is a useful tool to study both induction and functionality of the autophagy pathway (Reggiori et al., 2004). For the starvation-induced analysis, we grew wild-type and *vps4*Δ cells expressing GFP-Atg8 continuously for 1 day to ensure steady-state conditions, then induced starvation by transferring the cells into medium lacking leucine. We analyzed samples at time zero and after 2 hours of starvation by fluorescence microscopy and anti-GFP Western blot (Figure 3.7 B and C). For the recovery analysis, we grew wild-type and *vps4Δ* overnight (12 hours). At time zero, we

Figure 3.7. TORC2 Does Not Mediate Starvation-Induced Downregulation of Ftr1; Autophagy is Not Inhibited in ESCRT Mutants. (A) Localization of Ftr1-GFP in the TORC2-deletion mutants *avo2Δ* and *bit61Δ* singly, or in combination with deletion of *NPR1* under normal conditions (con.) and following 1 hr. of leucine starvation. 'Minus' (-) designates minimal internalization of Ftr1, 'plus' (+) designates heightened internalization and accompanying late endosomal/vacuolar staining. (B) Wild-type and *vps4*Δ cells expressing GFP-Atg8 were starved for leucine at time = 0 following 24 hours of continuous growth. Samples were taken at indicated time points and analyzed by anti-GFP Western blot. (C) Fluorescence microscopy of the cells used for the Western blot analysis shown in B. The amount of GFP-Atg8 and its GFP-containing degradation product were determined based on the Western blot shown in B and two other Western blots performed in parallel experiments (amounts are shown relative to loading control Snf7, +/- standard deviation). (D) Cells were grown overnight for 12 hours. At time zero, cells were diluted to OD=0.2 in selective media. Samples were analyzed by anti-GFP Western blot.

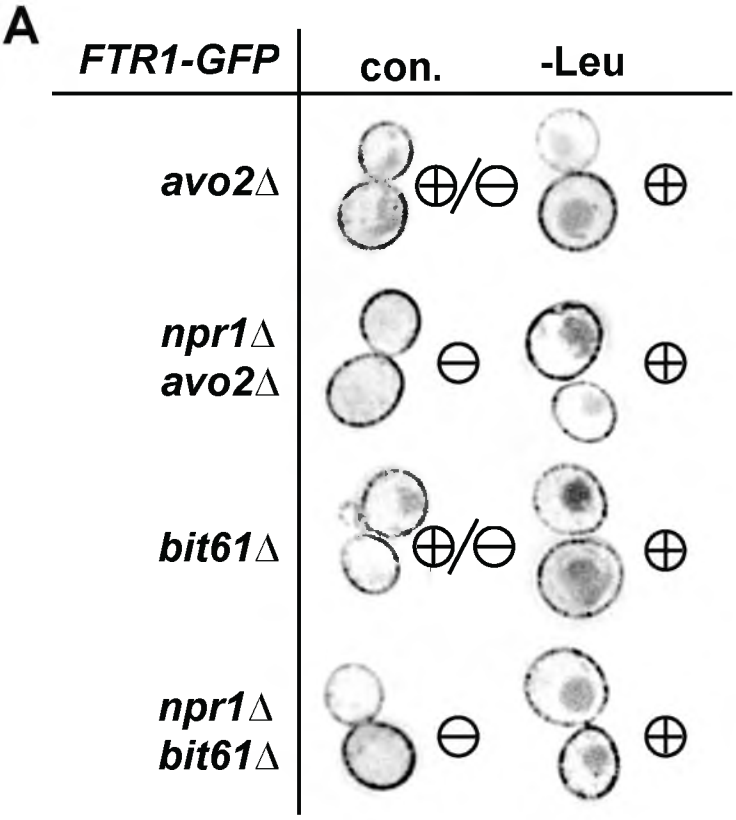
A
FTR1-GFP
con.
-Leu
avo2Δ
⊕/⊖
⊕
npr1Δ
avo2Δ
⊖
⊕
bit61Δ
⊕/⊖
⊕
npr1Δ
bit61Δ
⊖
⊕

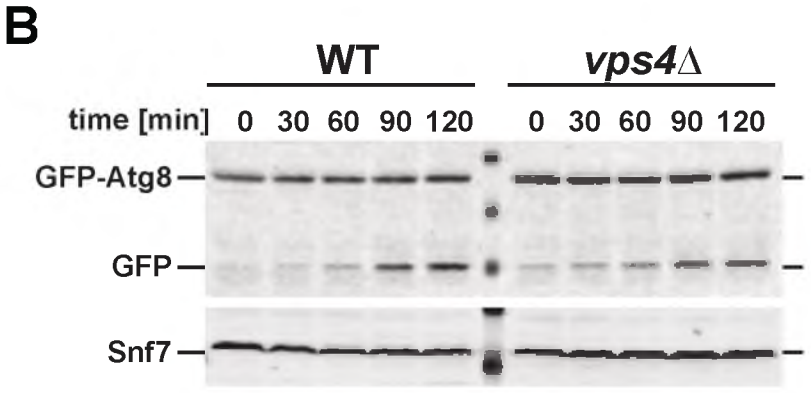
B
WT
vps4Δ
time [min]
0 30 60 90 120
0 30 60 90 120
GFP-Atg8
GFP
Snf7

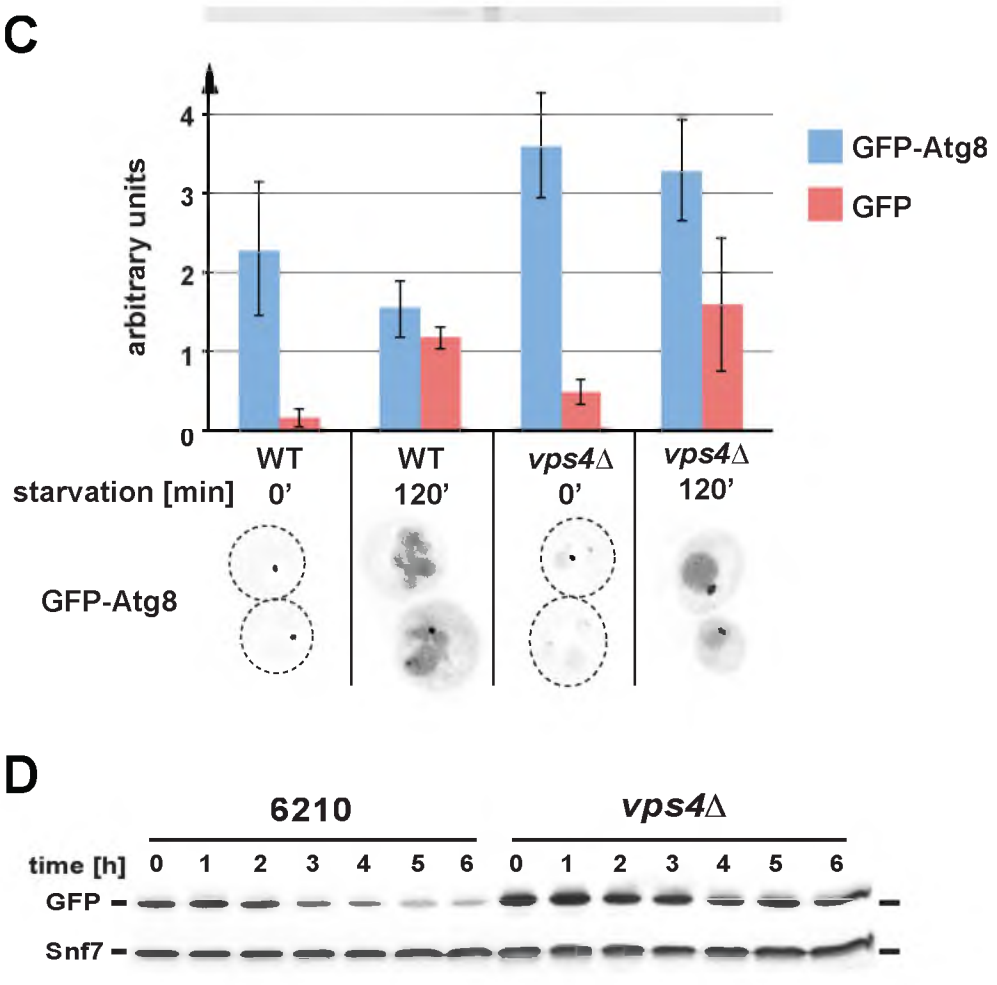

Figure 3.7 Cont.

diluted cells in fresh medium. Samples were analyzed at time zero and every hour after for 6 hours by anit-GFP Western blot. The results of amino acid-induced starvation showed that within 2 hours of starvation both strains accumulated a stable intermediate of GFP-Atg8 degradation in the vacuole. This observation indicated that the efficiency of autophagy induction and execution was similar in both strains. However, *vps4Δ* cells showed increased levels of GFP-Atg8 and the stable intermediate before starvation, suggesting that ESCRT mutants might exhibit a low-level autophagic response under normal growth conditions. The results of starvation recovery (Figure 3.7 D) showed that wild-type cells recovered from starvation in 5 hours, whereas *vps4Δ* cells showed no recovery after 6 hours. This result suggests that the autophagy pathway is highly active and stays active longer in *vps4Δ* than wild-type cells.

Taken together, the data demonstrated that, unlike mammalian cells, yeast does not require MVBs for a functional autophagy pathway. Rather, the deletion of the MVB pathway requires the activity of the autophagic pathway to recover from starvation. Therefore, the observed phenotypes in the starvation response of ESCRT mutants are likely a direct consequence of a defective MVB pathway. The role of the MVB pathway in the degradation of membrane proteins is well established (Piper and Katzmann, 2007). The MVB pathway delivers these proteins into the lumen of vacuoles/lysosomes where they are degraded by hydrolases. Resident transporters at the vacuolar membrane pump the resulting amino acids into the cytoplasm for reuse in protein synthesis. Here we

demonstrate that this recycling pathway provides a vital source of amino acids for the cell during starvation conditions.

3.4 *Discussion*

Our studies indicated that yeast cells have a very limited storage capacity for amino acids, and, as a consequence, amino acid levels drop rapidly during starvation (<15 minutes). Furthermore, we found that the MVB pathway plays an important role in maintaining minimal amino acid levels during starvation, which explains the rapid loss of viability of ESCRT mutants when starved for amino acids (Figure 3.2). Similarly, studies in mammalian cells have shown a role for the proteasomal degradation pathway in maintaining amino acid levels during acute starvation (Vabulas and Hartl, 2005). Thus, both of the major protein degradation systems, the proteasome and the MVB pathway, provide an immediate source of amino acids when limitations occur. These amino acids allow for synthesis of starvation-response proteins, which are vital for the cell to adapt to stress conditions. Such proteins include vacuolar hydrolases and components of the autophagy pathway. Full induction of autophagy requires hours, during which requisite autophagic proteins must be synthesized (Kirisako et al., 1999; Kuma et al., 2004). Therefore, during acute starvation, the MVB pathway and the proteasome serve to maintain translational capability until the major starvation response system, autophagy, is fully active. Similarly, during recovery from starvation, the MVB pathway provides a cache of amino acids enabling quick recovery, as evidenced by the long recovery time of the MVB mutant.

We found that activity of the MVB pathway can be modulated according to metabolic conditions through changes in the cellular concentration of Ist1, a protein that binds to the essential ESCRT factor Vps4 (Figure 3.4). Exponentially growing cells have high Ist1 levels; whereas, cells approaching stationary phase show a dramatic decrease in Ist1 levels. Our model predicts that low cellular Ist1 concentrations promote efficient Vps4 recruitment to endosomes in the form of a trimeric Vps4-Ist1-Did2 complex, whereas high Ist1 levels promote the formation of binary Vps4-Ist1 and Ist1-Did2 complexes that impair Vps4 recruitment (Figure 3.8 A). Loss of Ist1 results in intermediate Vps4 recruitment efficiency.

Exponentially growing *ist1*Δ cells exhibit increased turnover of plasma membrane proteins compared to wild-type cells (Figure 3.3 C), suggesting that the high Ist1 concentration in rapidly-growing cells suppresses MVB-dependent degradation of membrane proteins. Consistent with this idea, a recent study has shown that deletion of *IST1* resulted in an increase in the size and number of MVB vesicles, suggestive of an increased flux of cargo through the MVB pathway (Nickerson et al.). Therefore, an important function of Ist1 might be to suppress membrane protein degradation during the exponential growth phase of the cell, a phase in which cells focus on protein production and cell expansion. Inducing starvation in exponentially growing cells resulted in a rapid drop of Ist1 levels (Figure 3.5), which increases MVB pathway throughput and, in turn, membrane protein turnover.

Figure 3.8. Regulation of Translation, Autophagy and the MVB Pathway by Nutrient-Sensing Systems. (A) Model for the regulation of Vps4 recruitment to ESCRT-III by cellular Ist1 levels. (B) Model for the concerted regulation of translation initiation, autophagy, the MVB pathway and endocytosis by amino acid levels.

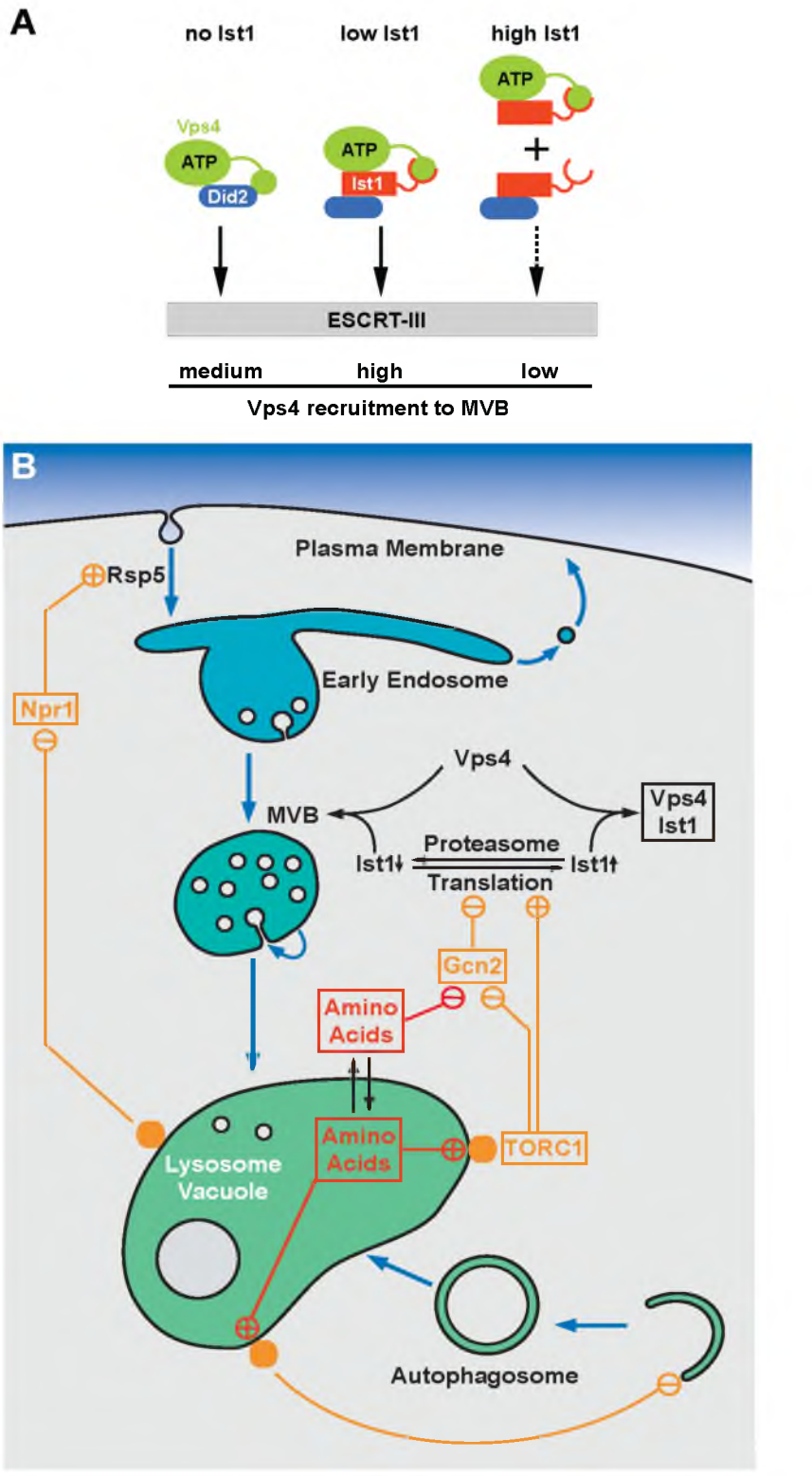
A
no Ist1
low Ist1
high Ist1
Vps4
ATP
Did2
ATP
Ist1
ATP
+
ESCRT-III
medium
high
low
Vps4 recruitment to MVB
B
Plasma Membrane
Rsp5
Early Endosome
Npr1
Vps4
MVB
Vps4
Ist1
Proteasome
Ist1↓
Translation
Ist1↑
Gcn2
Amino
Acids
Amino
Acids
TORC1
Lysosome
Vacuole
Autophagosome

The variation in Ist1 levels is not transcriptionally generated, but is the result of changes in the translational output of the cell combined with a rapid turnover rate of Ist1 (Figure 3.5). As such, Ist1 levels are a direct readout of the metabolic state of the cell, providing a connection between the MVB pathway and the TOR and Gcn2 regulatory systems that govern translation initiation. This connection results in an inverse coupling of protein synthesis and protein degradation via the MVB pathway: high levels of protein synthesis result in reduced MVB pathway throughput, and conversely, low levels of protein synthesis during starvation result in heightened protein degradation via the MVB pathway (Figure 3.8 B).

Starvation conditions or addition of rapamycin have been shown to induce endocytosis and subsequent degradation of numerous plasma membrane transporters, indicating that the TOR signaling pathway is involved in the regulation of membrane protein turnover (Beck et al., 1999; Galan et al., 1994; Krampe and Boles, 2002; Omura et al., 2001; Penalver et al., 1998). Similarly, we observed that starvation caused rapid internalization and degradation of the iron-transporter Ftr1 and the arginine-transporter Can1. We found that this downregulation is not solely caused by the degradation of Ist1 and subsequent upregulation of the MVB pathway (Figure 3.6), but also seems to involve increased internalization of the transporters through separate mechanisms. Taken together, these observations suggest that starvation induces both endocytosis and MVB sorting of a large set of plasma membrane proteins, leading to increased amino acid recycling. Importantly, the general amino acid

transporter Gap1 has been shown to be stabilized at the plasma membrane during starvation (De Craene et al., 2001), further support that starvation does not increase bulk flow uptake of plasma membrane proteins, but enhances endocytosis of a specific set of proteins that are not essential for survival under the given stress conditions.

Under normal growth conditions, Ftr1 degradation is regulated in response to levels of available iron. High iron concentrations result in the ubiquitination of Ftr1 by Rsp5 and the subsequent degradation of Ftr1 via the MVB pathway (Strochlic et al., 2008). Starvation-induced degradation of Ftr1 was also found to require Rsp5, suggesting that similar mechanisms are involved in both starvation- and iron-induced Ftr1 downregulation. Npr1 is a downstream effector of TOR, and we found this kinase to be important for the rapamycin-induced downregulation of Ftr1 and other cell-surface proteins. A recent proteomics study identified Rsp5 as a target of Npr1 (Breitkreutz et al., 2010), suggesting that TOR regulates the activity of Rsp5 via Npr1. However, deletion of *NPR1*, or genes encoding subunits of the TORC2 complex, did not impair the rapid downregulation of Ftr1 during leucine starvation or cycloheximide treatment (Figure S3.3), suggesting that an additional, TOR-independent pathway also regulates membrane protein degradation.

Long-term starvation induces autophagy, which, in mammalian cells, is impaired in ESCRT mutants (Lee et al., 2007; Rusten et al., 2007). Our analysis indicated that yeast ESCRT mutants are not defective in autophagy induction or autophagosome fusion with the vacuole. In contrast, ESCRT mutants showed

slightly induced autophagy even in rich medium and had a longer starvation-recovery period, indicating that loss of the MVB pathway likely decreases steady-state TOR activity.

In summary, we propose a model in which MVB-dependent protein degradation is regulated by the growth phase and metabolic state of a cell (Figure 3.8 B). Ist1 is a central factor in this regulation: its levels are regulated by the translational output of the cell, and these varying levels impact the activity of Vps4. High translational output in rapidly growing cells results in high Ist1 protein levels, which impair the function of Vps4 in the MVB pathway. Under these conditions, degradation of membrane proteins is low. Decreased translational activity, as observed in non-growing or starving cells, causes a drop in Ist1 levels due to its intrinsically rapid degradation. This drop increases Vps4 recruitment to MVBs, thereby increasing protein degradation. Additionally, starvation causes increased endocytosis of a large number of plasma membrane proteins, and their subsequent delivery to the MVB pathway.

TORC1 plays an important role in regulating both endocytosis and, via Ist1, the MVB pathway. The TORC1 complex localizes to the vacuolar membrane, which has led to speculation that TORC1 is regulated by the vacuolar amino acid pool rather than the cytoplasmic pool (Sturgill et al., 2008). The result of starvation-induced upregulation of endocytosis and vacuolar degradation is a pool of free amino acids that is important for the adaptive synthesis of stress-response proteins. Thus the MVB pathway helps to maintain translation during

acute starvation until autophagy, the long-term starvation-response pathway, is fully active.

3.5 *Supplemental Information*

The following supporting table and figures are discussed in the previous section and function to further support our findings. Refer to section 3.4 for more detailed information.

Table S3.1. Function and regulation of Vps4. (A) Free amino acid analysis of WT and *vps4Δ* cells following one hour of leucine starvation. Values are represented as change relative to starting conditions. (B) *In vitro* binding studies using recombinant Vps4(E233Q), Ist1 and GST-Did2(CT) (amino acids 113-204). GST-Did2(CT) was immobilized on GSH-sepharose and approximately equimolar amounts of Vps4(E233Q) was added in the presence of ATP. The Ist1 concentrations were varied from zero to approximately four times the molar amount of Vps4(E233Q). Bound fractions were analyzed by SDS-PAGE and coomassie staining, and the amount of bound Vps4(E233Q) relative to GST-Did2(CT) was determined by densitometric scanning. The obtained values were plotted relative to the negative control (no GST-Did2(CT) = 0) and the maximum signal (2xIst1 = 1).

A

Leucine Starvation

Free cellular amino acid levels (arbitrary units)

Wild type					
Time [min]	0	15	30	45	60
Glu	22.37	17.04	17.18	19.10	18.51
Gly	2.74	2.74	2.09	2.01	1.66
Ala	7.31	17.11	21.93	26.02	25.87
Val	0.87	0.95	1.11	1.08	0.91
Met	0.47	0.13	0.06	0.06	0.05
Ile	0.34	1.38	1.17	1.05	0.92
Leu	0.99	0.05	0.03	0.04	0.02
Tyr	0.25	0.94	1.35	1.65	1.79
Phe	0.23	1.24	1.23	1.20	1.11
Lys	14.26	13.33	14.92	15.59	16.05
His	1.57	1.02	0.97	0.97	0.90

B

*vps4*Δ					
Time [min]	0	15	30	45	60
Glu	18.77	16.97	16.23	18.16	18.02
Gly	2.52	2.99	2.37	2.00	1.48
Ala	6.00	17.83	19.23	23.36	23.56
Val	0.54	0.85	0.87	0.94	0.63
Met	0.54	0.27	0.06	0.03	0.01
Ile	0.23	1.75	1.46	1.24	0.83
Leu	1.00	0.00	0.00	0.00	0.00
Tyr	0.36	1.11	1.36	1.50	1.48
Phe	0.26	1.26	1.10	0.95	0.83
Lys	13.79	14.90	15.62	16.33	17.00
His	3.92	3.34	3.08	3.08	2.87

Figure S3.1. Ist1 Protein Levels and Subcellular Localization. (A) Western blot analysis of Ist1-HA following leucine starvation in strains containing functional Rsp5 (*RSP5*) or an Rsp5 mutant deficient in ubiquitin conjugation (*rsp5-1)* (panel 1), and cells expressing either wild-type Ist1 or Ist1 containing a point mutation in a reported C-terminal phosphorylation site, Ist1(S244A)-HA (panel 2). (B) Ist1-GFP localization under normal conditions (con.) and after 20 minutes of leucine starvation.

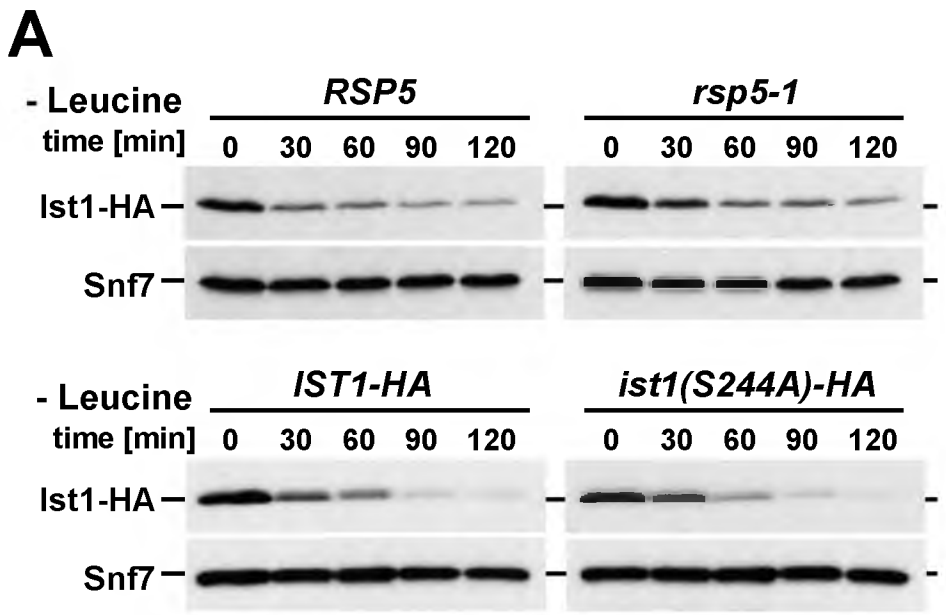
A
- Leucine
RSP5
rsp5-1
time [min]
0 30 60 90 120
0 30 60 90 120
Ist1-HA
Snf7
- Leucine
IST1-HA
ist1(S244A)-HA
time [min]
0 30 60 90 120
0 30 60 90 120
Ist1-HA
Snf7

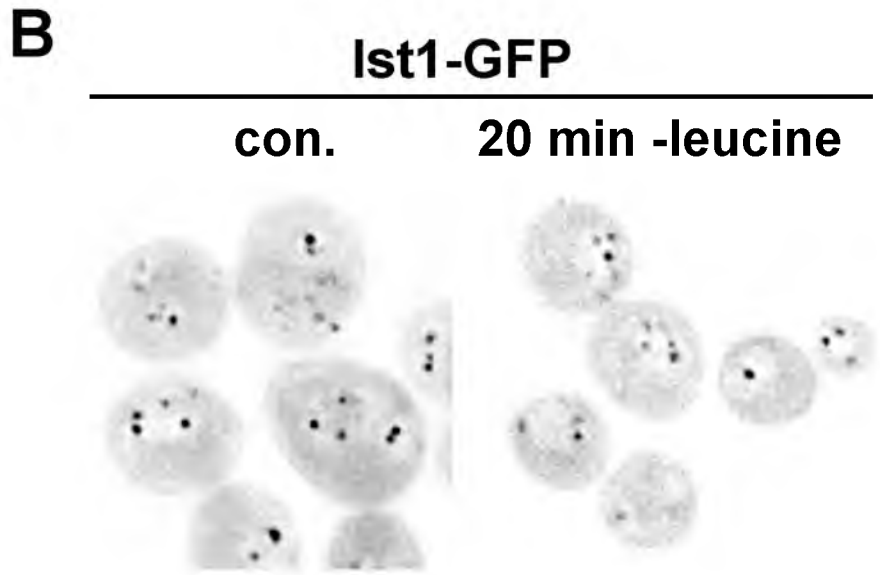
B
Ist1-GFP
con.
20 min -leucine

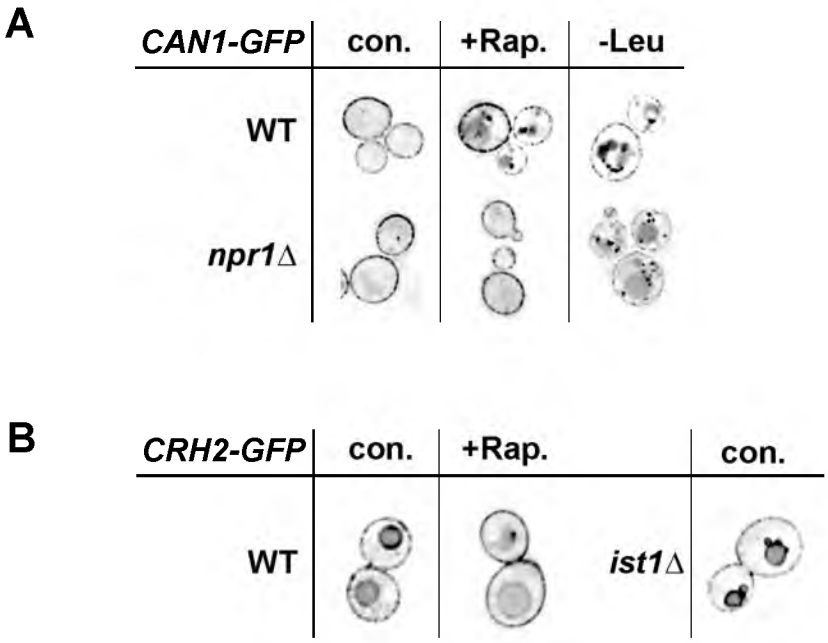

Figure S3.2 Downregulation of Can1, Crh2, and Ftr1 During Starvation. (A) Localization of Can1-GFP in untreated (con.), rapamycin-treated, or leucine-starved wild-type or *npr1Δ* cells. Cells grown to exponential phase in YNB CSM, then treated with rapamycin or transferred to YNB (-Leu). (B) Localization of Crh2-GFP in cells before (con.) and after 1 hr. of rapamycin-treatment, as well as under normal conditions in *ist1Δ* cells.

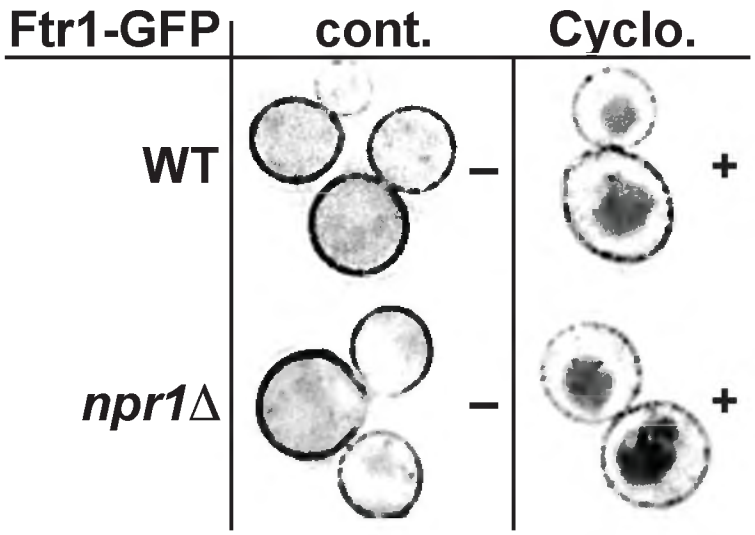

Figure S3.3 Inhibition of Translation Initiates a TORC1-Denependent Starvation Response. Localization of Ftr1-GFP in untreated (cont.), or cycloheximide-treated wild-type or *npr1Δ* cells after 1 hour. Cells grown to exponential phase in YNB CSM, then treated with cycloheximide

3.6 *Materials and Methods*

3.6.1 *Materials*

3.6.1.1 Antibodies. HA (hemagglutinin) specific antibody was purchased from Covance (Princeton, NJ). GFP-specific monoclonal antibody was purchased from Roche Applied Science (Indianapolis, IN). Antiserum specific to phosphor(S51)-eIF2α was purchased from Abcam (Cambridge, MA). Antisera against Snf7 has been characterized previously (Babst et al., 1998).

3.6.2 *Methods*

3.6.2.1 Survival assay. Survival assays used exponentially growing cells diluted uniformly into YNB (-Leu) composed as detailed above. Cells were grown at 30°C with agitation. Samples were collected daily, diluted 1:10^6 then plated on YPD (Yeast Extract Peptone Dextrose). Colonies were counted following 2 days of growth at 30°C; viability was gauged as number of colonies with respect to starting point. Free amino acid analysis of yeast was performed using a Hitachi L8800 Analyzer (Hitachi, Schaumburg, IL).

3.6.2.2 Strains and media. *S. cerevisiae* strains used in this study are listed in Table 3.1. To maintain plasmids, yeast were grown in appropriate complete synthetic dropout medium. Wild type cells as well as those containing genomic integrations or deletions were grown in either rich YPD medium (yeast extract-peptone-dextrose) or complete synthetic media YNB (Yeast Nitrogen Base) with 2% Glucose + Drop-out Mix Synthetic from US Biological (Swampscott, MA) containing the following components in [mg/L]: Adenine [10], Ala [40], Arg [40], Asn [40], Asp [40], Cys [40], Gln [40], Glu [40], Gly [40], His

[40], Myo-Inositol [40], Ile [40], Leu [200], Lys [40], Met [40], Para-Aminobenzoic Acid [4], Phe [40], Pro [40], Ser [40], Thr [40], Trp [40], Tyr [40], Uracil [40], Val [40].

3.6.2.3 DNA manipulations. Plasmids used in this study are listed in Table 3.1. All plasmids were constructed using standard cloning techniques. The pRS4XX shuttle vectors used in this study have been described previously (Christianson et al., 1992). Plasmid-based GFP fusions used pEGFP-C1 obtained from Clontech Laboratories Inc. (Palo Alto, CA).

3.6.2.4 Protein purification. Proteins used in pulldown assays were expressed in *Escherichia coli*. Vps4(E233Q) (pMB63), GST-Did2(CT) (pAH32) and Ist1 (pCD2) were purified previously reported (Babst et al., 1997; Dimaano et al., 2008; Shestakova et al., 2010).

3.6.2.5 Amino acid analysis. For amino acid analysis of cells starved for leucine, exponentially growing cultures were spun down, washed twice in YNB (-Leu) and resuspended in YNB (-Leu). For each time point, 5 ODV of cells was harvested, washed 3X on ice with Milli-Q water and resuspended in 10% TCA. Cells were lysed with glass beads and vortexing, cell debris was pelleted, and soluble material was spun hard at 4°C for 10 minutes. Supernatants were kept overnight at -20°C, spun hard again at 4°C, and diluted for analysis. Quantitative RT-PCR was performed using standard techniques with actin mRNA as a control. Subcellular fractionation was performed as previously described (Babst et al., 2002a). Western blot samples tracking transmembrane protein degradation (Figure 3.6B) were initially TCA precipitated, acetone washed, then lysed with

glass beads in SDS-PAGE sample buffer (2% SDS, 0.1 M Tris, pH 6.8, 10% glycerol, 0.01% bromophenol blue, 5% β-mercaptoethanol) containing 6 M Urea. All other Western blot samples were collected and lysed with glass beads in the presence of SDS-PAGE sample buffer.

3.6.2.6 Other. Western blots were performed using standard techniques. Rapamycin was used at a final concentration of 200 ng/mL. Cycloheximide was used at a final concentration of 25 mg/L. Fluorescence microscopy was performed on a deconvolution microscope (DeltaVision, Applied Precision, Issaquah, WA). GST-pulldown assays were performed using recombinant proteins as previously described (Shestakova et al., 2010).

3.7 *Acknowledgements*

Special thanks to Inge Stijleman and Philip Bernard for assistance with the RT-PCR experiments. Kelsey Fulkerson aided in strain construction. The yeast strain CBY118 was a gift from Chris Burd. This work has been supported by NIH Grant R01 GM074171.

3.8 *References*

Agromayor, M., J.G. Carlton, J.P. Phelan, D.R. Matthews, L.M. Carlin, S. Ameer-Beg, K. Bowers, and J. Martin-Serrano. 2009. Essential role of hIST1 in cytokinesis. *Mol Biol Cell*. 20:1374-1387.

Babst, M., D.J. Katzmann, E.J. Estepa-Sabal, T. Meerloo, and S.D. Emr. 2002a. Escrt-III: an endosome-associated heterooligomeric protein complex required for mvb sorting. *Dev Cell*. 3:271-282.

Babst, M., D.J. Katzmann, W.B. Snyder, B. Wendland, and S.D. Emr. 2002b. Endosome-associated complex, ESCRT-II, recruits transport machinery for protein sorting at the multivesicular body. *Dev Cell*. 3:283-289.

Babst, M., T.K. Sato, L.M. Banta, and S.D. Emr. 1997. Endosomal transport function in yeast requires a novel AAA-type ATPase, Vps4p. *EMBO J.* 16:1820-1831.

Babst, M., B. Wendland, E.J. Estepa, and S.D. Emr. 1998. The Vps4p AAA ATPase regulates membrane association of a Vps protein complex required for normal endosome function. *Embo J*. 17:2982-2993.

Bajorek, M., E. Morita, J.J. Skalicky, S.G. Morham, M. Babst, and W.I. Sundquist. 2009a. Biochemical analyses of human IST1 and its function in cytokinesis. *Mol Biol Cell*. 20:1360-1373.

Bajorek, M., H.L. Schubert, J. McCullough, C. Langelier, D.M. Eckert, W.M. Stubblefield, N.T. Uter, D.G. Myszka, C.P. Hill, and W.I. Sundquist. 2009b. Structural basis for ESCRT-III protein autoinhibition. *Nat Struct Mol Biol*. 16:754-762.

Beck, T., A. Schmidt, and M.N. Hall. 1999. Starvation induces vacuolar targeting and degradation of the tryptophan permease in yeast. *J Cell Biol*. 146:1227-1238.

Belgareh-Touze, N., S. Leon, Z. Erpapazoglou, M. Stawiecka-Mirota, D. Urban-Grimal, and R. Haguenauer-Tsapis. 2008. Versatile role of the yeast ubiquitin ligase Rsp5p in intracellular trafficking. *Biochem Soc Trans*. 36:791-796.

Bordallo, J., and P. Suarez-Rendueles. 1993. Control of Saccharomyces cerevisiae carboxypeptidase S (CPS1) gene expression under nutrient limitation. *Yeast*. 9:339-349.

Breitkreutz, A., H. Choi, J.R. Sharom, L. Boucher, V. Neduva, B. Larsen, Z.Y. Lin, B.J. Breitkreutz, C. Stark, G. Liu, J. Ahn, D. Dewar-Darch, T. Reguly, X. Tang, R. Almeida, Z.S. Qin, T. Pawson, A.C. Gingras, A.I. Nesvizhskii,

and M. Tyers. 2010. A global protein kinase and phosphatase interaction network in yeast. *Science*. 328:1043-1046.

Carlton, J.G., and J. Martin-Serrano. 2007. Parallels between cytokinesis and retroviral budding: a role for the ESCRT machinery. *Science*. 316:1908-1912.

Chang, Y.Y., G. Juhasz, P. Goraksha-Hicks, A.M. Arsham, D.R. Mallin, L.K. Muller, and T.P. Neufeld. 2009. Nutrient-dependent regulation of autophagy through the target of rapamycin pathway. *Biochem Soc Trans*. 37:232-236.

Christianson, T.W., R.S. Sikorski, M. Dante, J.H. Shero, and P. Hieter. 1992. Multifunctional yeast high-copy-number shuttle vectors. *Gene*. 110:119-122.

De Craene, J.O., O. Soetens, and B. Andre. 2001. The Npr1 kinase controls biosynthetic and endocytic sorting of the yeast Gap1 permease. *J Biol Chem*. 276:43939-43948.

Dimaano, C., C.B. Jones, A. Hanono, M. Curtiss, and M. Babst. 2008. Ist1 regulates vps4 localization and assembly. *Mol Biol Cell*. 19:465-474.

Enyenihi, A.H., and W.S. Saunders. 2003. Large-scale functional genomic analysis of sporulation and meiosis in Saccharomyces cerevisiae. *Genetics*. 163:47-54.

Felice, M.R., I. De Domenico, L. Li, D.M. Ward, B. Bartok, G. Musci, and J. Kaplan. 2005. Post-transcriptional regulation of the yeast high affinity iron transport system. *J Biol Chem*. 280:22181-22190.

Galan, J.M., C. Volland, D. Urban-Grimal, and R. Haguenauer-Tsapis. 1994. The yeast plasma membrane uracil permease is stabilized against stress induced degradation by a point mutation in a cyclin-like "destruction box". *Biochem Biophys Res Commun*. 201:769-775.

Gruhler, A., J.V. Olsen, S. Mohammed, P. Mortensen, N.J. Faergeman, M. Mann, and O.N. Jensen. 2005. Quantitative phosphoproteomics applied to the yeast pheromone signaling pathway. *Mol Cell Proteomics*. 4:310-327.

Kamura, T., D. Burian, H. Khalili, S.L. Schmidt, S. Sato, W.J. Liu, M.N. Conrad, R.C. Conaway, J.W. Conaway, and A. Shilatifard. 2001. Cloning and characterization of ELL-associated proteins EAP45 and EAP20: A role for yeast EAP-like proteins in regulation of gene expression by glucose. *J Biol Chem*. 5:5.

Kirisako, T., M. Baba, N. Ishihara, K. Miyazawa, M. Ohsumi, T. Yoshimori, T. Noda, and Y. Ohsumi. 1999. Formation process of autophagosome is traced with Apg8/Aut7p in yeast. *J Cell Biol*. 147:435-446.

Krampe, S., and E. Boles. 2002. Starvation-induced degradation of yeast hexose transporter Hxt7p is dependent on endocytosis, autophagy and the terminal sequences of the permease. *FEBS Lett*. 513:193-196.

Kuma, A., M. Hatano, M. Matsui, A. Yamamoto, H. Nakaya, T. Yoshimori, Y. Ohsumi, T. Tokuhisa, and N. Mizushima. 2004. The role of autophagy during the early neonatal starvation period. *Nature*. 432:1032-1036.

Lee, J.A., A. Beigneux, S.T. Ahmad, S.G. Young, and F.B. Gao. 2007. ESCRT-III dysfunction causes autophagosome accumulation and neurodegeneration. *Curr Biol*. 17:1561-1567.

Luhtala, N., and G. Odorizzi. 2004. Bro1 coordinates deubiquitination in the multivesicular body pathway by recruiting Doa4 to endosomes. *J Cell Biol*. 166:717-729.

Nickerson, D.P., M. West, R. Henry, and G. Odorizzi. 2010. Regulators of vps4 ATPase activity at endosomes differentially influence the size and rate of formation of intralumenal vesicles. *Mol Biol Cell*. 21:1023-1032.

Omura, F., Y. Kodama, and T. Ashikari. 2001. The N-terminal domain of the yeast permease Bap2p plays a role in its degradation. *Biochem Biophys Res Commun*. 287:1045-1050.

Penalver, E., P. Lucero, E. Moreno, and R. Lagunas. 1998. Catabolite inactivation of the maltose transporter in nitrogen-starved yeast could be due to the stimulation of general protein turnover. *FEMS Microbiol Lett*. 166:317-324.

Piper, R.C., and D.J. Katzmann. 2007. Biogenesis and Function of Multivesicular Bodies. *Annu Rev Cell Dev Biol*.

Reggiori, F., C.W. Wang, U. Nair, T. Shintani, H. Abeliovich, and D.J. Klionsky. 2004. Early stages of the secretory pathway, but not endosomes, are required for Cvt vesicle and autophagosome assembly in Saccharomyces cerevisiae. *Mol Biol Cell*. 15:2189-2204.

Robinson, J.S., D.J. Klionsky, L.M. Banta, and S.D. Emr. 1988. Protein sorting in *Saccharomyces cerevisiae*: isolation of mutants defective in the delivery and processing of multiple vacuolar hydrolases. *Mol. Cell. Biol.* 8:4936-4948.

Rodriguez-Pena, J.M., V.J. Cid, J. Arroyo, and C. Nombela. 2000. A novel family of cell wall-related proteins regulated differently during the yeast life cycle. *Mol Cell Biol*. 20:3245-3255.

Rue, S.M., S. Mattei, S. Saksena, and S.D. Emr. 2008. Novel Ist1-Did2 complex functions at a late step in multivesicular body sorting. *Mol Biol Cell*. 19:475-484.

Rusten, T.E., T. Vaccari, K. Lindmo, L.M. Rodahl, I.P. Nezis, C. Sem-Jacobsen, F. Wendler, J.P. Vincent, A. Brech, D. Bilder, and H. Stenmark. 2007. ESCRTs and Fab1 regulate distinct steps of autophagy. *Curr Biol*. 17:1817-1825.

Sekito, T., Y. Fujiki, Y. Ohsumi, and Y. Kakinuma. 2008. Novel families of vacuolar amino acid transporters. *IUBMB Life*. 60:519-525.

Shestakova, A., A. Hanono, S. Drosner, M. Curtiss, B.A. Davies, D.J. Katzmann, and M. Babst. 2010. Assembly of the AAA ATPase Vps4 on ESCRT-III. *Mol Biol Cell*.

Sonenberg, N., and A.G. Hinnebusch. 2009. Regulation of translation initiation in eukaryotes: mechanisms and biological targets. *Cell*. 136:731-745.

Staschke, K.A., S. Dey, J.M. Zaborske, L.R. Palam, J.N. McClintick, T. Pan, H.J. Edenberg, and R.C. Wek. 2010. Integration of general amino acid control and TOR regulatory pathways in nitrogen assimilation in yeast. *J Biol Chem*.

Strochlic, T.I., B.C. Schmiedekamp, J. Lee, D.J. Katzmann, and C.G. Burd. 2008. Opposing activities of the Snx3-retromer complex and ESCRT proteins mediate regulated cargo sorting at a common endosome. *Mol Biol Cell*. 19:4694-4706.

Sturgill, T.W., A. Cohen, M. Diefenbacher, M. Trautwein, D.E. Martin, and M.N. Hall. 2008. TOR1 and TOR2 have distinct locations in live cells. *Eukaryot Cell*. 7:1819-1830.

Vabulas, R.M., and F.U. Hartl. 2005. Protein synthesis upon acute nutrient restriction relies on proteasome function. *Science*. 310:1960-1963.

Wang, X., and C.G. Proud. 2009. Nutrient control of TORC1, a cell-cycle regulator. *Trends Cell Biol*. 19:260-267.

Wullschleger, S., R. Loewith, and M.N. Hall. 2006. TOR signaling in growth and metabolism. *Cell*. 124:471-484.

CHAPTER 4

STARVATION INDUCED DOWNREGULATION OF PLASMA MEMBRANE PROTEINS

4.1 *Abstract*

Metabolic regulation is essential for cell growth and survival. The TORC1 signaling complex plays a crucial role in regulating metabolic homeostasis. We have previously shown that amino acid starvation induces the downregulation and degradation of plasma membrane proteins through the MVB pathway and that Npr1 and Rsp5 have been implicated in this response. The ubiquitin ligase Rsp5 and MVB pathway are required for starvation-induced endocytosis however the mechanisms that regulate the endocytosis of plasma membrane proteins during starvation are unclear. Here, we show that starvation induces the accumulation of PI(3)P and ESCRT-0 on endosomal membranes, increasing the sorting efficacy of the MVB pathway. We also show that TORC1 activation of Npr1 is require for the localization of Rsp5 to the plasma membrane and endosomes, which functions to increase the ubiquitination of membrane proteins. Finally, we show that the Rsp5 adaptors, Bul1 and Bul2, are required for the polyubiquitination and downregulation of the iron transporter, Ftr1. Together these results demonstrate a starvation-response pathway where TORC1 activation of Npr1 regulates the localization and activity of Rsp5 to enhance the sorting of plasma membrane proteins into the MVB pathway. The function of this starvation-response pathway is to provide the amino acids necessary to synthesize the proteins required to adapt to long-term starvation conditions.

4.2 *Background*

Metabolism encompasses the all the chemical reactions that occur to maintain life. There are two main categories of metabolism. Catabolism, the break down of biological molecules, and anabolism is the synthesis of biological molecules. Metabolic regulation is the process by which the cell balances these two reactions and is dependent upon the nutrient supply and demand of the cell. Central to metabolic regulation is the Target Of Rapamycin (TOR) kinase, a highly conserved nutrient sensing system that regulates homeostasis through a variety of signaling pathways (reviewed in (Wullschleger et al., 2006). TOR was identified through a screen designed to identify mutants that confer resistance to rapamycin, a potent antifungal bacterial metabolite (Heitman et al., 1991). TOR is a highly conserved kinase with orthologs found throughout eukaryotes (Wang et al., 2009). Yeast cells have two TOR Ser/Thr kinase homologs that form two distinct protein complexes, TORC1 (TOR complex 1), and TORC2, in contrast to mammalian cells, which only contain one *TOR* gene (Schmidt et al., 1996; Wang and Proud, 2009). The TOR complexes function in regulating temporal and spatial growth in response to nutrient availability through different mechanisms. Interestingly, only TORC1 is sensitive to rapamycin treatment. TORC1 is inactivated by the binding of a cofactor, FKBP12 (peptidyl-prolyl cis/trans isomerase), in complex with rapamycin, such that mutations that prevent FKBP12 binding to TORC1 inhibit the cytotoxic effects of rapamycin (Heitman et al., 1991). TORC2 is comprised of TOR2, Avo2, Lst8, and Bit61 (Loewith et al., 2002; Reinke et al., 2004) and is involved in cell-cycle dependent actin

cytoskeleton organization, endocytosis important for bud development (Loewith et al., 2002). Recently, NIP7, a protein involved in RNA maturation and ribosome biogenesis, was identified as an activator of mTORC2, the mammalian ortholog of yeast TORC2. Mutation of NIP7 phenocopies loss-of-function mutants of mTORC2, strongly supporting they are functionally related (Zinzalla et al., 2011). The supply of ribosomes in the cell is relative to its ability to respond to growth stimuli, therefore, activation of mTORC2 in a ribosome dependent mechanism co-regulates growth with growth-capacity (Zinzalla et al., 2011). Based on the degree of homology between TOR complexes in yeast (Wullschleger et al., 2006), it is likely that yeast TORC2 is activated similarly.

The TORC1 complex is a nutrient sensing mechanism that positively regulates general translation, ribosome biogenesis and represses the autophagy pathway when nutrients are plentiful (Wang et al., 2009). The combination of ribosome biogenesis by TORC1 and TORC2-dependent ribosome activation suggests there is an elegant regulatory network combining these two important growth regulators (Zinzalla et al., 2011). TORC1 is comprised of the kinase Tor1 or Tor2, Lst8, TCO89 and Kog1 (Loewith et al., 2002; Reinke et al., 2004). It is currently unknown how nutrients stimulate TORC1 activity, however nutrient depletion, especially of amino acids, causes rapid inactivation of TORC1, which subsequently stimulates starvation response pathways (Wullschleger et al., 2006). Rapamycin treatment also induces rapid inactivation of TORC1 mimicking starvation and initiating cell cycle arrest, general translation attenuation, upregulation of stress-response genes and derepression of autophagy.

Autophagy is a long-term starvation pathway where a double membrane randomly engulfs portions of the cytoplasm, forming an autophagosome (Nakatogawa et al., 2009). Autophagasomes fuse with the vacuole in a PI(3)P dependent mechanism providing an emergency source of nutrients. Vps34 is the only known kinase that converts phosphotidylinositol to PI(3)P and is recruited to autophagosomal membranes in complex with Vps15, Vps30 and Atg14 to produce PI(3)P and promote fusion of the autophagosome to vacuoles (Kihara et al., 2001). TORC1 dependent translation attenuation is mediated by the inactivation of the general translation initiation factor eIF2α by Gcn2, a kinase downstream of TORC1. TORC1 inactivation results in the activation of Gcn2, though Gcn2 is also activated by uncharged t-RNAs that result from amino acid starvation (De Craene et al., 2001; Kamura et al., 2001). The TORC1-dependent regulation of Ribosome biogenesis is mediated by the kinase Sch9 (Urban et al., 2007). During growth, TORC1 phosphorylates and activates Sch9. Activated Sch9 stimulates the transcription of tRNA and ribosomal proteins by phosphorylating transcription initiation factors, localizing them to the nucleus (Lempiainen and Shore, 2009). TORC1 inactivation results in the dephosphorylation and inactivation of Sch9 minimizing ribosomal production and curbing biomolecule synthesis (Urban et al., 2007). Another kinase downstream of TORC1 is Npr1, identified by its role a protein trafficking regulator of Gap1 (general amino acid permease) (De Craene et al., 2001; Helliwell et al., 2001). When nitrogen and amino acid levels are sufficient, Npr1 is inactivated by TORC1-dependent phosphorylation, directing Gap1 trafficking to the vacuole.

However during starvation, Npr1 is dephosphorylated and stabilizes Gap1 on the plasma membrane to import amino acids as a source of nitrogen from the environment (De Craene et al., 2001). Npr1 is also involved in the trafficking of the tryptophan transporter, Tat2, although when Npr1 is active, Tat2 is downregulated (Schmidt et al., 1998). Furthermore, starvation also induces the downregulation of several other transporters from the plasma membrane and is discussed in Chapter 3 (Beck et al.; Galan et al.; Krampe and Boles; Omura et al.; Penalver et al.).

TORC1 is especially tuned to sense amino acids levels likely because protein synthesis is an expensive energy process that requires large amounts of amino acids. The synthesis of amino acids is also a costly process and is avoided when possible through the import of nutrients, including amino acids, from the environment. During starvation, energy consumption is restricted and instead favors the reutilization of dispensable biomass (Wullschleger et al., 2006).

Amino acids, sugars and other nutrients are pumped into the cell from the environment by transporters on the plasma membrane (Jauniaux and Grenson, 1990; Ozcan et al., 1998). Nutrient import is regulated by the expression and trafficking of specific transporters to and from the plasma membrane. Fur4 is trafficked to the vacuole upon activation of the transporter by exposure to its ligand, uracil or starvation (Blondel et al., 2004; Galan et al.). The downregulation of Fur4 from the plasma membrane is dependent upon polyubiquitination by the ubiquitin ligase, Rsp5. Polyubiquitination chains formed by Rsp5 are linked to each other through UbK63 and are specific for the endocytic and MVB pathways,

whereas UbK48 polyubiquitin chains are recognized by the proteasomal degradation pathway (Galan and Haguenauer-Tsapis, 1997). The MVB pathway is critical role in regulating the composition of transporters expressed at the cell surface by downregulating transmembrane proteins from the plasma membrane (reviewed in(Hanson et al., 2009; Hurley, 2010; Raiborg and Stenmark, 2009) (Figure 1.1). In this sorting pathway, the ubiquitination of plasma membrane protein is sufficient for entry into the MVB pathway and subsequent degradation in the vacuole (Katzmann et al., 2001). The retromer complex competes for cargoes at the MVB where it cycles a subset of proteins in the late endosome to the Golgi or the plasma membrane (reviewed in (Attar and Cullen, 2010). Retromer is composed of Vps26, Vps29, Vps35, Vps5 and Vps17 and is recruited to endosomal membranes through the PI(3)P binding PX domains in the sorting nexins, Vps17 and Vps5 (Seaman and Williams, 2002). Vps26, Vps29 and Vps35 make up the cargo-selection subcomplex and are responsible for cargo recognition (Nothwehr et al., 1999; Nothwehr et al., 2000).

In Chapter 3, we present compelling evidence that starvation upregulates the MVB pathway inducing the endocytosis and degradation of plasma membrane proteins. The activity of Rsp5 was required for the internalization of plasma membrane proteins during starvation. TORC1 and Gcn2 mediate regulation of the MVB pathway, which regulate the ubiquitination of cargoes and expression levels of Ist1 respectively. Deletion of Npr1, a kinase downstream of TORC1, inhibited TORC1-dependent degradation of plasma membrane proteins. Together, our results from Chapter 3 strongly suggest that ubiquitination of

plasma membrane proteins is regulated by Npr1 and upstream TORC1 to increase soring of cargoes into the MVB pathway. The following work provides evidence that the starvation-induced activity of Npr1 and Rsp5 regulate plasma membrane protein sorting and degradation via the MVB pathway.

4.3 *Results and Discussion*

4.3.1 *Starvation Induces PI(3)P Accumulation and ESCRT-0 Localization to Late Endosomes*

Phosphositides are required for the function of signal transduction pathways and membrane trafficking pathways, including the endocytic pathway, by recruiting proteins to the membranes that function in cargo sequestration and vesicle formation (Stenmark, 2009). The head group of phosphatidyloinositol can be reversibly phosphorylated at three positions: D-2, D-3 and D-4 to form a variety of phosphoinositides (Strahl and Thorner, 2007). The enrichment of PI(3)P in the endomembrane system is crucial for the localization and function of ESCRT-0, ESCRT-I and ESCRT-II proteins required for protein sorting and ILV formation during MVB maturation (Piper and Katzmann, 2007). The influx and efflux of lipids through the endosomal membrane necessitates constant activity of kinases and phosphatases to maintain PI(3)P levels. Vps34 is localized to endosomes by recruitment of the Vps34, Vps15, Vps38 and Vps30 complex (Kihara et al., 2001; Stack and Emr, 1994). Yeast have several phosphatases that can convert di-phosphoinositides and tri- phosphoinositides to phosphatidylinositol and PI(3)P including *YMR1,* an ortholog of the Myotubularin family of PI(3)P phosphatases (Laporte et al., 1998) and the Snaptojanin Like

phosphatases *SJL2* and *SJL3* (Singer-Kruger et al., 1998; Strahl and Thorner, 2007) (Figure 1.3). Yeast also contains to other phosphatases, Sac1 and Fig4 (Robinson 2004). Sac1, Fig4, Sjl2 and Sjl3 contain Sac1-domains (guo, 1999). Fig4 is specific for the D-5 position of $PI(3,5)P_2$ (rudge, 2004), where as Sac1, Sjl2 and Sjl3 can convert PI(3)P, PI(4)P, PI(5)P and $PI(3,5)P_2$ to phosphatidylinositol. In addition, Sjl2 and Sjl3 can act on $PI(4,5)P_2$ (guo, 1999). The localization of Ymr1 and Sjl1,2and 3 is mostly cytoplasmic and unclear where they enact their function (Robinson, 2006), although Sjl3 has ben shown to localize to cortical actin patches following osmotic stress (Ooms, 2000). Single deletions of Ymr1, Sjl1, Sjl2 and Sjl3 had little effect on PI(3)P levels, although FM-464 treatment revealed a fragmented vacuole pheonotype (Parrish et al., 2004). Combinatory double deletions between Ymr1 and the Sjls also exhibited normal PI(3)P levels with the exception of the *ymr1Δsjl3Δ* double mutant (Parrish et al., 2004). The *ymr1Δsjl3Δ* mutant show a two-fold increase in PI(3)P levels displayed drastic accumulation of GFP-FYVE at the vacuole, indicating the dephosphorylation of PI(3)P was disrupted (Parrish et al., 2004). The trafficking of two MVB cargoes, CPY and CPS, were also disrupted in this mutant (Parrish et al., 2004).

We used similar mutant strains to determine whether the disruption of PI(3)P levels induced changes in the trafficking of the iron transporter Ftr1 through the MVB pathway (Table 4.1). To study this, we analyzed Ftr1-GFP localization after inducing starvation in the mutants (Figure 4.1A). Cells were

Table 4.1 List of Plasmids and Strains

Strain or Plasmid	Descriptive Name	Genotype or Description	Reference or Source
Yeast Strains			
SEY6210	WT	MATα leu2-3,112 ura3-52 his3-Δ200 trp1-Δ901 lys2-801 suc2-Δ9	(Robinson et al., 1988)
EOY72	*FTR1-GFP ymr1Δ*	SEY6210, *FTR1-GFP::KanMX6*, *YMR1::HIS3*	This Study
MCY52	*npr1Δ*	SEY6210, *NPR1::KanMX6*	This study
CBY118	*FTR1-GFP*	SEY6210.1, *FTR1-GFP::HISMX*	C. Burd, unpublished
EOY54	*ymr1Δsjl3Δ FTR1-GFP*	SEY6210.1 *YMR1::HIS3, SJL3::HIS3, FTR1-GFP::KanMX6*	This Study
EOY70	*ymr1Δslj2Δ FTR1-GFP*	SEY6210, *YMR1::HIS, SJL2::HIS), FTR1-GFP::KanMX6*	This Study
EOY69	*ymr1Δslj3Δ FTR1-GFP*	SEY6210.1, *YMR1::HIS, SJL3::Trp, Ftr1-GFP::KanMX6*	This Study
EOY81	*tor1Δ FTR1-GFP*	SEY6210, *TOR1::KanMX6, FTR1-GFP::HIS3*	This Study
TSY183	*FTR1-GFP rsp5Δ*	SEY6210, *RSP5::HIS3* + *pDsRED415-rsp5^{L733S}*, *FTR1-GFP::URA3*	(Strochlic et al., 2008b)
EOY3	*vps35Δ FTR-GFP*	SEY6210, *VPS35::HIS3, FTR1-GFP::KanMX6*	This Study

Table 4.1 Cont.

Strain or Plasmid	Descriptive Name	Genotype or Description	Reference or Source
E. coli			
XL1-Blue		recA1 endA1 gyrA96 thi-1 hsdR17 supE44 relA1 lac [F' proAB lacIqZDM15 Tn10(tetr)]	Stratagene (La Jolla, CA)
Plasmids			
pMB103	*vps4(E233Q)*	*URA3* Ap^r (pRS416) *vps4(E233Q)*	(Babst et al., 1997)
pMB342	Vps4-GFP	*URA3* Ap^r (pRS416) *VPS4*-HA-GFP	
pEE27-5	GFP-Vps27	*URA3* Ap^r (pRS426) *VPS27*-GFP	
pDsRED415*RSP5*	DsRED-Rsp5	*LEU2* Ap^r (pRS415) DsRED-RSP5	(Lee et al., 2009)
pDsRED415*rsp5*	DsRED-*rsp5-1*	*LEU2 Ap^r (pRS415) DsRED-rsp5-1*	(Lee et al., 2009)
pAH77	GFP-Did2	*URA3* Ap^r (pRS416) GFP-*DID2*	
pTAP*RSP5*	TAP-Rsp5	*URA3* Ap^r (pRS416) TAP-Rsp5	(Oestreich et al., 2007)
pEO70	TAP-*rsp5(S216A)*	*URA3* Ap^r (pRS416) TAP-rsp5(S216A)	This Study
pEO71	TAP-*rsp5(S216E)*	*URA3* Ap^r (pRS416) TAP-rsp5(S216E)	This Study
pTER103	*CUP1*-Ub(K63R)	*TRP* Ap^r (pRS	(Swaminathan et al., 1999)

grown in complete medium until mid-log phase. At time zero, untreated cells were analyzed by fluorescence microscopy and then transferred to selective medium lacking leucine or rapamycin was added. After an hour of incubation, the cells were analyzed again by fluorescence microscopy to determine the localization and trafficking of Ftr1-GFP (Figure 4.1A). Before starvation-induction Ftr1-GFP localization in the *ymr1Δ* mutant and wilt-type cells was similar. Following starvation, Ftr1-GFP was stabilized on the plasma membrane the *ymr1Δ* mutant. In contrast, starvation of wild-type cells caused Ftr1-GFP to accumulate in the vacuole. This result indicates that the small perturbation of the PI(3)P levels in the *ymr1Δ* mutant altered the trafficking of Ftr1-GFP through the MVB pathway by favoring recycling by retromer over MVB sorting. The double deletion mutants of *ymr1Δ*sjl1*Δ*, *ymr1Δ*sjl2*Δ*, and *ymr1Δ*sjl3*Δ* displayed increased sorting of Ftr1-GFP to the vacuole under nutrient-rich (control) conditions. Leucine starvation and rapamycin treatment did not cause a significant change in the trafficking of Ftr1-GFP in the *ymr1Δsjl1Δ* or the *ymr1Δsjl2Δ*, indicating Ftr1-GFP was sorted into the vacuole. Leucine deprivation and rapamycin treatment of the *sjl3Δymr1Δ* mutant caused a disturbance in the MVB pathway as evidenced by the accumulation of Ftr1-GFP in late endosomal/perivacuolar structures. There was slight vacuolar signal in these strains, however most of the signal seemed to be in perivacuolar structures. This Ftr1-GFP sorting phonotype is likely a result of the highly increased PI(3)P levels in *ymr1Δsjl3Δ* mutant previously reported, which causes a severe MVB trafficking phenotype (Parrish et al., 2004).

Figure 4.1. Starvation Induces the Accumulation Endosomal Membranes and Increases Efficiency of MVB Sorting. (A) Cells were grown to mid-log phase in CSM complete or selective media. At time zero, cells were moved to leucine minus medium (-Leu) or rapamycin (+Rap) was added. (B) The localization of GFP-Vps27 was analyzed in wild-type, *ymrΔ* and *ymr1Δsjl3Δ* cells. Cells were treated similar to the technique in A. (C) Ftr1-GFP trafficking in an MVB mutant following starvation. (D) Ftr1-GFP trafficking in a retromer mutant (*vps35Δ*) under control conditions, starvation conditions, or iron shock.

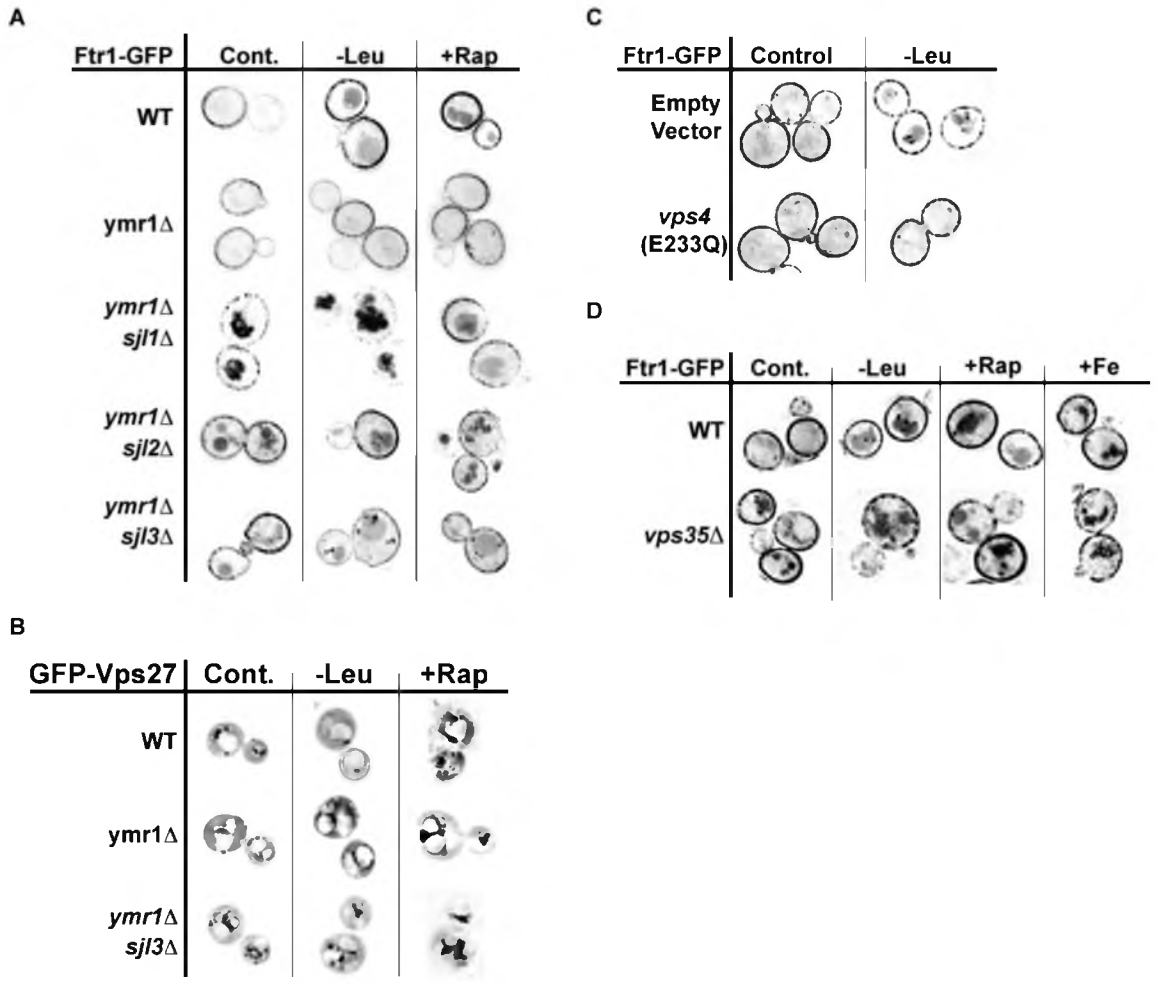
A
Ftr1-GFP
Cont.
-Leu
+Rap
WT
ymr1Δ
ymr1Δ sjl1Δ
ymr1Δ sjl2Δ
ymr1Δ sjl3Δ
B
GFP-Vps27
Cont.
-Leu
+Rap
WT
ymr1Δ
ymr1Δ sjl3Δ
C
Ftr1-GFP
Control
-Leu
Empty Vector
vps4 (E233Q)
D
Ftr1-GFP
Cont.
-Leu
+Rap
+Fe
WT
vps35Δ

To visualize the pool of PI(3)P in endosomal membranes, we analyzed the localization of GFP-Vps27 in wild-type cells, the *ymr1Δ* and *ymr1Δsjl3Δ* phosphatase mutants by fluorescent microscopy (Figure 4.1B). Vps27 function in the MVB pathway is to localize ESCRT-0 to endosomal membranes by binding to PI(3)P through its FYVE domain (Burd and Emr; Katzmann et al., 2001). ESCRT-0 localization to endosomes is necessary for the recruitment of downstream ESCRT proteins and ILV formation (Piper and Katzmann, 2007) (Chapter 1 Figure 4.1). The localization of PI(3)P and thus Vps27, might reveal the source of the Ftr1-GFP trafficking defect in the *ymr1Δ* and *ymr1Δsjl3Δ* mutants.

Wild-type cells expressing GFP-Vps27 from a high-copy plasmid were examined before and after starvation (Figure 4.1B). Starvation was induced in these cells through leucine depletion and rapamycin treatment. GFP-Vps27 was localized to the cytoplasm and endosomes in wild-type cells as previously reported (Burd and Emr, 1998), although there was slight vacuolar membrane signal likely caused by the overexpression of the protein. Leucine starvation of wild-type cells caused a slight increase in the localization of GFP-Vps27 to endosomes and the vacuolar membrane, whereas rapamycin treatment surprisingly caused a dramatic relocalization of GFP-Vps27 to the vacuolar membrane and perivacuolar compartments, which likely represent late endosomes. These data suggest that rapamycin-induced starvation causes the accumulation of PI(3)P in late endosomes. The localization of GFP-Vps27 in *ymr1Δ* mutants showed slightly more GFP signal on endosome-like and vacuolar membranes than untreated wild-type cells. Leucine starvation of the *ymr1Δ*

mutant cells resulted in increased accumulation of GFP-Vps27 to the perivacuolar/vacuolar compartments compared to GFP-Vps27 localization in wild-type cells. Rapamycin treatment caused a more dramatic relocalization of GFP-Vps27 to endosomal/perivacuolar structures and the vacuolar membrane in the *ymr1Δ* mutant cells, although cytoplasmic signal was detectable in both starvation treatments.

GFP-Vps27 was accumulated on the vacuolar membrane and endosomal-like structures in the *ymr1Δsjl3Δ* mutant in untreated cells, in agreement with previous observations (Parrish et al., 2004). Amino acid starvation dramatically induced the localization of GFP-Vps27 to endosomal/perivacuolar structures and the vacuolar membrane in *ymr1Δsjl3Δ* mutant cells and was even more prominent in rapamycin treated cells. Under both starvation conditions, the cytoplasmic pool of GFP-Vps27 was almost completely depleted.

Together these results suggest that starvation induces the accumulation of PI(3)P on late endosomes which disrupts the MVB pathway in *ymr1Δ* cells, however the retromer is still functional and recycles Ftr1 to the plasma membrane. In the *ymr1Δsjl3Δ*, however, the accumulation of PI(3)P levels at the endosomal/perivacuolar compartment is enough to disrupt the endocytic pathway, including retromer. Therefore Ftr1-GFP accumulates in endosomes near the vacuole. These data also suggest that Npr1 might have another function in the endocytic pathway that affects the trafficking Ftr1-GFP, as the trafficking of Ftr1-GFP in this strain is different from the *ymr1Δsjl1Δ* and *ymr1Δsjl2Δ* trafficking

phonotype. In both the *ymr1Δsjl1Δ* and *ymr1Δsjl2Δ*, Ftr1-GFP was continually trafficked to the vacuole.

The increased localization of PI(3)P to endosomes during starvation supports our previous observation that endocytic trafficking is also upregulated (Chapter 3). PI(3)P was also accumulated on the perivascular region in *ymr1Δ*, indicating that the endocytic pathway was upregulated as a result of starvation, although Ftr1-GFP was not endocytosed. The lack of Ftr1-GFP endocytosis in the *ymr1Δ* during starvation suggests that Ymr1 function is involved in Ftr1 trafficking, although through an unknown mechanism.

To determine whether Ftr1-GFP accumulates in late endosomes of an MVB mutant during starvation, we analyzed Ftr1-GFP trafficking in a strain expressing a dominant-negative form of Vps4 (*vps4E233Q*) during starvation (Figure 4.1C). Cells expressing chromosomally integrated Ftr1-GFP were transformed with empty vector or *vps4*(E233Q) and were grown selective medium until mid-log phase. At time zero, untreated cells were analyzed by fluorescence microscopy and transferred to selective medium lacking leucine or rapamycin was added. After an hour of incubation, the cells were analyzed again to determine the localization and trafficking of Ftr1-GFP. The vacuoles in cells expressing empty vector control and cells expressing *vps4*(E233Q) were devoid of signal. Leucine starvation of cells expressing empty vector induced downregulation of Ftr1-GFP as evidenced by the accumulation of GFP signal in the vacuole. Ftr1-GFP was stabilized on the plasma membrane in leucine-starved of cells expressing the *vps4*(E233Q). This result suggested that in MVB

mutants even under starvation conditions Ftr1-GFP is likely recycled from the late endosome by retromer sorting. To test this idea we analyzed Ftr1-GFP trafficking in a strain deleted for the retromer subunit Vps35 (Nothwehr et al., 1999; Nothwehr et al., 2000) (Figure 4.1 D). Starvation was induced in both the wild-type cells and *vps35Δ* cells as in Figure 4.1. Iron was also added to discrete cultures of both wild-type and *vps35Δ* cells at time zero. Both wild-type and control cells were devoid of vacuolar GFP signal in untreated cells. Following starvation, GFP accumulation was observed in the vacuoles of wild-type leucine starved, rapamycin and Fe^{3+} treated cells. The *vps35Δ* cells displayed substantial GFP accumulation in the vacuole in all conditions, including the control. These results indicate that retromer is required for the recycling of Ftr1-GFP to the plasma membrane in starving cells. The accumulation of GFP signal in the vacuoles of untreated *vps35Δ* indicates that Ftr1 continually cycles through the retromer pathway in cells growing in mid-log phase, consistent with previously published results (Strochlic et al., 2008a).

Together these data indicate that starvation induces accumulation of PI(3)P to endosomal/perivacuolar membranes. The increase of PI(3)P is likely a result of the increased flow of lipids through the endocytic pathway as a consequence of starvation-induced upregulation of endocytosis. The increase in PI(3)P in late endosomal/perivacuolar membranes also resultes in increased localization of ESCRT-0 to these same membranes. The increased localization of ESCRT-0 during starvation likely increases the efficiency of cargo sorting into ILVs and subsequent degradation. Therefore the increase of PI(3)P levels in the

late endosome/perivacuolar membrane must be tightly regulated as a small increase of cellular PI(3)P levels, like in the *ymr1Δ* mutant sequesters enough ESCRT-0 to affect the sorting efficiency of the MVB. This explains why Ftr1-GFP is recycled by retromer in the *ymr1Δ*. In this model, the MVB pathway increases its sorting efficiency over retromer sorting by increasing PI(3)P levels and the localization of the ESCRTs to the endosomal membrane.

To further study the accumulation of PI(3)P during starvation to late endosomal/perivacuolar membranes during starvation, the localization of GFP-$FYVE_{EEA1}$ should also be analyzed during starvation (Burd 1998). In addition, the identity of the membranous structures where GFP-Vps27 was localizing in response to starvation should be characterized.

4.3.2 *Rsp5 Is Relocalized During Starvation*

We demonstrated in Chapter 3 that starvation-induced downregulation of plasma membrane proteins is dependent upon the catalytic activity of Rsp5. Here we sought to determine how the ubiquitination activity of Rsp5 is regulated to control the entry of cargoes into the MVB pathway during starvation. Rsp5 could be regulated during starvation through increasing its membrane localization where it could readily interact cargoes. Rsp5 is known to associate with adaptor proteins that act as cofactors. By assembling a starvation-specific cofactor complex, perhaps the activity of Rsp5 during starvation is increased, leading to the ubiquitination of more cargoes.

To test these hypotheses, we first sought to determine whether the localization of Rsp5 changes during starvation. We first analyzed the localization

of N-terminal DsRed-fusions of Rsp5 before and after amino acid starvation (Figure 4.2A). In complete medium, the majority of DsRed-Rsp5 was soluble in the cytoplasm, although there was some signal in punctate dots throughout the cell. Following amino acid starvation, DsRed-Rsp5 was re-localized to the plasma membrane and to more puncta throughout the cell. To determine whether the identity of the Rsp5-positive puncta were endosomes, we expressed the DsRed-Rsp5 chimera with various GFP-tagged ESCRT proteins including GFP-Vps27 (ESCRT-0) (Figure2B), GFP-Did2 (ESCRT-III) (Figure 4.2C) and Vps4-GFP (Figure 4.2D). DsRed-Rsp5 colocalized with GPF-Vps27 before and after amino acid starvation. DsRed-Rsp5 and GFP-Vps27 localized to endosomes in the control and accumulated on the vacuolar membrane during starvation, similar to our results in Figure 4.1B. These data suggest that GFP-Vps27 and Rsp5 remain on endosomal membranes throughout the MVB pathway during starvation. DsRed-Rsp5 was not colocalized with GFP-Did2 in the control, and was slightly more colocalized following leucine starvation and rapamycin treatment. Vps4-GFP did not colocalize with DsRed-Rsp5 under any condition. This result was not surprising as Vps4 is only transiently associated with the membrane at the late stage of ILV formation (Babst et al., 1998). The fast cycling of Vps4 on and off the membrane prevents the detection of colocalization between Vps4 and Rsp5. These analyses demonstrate that Rsp5 is localized to the cytoplasm and early endosomes in both control and starvation conditions. Following starvation, DsRed-Rsp5 distribution is shifted more towards membrane association, with plasma membrane and endosomes.

Figure 4.2. Starvation Induced Relocaizaton of Rsp5 is Dependent Upon TORC1 .(A) Rsp5 localization in cells expressing wild-type DsRED-Rsp5 and the *rsp5-1* mutant allele. Cells were grown to mid-log phase and at time zero, cells were resuspended in leucine minus (-Leu) medium or rapamycin (+Rap) was added. (B). Colocalization of ESCRT-0 (GFP-Vsp27) and DsRED-Rsp5 under similar conditions in A. (C) Localization of GFP-Vps27, GFP-Did2 (D) or Vps4-GFP (E).

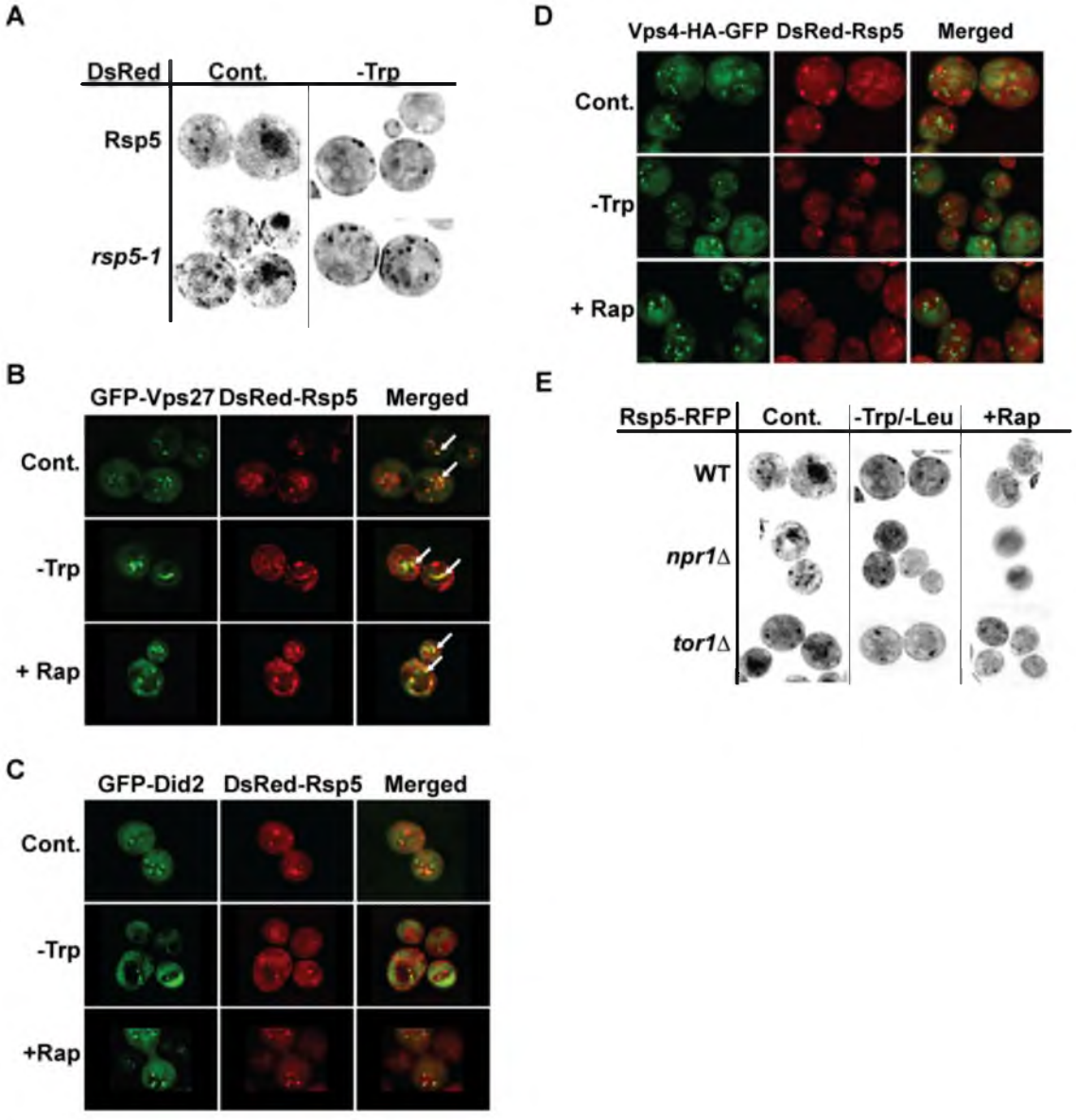
A
DsRed
Cont.
-Trp
Rsp5
rsp5-1
B
GFP-Vps27
DsRed-Rsp5
Merged
Cont.
-Trp
+ Rap
C
GFP-Did2
DsRed-Rsp5
Merged
Cont.
-Trp
+Rap
D
Vps4-HA-GFP
DsRed-Rsp5
Merged
Cont.
-Trp
+ Rap
E
Rsp5-RFP
Cont.
-Trp/-Leu
+Rap
WT
npr1Δ
tor1Δ

The localization of Rsp5 to the membrane might depend on interaction with the substrate or with another membrane associated protein. Our previous result from Chapter 3 demonstrated that deletion of *NPR1*, a kinase downstream of TORC1, inhibited Ftr1-GFP downregulation following rapamycin treatment, but did not block the amino acid starvation response. In addition, a recent proteomics analysis discovered an Npr1 phosphorylation site in Rsp5, indicating Npr1 could influence the function of Rsp5 (Breitkreutz 2010). Therefore we analyzed DsRED-Rsp5 localization in the *npr1Δ* and the *tor1Δ* following amino acid starvation and rapamycin treatment (Figure 4.2 E). The majority of Ds-RED-Rsp5 in *npr1Δ* untreated cells was accumulated on internal puncta with little cytoplasmic signal, whereas untreated wild-type cells had much more soluble DsRED-Rsp5 signal. Following rapamycin treatment of *npr1Δ* mutant cells, DsRED-Rsp5 was reloclazied completely to the cytoplasm. Amino acid starvation of *npr1Δ* mutant cells resulted in partial relocalization of DsRED-Rsp5 to membranes, although to a lesser degree than wild-type cells. The localization of DsRED-Rsp5 in *tor1Δ* mutant cells was similar under all conditions to wild-type cells. The normal behavior of DsRED-Rsp5 in *tor1Δ* mutant cells is most likely due to the presence of the Tor2 kinase, which can substitute for Tor1 in the TORC1 complex.

The cytoplasmic distribution of DsRED-Rsp5 in *npr1Δ* mutants following rapamycin treatment is in agreement with our previous results where Ftr1-GFP internalization is blocked by the deletion of *NPR1* following rapamycin treatment.

This result suggests that Rsp5 localization in rapamycin-treated cells is dependent upon the activity of Npr1.

Together, these data show that amino acid starvation and rapamycin treatment induce relocalization of Rsp5 from Vps27-positive early endosomes to late endosome/perivacuolar membrane structures. In addition, we further show that the relocalization of Rsp5 in rapamycin treated cells is dependent upon TORC1 inactivation. These results support a model in which starvation induces the relocalization of Rsp5 to the plasma membrane and to endosomes to maintain the ubiquitination of cargoes to increase the sorting of cargoes into MVBs and prevent recycling by retromer.

4.3.3 *Npr1 Regulates Rsp5 Relocalization During Starvation*

A recent proteomics study discovered that Npr1 phosphorylates Rsp5 at position S216 (Breitkreutz et al., 2010), in between the C2 lipid interaction domain and the WW cargo recognition domains (Figure 1.4). Npr1 is involved in membrane trafficking (De Craene et al., 2001; Kamura et al., 2001) and is activated upon TORC1 inactivation (Gander et al., 2008; Jacinto et al., 2001). To test whether the phosphorylation of Rsp5 at Ser216 by Npr1 has an effect on Ftr1-GFP trafficking during starvation, we analyzed Ftr1-GFP trafficking in wild-type and in the *rsp5-1* mutant strain transformed with plasmids expressing TAP-tagged wild-type Rsp5, TAP-Rsp5, the phosphorylation mutant, TAP-Rsp5(S216A) or the phosphomimetic mutant, TAP-Rsp5(S216E) (Figure 4.3). Cells were grown to mid-log phase in selective medium and analyzed by fluorescence microscopy. Wild-type cells expressing either TAP-Rsp5 or

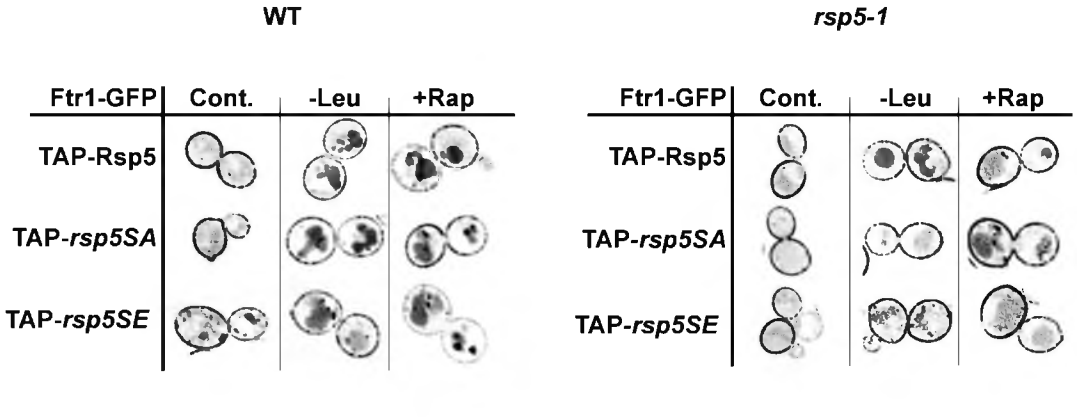

Figure 4.3. The Phosphorylation of Rsp5 Plays a Role in Starvation Induced Downregulation of Ftr1-GFP During Starvation. (A) The localization of Ftr1-GFP was analyzed in wild-type and *rsp5-1* cells were transformed with mutant forms of Rsp5.

TAP-Rsp5(S216A) localized Ftr1-GFP exclusively to the plasma membrane, however the expression of TAP-Rsp5(S216E) caused relocalization of Ftr1-GFP to endosomes. Following leucine starvation or rapamycin treatment, all wild-type cells were positive for vacuolar Ftr1-GFP signal. Ftr1-GFP localization in untreated *rsp5-1* mutants expressing TAP-Rsp5, TAP-Rsp5(S216A) or TAP-Rsp5(S216E) were devoid of internal GFP signal. Following 1 hour of incubation in leucine-depleted medium or in presence of rapamycin, all wild-type cells were positive for vacuolar Ftr1-GFP signal. In nonstarving *rsp5-1* mutants expressing TAP-Rsp5, TAP-Rsp5(S216A) or TAP-Rsp5(S216E) Ftr1-GFP localized to the plasma membrane. Following leucine starvation, only the cells expressing TAP-Rsp5(S216E) did not contain vacuolar GFP signal. Rapamycin treatment of all three strains induced the endocytosis of Ftr1-GFP and displayed vacuolar GFP-signal, although expression of TAP-Rsp5(S216E) caused less vacuolar GFP signal in both leucine starved and rapamycin treated cells than the corresponding wild-type cells. These results indicate that mutation of the Npr1 phosphorylation site in Rsp5 disrupts the starvation-induced endocytosis of Ftr1-GFP, suggesting that Npr1-dependent phosphorylation contributes to the regulation of Rsp5 during the starvation response.

Additional experiments are required to fully understand the regulation of Rsp5 activity during starvation. It is clear that mutating S216 in Rsp5 disrupted the starvation-induced endocytosis of Ftr1-GFP, however this experiment should be repeated where pTAP-Rsp5(S216A) or pTAP-Rsp5(S216E) expression is the only source of Rsp5. The trafficking of Ftr1-GFP in the *npr1Δ* expressing both

S216 mutants should also be analyzed to confirm that the altered trafficking of Ftr1-GFP is a result of Rsp5 mutation. The fact that starvation-induced relocalization of Rsp5 is inhibited in cells treated with rapamycin but in those starved for amino acids indicates TORC1 signaling is not required for the amino acid starvation induced response. This supports our previous observation from Chapter 3 that a TORC1-independent starvation response pathway is responsible for the reolocalization of Rsp5 in cells starving for amino acids.

4.3.4 *Rsp5 Adaptors Regulate Endocytosis of Ftr1-GFP*

Rsp5 forms complexes with many cargo adaptors that direct the ubiquitination activity of Rsp5 towards a wide variety of proteins. Rsp5 binds to proline-rich motifs (PPXY or PPXL) which are present in some target proteins and in adaptors (Chang et al., 2000). Many adaptors have been identified, including soluble and membrane localized adaptors (Lin et al., 2008; Sullivan et al., 2007). In addition Rsp5 cofactors have been identified that assemble with Rsp5 into protein complexes, thereby regulating the ubiquitination activity of Rsp5 (Helliwell et al., 2001; Leon et al., 2008). The Bul1-Bul2-Rsp5 complex was shown to regulate the intracellular trafficking of Gap1 through the polyubiquitination of Gap1 through UbK63-linked chains (Helliwell et al., 2001). The monoubiquitination of Gap1 at the Golgi results in sorting of the transporter to the plasma membrane. However polyubiquitination by the Bul1-Bul2-Rsp5 complex induces the sorting of Gap1 from the plasma membrane and the Golgi into the MVB pathway (Helliwell et al., 2001). Some deubiquitinating enzymes form complexes with Rsp5 adding another level of upiquitination regulation

(Baker et al.; Xiao et al.). Deubiqutinated proteins can be recycled to the plasma membrane by retromer (McGough and Cullen, 2011). Therefore polyubiquitination of cargoes increases the sorting efficiency of cargoes into the MVB pathway by preventing recycling.

To test whether a specific Rsp5 adaptor is required for starvation induced-receptor downregulation, we analyzed the trafficking of Ftr1-GFP following amino acid starvation of strains deleted for several known Rsp5 adaptors including *ear1Δ*, *ssh4Δ*, *ear1Δssh4Δ*, *hse1Δ*, *rup1Δ*, *ubp2Δ*, *bul1Δ*, and *bul2Δ* (not shown). No single deletion inhibited starvation-induced downregulation of Ftr1-GFP.

These results suggested redundancy in the recognition of Ftr1-GFP by Rsp5 adaptors. Because the Bul1-Bul2-Rsp5 complex has been shown to be involved in the polyubiqutination of cargo proteins, the result suggested that polyubiqutination might be required for sorting of Ftr1-GFP into the MVB pathway during starvation. Therefore we analyzed Ftr1-GFP localization in the *bul1Δbul2Δ* following starvation (Figure 4.4 A). Under all conditions, the double *bul1Δbul2Δ* mutant did not show internal GFP signal.

4.3.5 *Polyubiquitination of Ftr1-GFP is Required for Endocytosis*

To further test whether polyubiquitination of Ftr1-GFP is required for endocytosis during amino acid starvation and iron induced downregulation, we overexpressed the ubiquitin mutant Ub(K63R) in wild-type cells under the copper inducible promoter of the *CUP1* gene (Arnason and Ellison, 1994) (Figure 4.4 B). The Ub(K63R) mutant is incapable of forming polyubiquitn chains. Ubiquitin expression was induced by the addition of Cu^{2+} 30 minutes prior to time zero. At

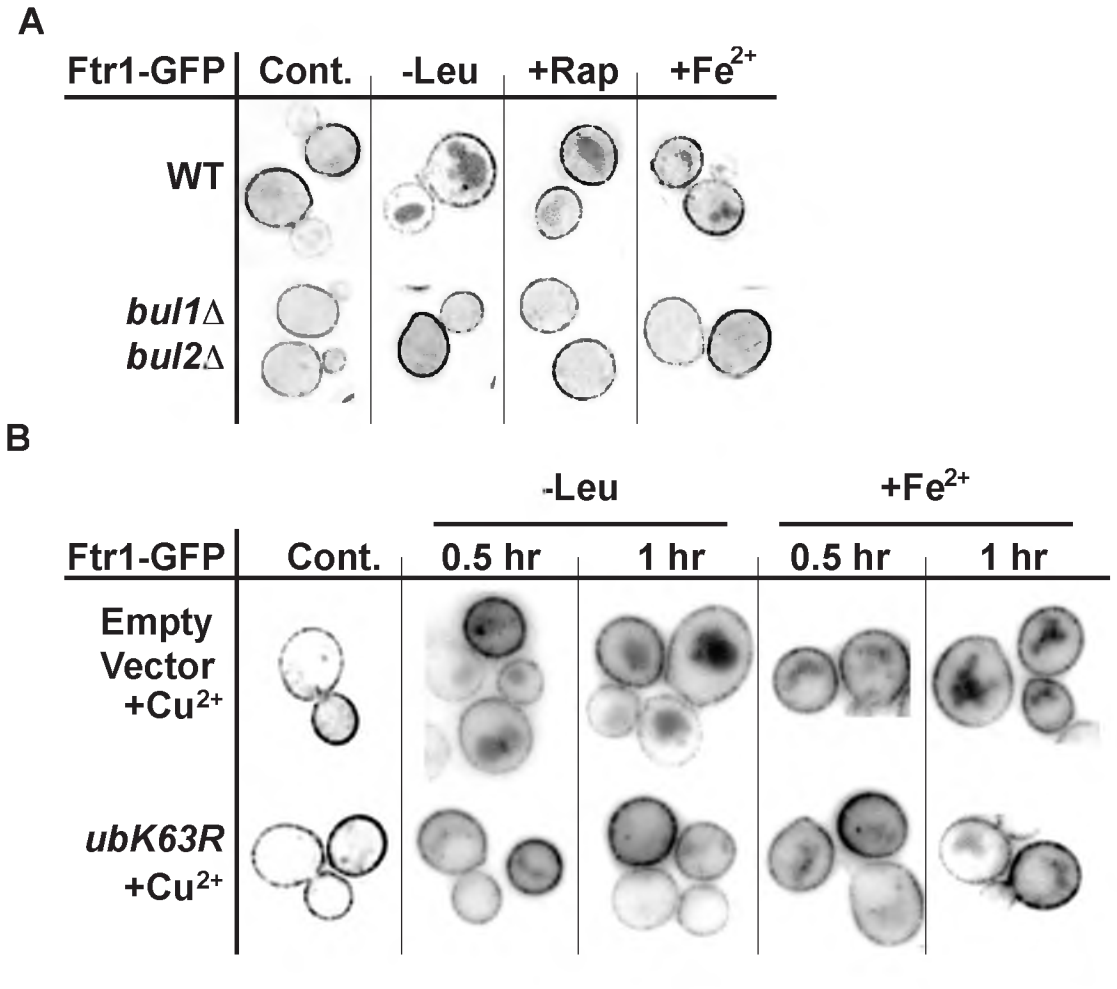

Figure 4.4. Bul1, Bul12 and Rsp5 are Required for the Polyubiquitination and Internalization of Ftr1-GFP During Starvation. (A) The trafficking of Ftr1-GFP was analyzed in wild-type cells and in the *bul1Δbul2Δ* were starved for leucine, treated with rapamycin or treated with iron. (B). Ftr1-GFP localization following overexpression of either the empty vector or the ubiquitin mutant, UbK62R by Cu^{2+} addition.

time zero, the cells were either transferred to leucine-depleted medium (containing Cu^{2+}) or Fe^{2+} or rapamycin was added to the culture. Ftr1-GFP in wild-type cells transformed with empty vector was sorted to the vacuole under all treatments. However, wild-type cells expressing Ub(K63R) did not internalize Ftr1-GFP under any condition, even with wild-type ubiquitin expression in the background. This result strongly suggests that the polyubiquitination is required for the downregulation of Ftr1-GFP. However, to directly test if Ftr1-GFP is indeed polyubiquitinated by the Bul1-Bul2-Rsp5 complex Western blot analysis of Myc-Ub expressing wild-type and *bul1Δbul2Δ* cells should be performed.

4.4. *Conclusions*

The MVB pathway is essential for the degradation of plasma membrane proteins. We previously showed that the MVB pathway plays a crucial role in mitigating acute starvation by trafficking membrane proteins to the vacuole where they are degraded. Vacuolar transporters pump the resulting amino acids from the lumen to the cytoplasm where they can be reused for the synthesis of proteins. The ubiquitination of plasma membrane proteins is required for efficient sorting of cargoes by the ESCRTs into the MVB pathway and is catalyzed by the ubiquitin ligase, Rsp5 (Piper and Katzmann). We show here that the efficiency of MVB sorting of Ftr1-GFP during starvation is regulated by the localization and activity of Rsp5 and by the recruitment of ESCRT-0 to the endosome.

Our analysis of PI(3)P localization indicates that starvation induces the accumulation of this lipid in late endosomal membranes and that ESCRT-0 is also accumulated on these membranes. We also show that increased

localization of ESCRT-0 to endosomes during starvation limits the recycling of Ftr1-GFP to the plasma membrane by retromer. Furthermore, we demonstrate that Rsp5 is also localized to the plasma membrane and to ESCRT-positive membranes during starvation, and that Rsp5 relocalization is partially regulated by TORC1. We previously showed that deletion of Npr1, a kinase downstream of TORC1, was required for TORC1-dependent downregulation of plasma membrane proteins. From our Rsp5 localization studies, it is clear that TORC1 activation of Npr1 functions to relocalize Rsp5 to membranes during starvation. Together these results suggest that starvation induced TORC1 inactivation causes increased Rsp5 localization to the plasma membrane and endosome, which results in efficient ubiquitination of membrane proteins. Furthermore, increased localization of ESCRT-0 to endosomes ensures efficient sorting of these ubiquitinated cargoes into the MVB pathway.

Finally we also demonstrated that Ftr1-GFP ubiquitination is dependent upon the Rsp5 cofactors Bul1 and Bul2. These cofactors have been shown to form a complex with Rsp5 to direct polyubiquitination of specific cargoes (De Craene et al., 2001; Galan and Haguenauer-Tsapis, 1997; Leon et al., 2008; Schmidt et al., 1998). We further show that the polyubiquitination of Ftr1-GFP is required for its endocytosis during starvation or iron shock.

Our results clearly demonstrate a starvation pathway that upregulates the flow of cargoes into the MVB pathway by localizing Rsp5 to cargo-rich membranes and limiting cargo recycling, thereby increasing the efficiency of ESCRT sorting at endosomes. The delivery of cargo to the vacuole during

starvation plays a critical role in supply the cell with the amino acids necessary to adapt to the starvation conditions as described in Chapter 3. Together, the results presented here describe a starvation-response pathway in which TORC1 regulation of Npr1 increases Rsp5 activity in order to enhance the sorting of plasma membrane proteins into the MVB pathway.

4.5 *Materials and Methods*

4.5.1 *Materials*

Iron was added to 0.5 mM (Fe^{2+}). Copper was added to 0.1 mM (Cu^{2+}). Rapamycin was used at a final concentration of 200 ng/mL. Fluorescence microscopy was performed on a deconvolution microscope (DeltaVision, Applied Precision, Issaquah, WA).

4.5.2 *Methods*

4.5.2.1 Strains and media. *S. cerevisiae* strains used in this study are listed in Table 4.1. To maintain plasmids, yeast were grown in appropriate complete synthetic dropout medium. Wild type cells as well as those containing genomic integrations or deletions were grown in either rich YPD medium (yeast extract-peptone-dextrose) or complete synthetic media YNB (Yeast Nitrogen Base) with 2% Glucose + Drop-out Mix Synthetic from US Biological (Swampscott, MA) containing the following components in [mg/L]: Adenine [10], Ala [40], Arg [40], Asn [40], Asp [40], Cys [40], Gln [40], Glu [40], Gly [40], His [40], Myo-Inositol [40], Ile [40], Leu [200], Lys [40], Met [40], Para-Aminobenzoic Acid [4], Phe [40], Pro [40], Ser [40], Thr [40], Trp [40], Tyr [40], Uracil [40], Val [40].

4.5.2.2 DNA manipulations. Plasmids used in this study are listed in Table 4.1. All plasmids were constructed using standard cloning techniques. The pRS4XX shuttle vectors used in this study have been described previously (Christianson et al., 1992). Plasmid-based GFP fusions used pEGFP-C1 obtained from Clontech Laboratories Inc. (Palo Alto, CA).

4.6 *References*

Arnason, T., and M.J. Ellison. 1994. Stress resistance in Saccharomyces cerevisiae is strongly correlated with assembly of a novel type of multiubiquitin chain. *Mol Cell Biol*. 14:7876-7883.

Attar, N., and P.J. Cullen. 2010. The retromer complex. *Adv Enzyme Regul*. 50:216-236.

Babst, M., T.K. Sato, L.M. Banta, and S.D. Emr. 1997. Endosomal transport function in yeast requires a novel AAA-type ATPase, Vps4p. *Embo J*. 16:1820-1831.

Babst, M., B. Wendland, E.J. Estepa, and S.D. Emr. 1998. The Vps4p AAA ATPase regulates membrane association of a Vps protein complex required for normal endosome function. *Embo J*. 17:2982-2993.

Baker, R.T., J.W. Tobias, and A. Varshavsky. 1992. Ubiquitin-specific proteases of Saccharomyces cerevisiae. Cloning of UBP2 and UBP3, and functional analysis of the UBP gene family. *J Biol Chem*. 267:23364-23375.

Beck, T., A. Schmidt, and M.N. Hall. 1999. Starvation induces vacuolar targeting and degradation of the tryptophan permease in yeast. *J Cell Biol*. 146:1227-1238.

Blondel, M.O., J. Morvan, S. Dupre, D. Urban-Grimal, R. Haguenauer-Tsapis, and C. Volland. 2004. Direct sorting of the yeast uracil permease to the endosomal system is controlled by uracil binding and Rsp5p-dependent ubiquitylation. *Mol Biol Cell*. 15:883-895.

Breitkreutz, A., H. Choi, J.R. Sharom, L. Boucher, V. Neduva, B. Larsen, Z.Y. Lin, B.J. Breitkreutz, C. Stark, G. Liu, J. Ahn, D. Dewar-Darch, T. Reguly, X. Tang, R. Almeida, Z.S. Qin, T. Pawson, A.C. Gingras, A.I. Nesvizhskii, and M. Tyers. 2010. A global protein kinase and phosphatase interaction network in yeast. *Science*. 328:1043-1046.

Burd, C.G., and S.D. Emr. 1998. Phosphatidylinositol(3)-phosphate signaling mediated by specific binding to RING FYVE domains. *Mol Cell*. 2:157-162.

Chang, A., S. Cheang, X. Espanel, and M. Sudol. 2000. Rsp5 WW domains interact directly with the carboxyl-terminal domain of RNA polymerase II. *J Biol Chem*. 275:20562-20571.

Christianson, T.W., R.S. Sikorski, M. Dante, J.H. Shero, and P. Hieter. 1992. Multifunctional yeast high-copy-number shuttle vectors. *Gene*. 110:119-122.

De Craene, J.O., O. Soetens, and B. Andre. 2001. The Npr1 kinase controls biosynthetic and endocytic sorting of the yeast Gap1 permease. *J Biol Chem*. 276:43939-43948.

Galan, J.M., and R. Haguenauer-Tsapis. 1997. Ubiquitin lys63 is involved in ubiquitination of a yeast plasma membrane protein. *Embo J*. 16:5847-5854.

Galan, J.M., C. Volland, D. Urban-Grimal, and R. Haguenauer-Tsapis. 1994. The yeast plasma membrane uracil permease is stabilized against stress induced degradation by a point mutation in a cyclin-like "destruction box". *Biochem Biophys Res Commun*. 201:769-775.

Gander, S., D. Bonenfant, P. Altermatt, D.E. Martin, S. Hauri, S. Moes, M.N. Hall, and P. Jenoe. 2008. Identification of the rapamycin-sensitive phosphorylation sites within the Ser/Thr-rich domain of the yeast Npr1 protein kinase. *Rapid Commun Mass Spectrom*. 22:3743-3753.

Hanson, P.I., S. Shim, and S.A. Merrill. 2009. Cell biology of the ESCRT machinery. *Curr Opin Cell Biol*. 21:568-574.

Heitman, J., N.R. Movva, and M.N. Hall. 1991. Targets for cell cycle arrest by the immunosuppressant rapamycin in yeast. *Science*. 253:905-909.

Helliwell, S.B., S. Losko, and C.A. Kaiser. 2001. Components of a ubiquitin ligase complex specify polyubiquitination and intracellular trafficking of the general amino acid permease. *J Cell Biol*. 153:649-662.

Hurley, J.H. 2010. The ESCRT complexes. *Crit Rev Biochem Mol Biol*. 45:463-487.

Jacinto, E., B. Guo, K.T. Arndt, T. Schmelzle, and M.N. Hall. 2001. TIP41 interacts with TAP42 and negatively regulates the TOR signaling pathway. *Mol Cell*. 8:1017-1026.

Jauniaux, J.C., and M. Grenson. 1990. GAP1, the general amino acid permease gene of Saccharomyces cerevisiae. Nucleotide sequence, protein similarity with the other bakers yeast amino acid permeases, and nitrogen catabolite repression. *Eur J Biochem*. 190:39-44.

Kamura, T., D. Burian, H. Khalili, S.L. Schmidt, S. Sato, W.J. Liu, M.N. Conrad, R.C. Conaway, J.W. Conaway, and A. Shilatifard. 2001. Cloning and characterization of ELL-associated proteins EAP45 and EAP20. a role for yeast EAP-like proteins in regulation of gene expression by glucose. *J Biol Chem*. 276:16528-16533.

Katzmann, D.J., M. Babst, and S.D. Emr. 2001. Ubiquitin-dependent sorting into the multivesicular body pathway requires the function of a conserved endosomal protein sorting complex, ESCRT-I. *Cell*. 106:145-155.

Kihara, A., T. Noda, N. Ishihara, and Y. Ohsumi. 2001. Two distinct Vps34 phosphatidylinositol 3-kinase complexes function in autophagy and carboxypeptidase Y sorting in Saccharomyces cerevisiae. *J Cell Biol*. 152:519-530.

Krampe, S., and E. Boles. 2002. Starvation-induced degradation of yeast hexose transporter Hxt7p is dependent on endocytosis, autophagy and the terminal sequences of the permease. *FEBS Lett*. 513:193-196.

Laporte, J., F. Blondeau, A. Buj-Bello, D. Tentler, C. Kretz, N. Dahl, and J.L. Mandel. 1998. Characterization of the myotubularin dual specificity phosphatase gene family from yeast to human. *Hum Mol Genet*. 7:1703-1712.

Lee, J.R., A.J. Oestreich, J.A. Payne, M.S. Gunawan, A.P. Norgan, and D.J. Katzmann. 2009. The HECT domain of the ubiquitin ligase Rsp5 contributes to substrate recognition. *J Biol Chem*. 284:32126-32137.

Lempiainen, H., and D. Shore. 2009. Growth control and ribosome biogenesis. *Curr Opin Cell Biol*. 21:855-863.

Leon, S., Z. Erpapazoglou, and R. Haguenauer-Tsapis. 2008. Ear1p and Ssh4p are new adaptors of the ubiquitin ligase Rsp5p for cargo ubiquitylation and sorting at multivesicular bodies. *Mol Biol Cell*. 19:2379-2388.

Lin, C.H., J.A. MacGurn, T. Chu, C.J. Stefan, and S.D. Emr. 2008. Arrestin-related ubiquitin-ligase adaptors regulate endocytosis and protein turnover at the cell surface. *Cell*. 135:714-725.

Loewith, R., E. Jacinto, S. Wullschleger, A. Lorberg, J.L. Crespo, D. Bonenfant, W. Oppliger, P. Jenoe, and M.N. Hall. 2002. Two TOR complexes, only one of which is rapamycin sensitive, have distinct roles in cell growth control. *Mol Cell*. 10:457-468.

McGough, I.J., and P.J. Cullen. 2011. Recent advances in retromer biology. *Traffic*.

Nakatogawa, H., K. Suzuki, Y. Kamada, and Y. Ohsumi. 2009. Dynamics and diversity in autophagy mechanisms: lessons from yeast. *Nat Rev Mol Cell Biol*. 10:458-467.

Nothwehr, S.F., P. Bruinsma, and L.A. Strawn. 1999. Distinct domains within Vps35p mediate the retrieval of two different cargo proteins from the yeast prevacuolar/endosomal compartment. *Mol Biol Cell*. 10:875-890.

Nothwehr, S.F., S.A. Ha, and P. Bruinsma. 2000. Sorting of yeast membrane proteins into an endosome-to-Golgi pathway involves direct interaction of their cytosolic domains with Vps35p. *J Cell Biol*. 151:297-310.

Oestreich, A.J., M. Aboian, J. Lee, I. Azmi, J. Payne, R. Issaka, B.A. Davies, and D.J. Katzmann. 2007. Characterization of multiple multivesicular body sorting determinants within Sna3: a role for the ubiquitin ligase Rsp5. *Mol Biol Cell*. 18:707-720.

Omura, F., Y. Kodama, and T. Ashikari. 2001. The N-terminal domain of the yeast permease Bap2p plays a role in its degradation. *Biochem Biophys Res Commun*. 287:1045-1050.

Ozcan, S., J. Dover, and M. Johnston. 1998. Glucose sensing and signaling by two glucose receptors in the yeast Saccharomyces cerevisiae. *Embo J*. 17:2566-2573.

Parrish, W.R., C.J. Stefan, and S.D. Emr. 2004. Essential role for the myotubularin-related phosphatase Ymr1p and the synaptojanin-like phosphatases Sjl2p and Sjl3p in regulation of phosphatidylinositol 3-phosphate in yeast. *Mol Biol Cell*. 15:3567-3579.

Penalver, E., P. Lucero, E. Moreno, and R. Lagunas. 1998. Catabolite inactivation of the maltose transporter in nitrogen-starved yeast could be due to the stimulation of general protein turnover. *FEMS Microbiol Lett*. 166:317-324.

Piper, R.C., and D.J. Katzmann. 2007. Biogenesis and function of multivesicular bodies. *Annu Rev Cell Dev Biol*. 23:519-547.

Raiborg, C., and H. Stenmark. 2009. The ESCRT machinery in endosomal sorting of ubiquitylated membrane proteins. *Nature*. 458:445-452.

Reinke, A., S. Anderson, J.M. McCaffery, J. Yates, 3rd, S. Aronova, S. Chu, S. Fairclough, C. Iverson, K.P. Wedaman, and T. Powers. 2004. TOR complex 1 includes a novel component, Tco89p (YPL180w), and cooperates with Ssd1p to maintain cellular integrity in Saccharomyces cerevisiae. *J Biol Chem*. 279:14752-14762.

Robinson, J.S., D.J. Klionsky, L.M. Banta, and S.D. Emr. 1988. Protein sorting in *Saccharomyces cerevisiae*: isolation of mutants defective in the delivery and processing of multiple vacuolar hydrolases. *Mol. Cell. Biol.* 8:4936-4948.

Schmidt, A., T. Beck, A. Koller, J. Kunz, and M.N. Hall. 1998. The TOR nutrient signalling pathway phosphorylates NPR1 and inhibits turnover of the tryptophan permease. *Embo J*. 17:6924-6931.

Schmidt, A., J. Kunz, and M.N. Hall. 1996. TOR2 is required for organization of the actin cytoskeleton in yeast. *Proc Natl Acad Sci U S A*. 93:13780-13785.

Seaman, M.N., and H.P. Williams. 2002. Identification of the functional domains of yeast sorting nexins Vps5p and Vps17p. *Mol Biol Cell*. 13:2826-2840.

Singer-Kruger, B., Y. Nemoto, L. Daniell, S. Ferro-Novick, and P. De Camilli. 1998. Synaptojanin family members are implicated in endocytic membrane traffic in yeast. *J Cell Sci*. 111 (Pt 22):3347-3356.

Stack, J.H., and S.D. Emr. 1994. Vps34p required for yeast vacuolar protein sorting is a multiple specificity kinase that exhibits both protein kinase and phosphatidylinositol-specific PI 3-kinase activities. *J Biol Chem*. 269:31552-31562.

Stenmark, H. 2009. Rab GTPases as coordinators of vesicle traffic. *Nat Rev Mol Cell Biol*. 10:513-525.

Strahl, T., and J. Thorner. 2007. Synthesis and function of membrane phosphoinositides in budding yeast, Saccharomyces cerevisiae. *Biochim Biophys Acta*. 1771:353-404.

Strochlic, T.I., B.C. Schmiedekamp, J. Lee, D.J. Katzmann, and C.G. Burd. 2008a. Opposing activities of the Snx3-retromer complex and ESCRT proteins mediate regulated cargo sorting at a common endosome. *Mol Biol Cell*. 19:4694-4706.

Strochlic, T.I., B.C. Schmiedekamp, J. Lee, D.J. Katzmann, and C.G. Burd. 2008b. Opposing activities of the Snx3-retromer complex and ESCRT proteins mediate regulated cargo sorting at a common endosome. *Mol Biol Cell*. 19:4694-4706.

Sullivan, J.A., M.J. Lewis, E. Nikko, and H.R. Pelham. 2007. Multiple interactions drive adaptor-mediated recruitment of the ubiquitin ligase rsp5 to membrane proteins in vivo and in vitro. *Mol Biol Cell*. 18:2429-2440.

Swaminathan, S., A.Y. Amerik, and M. Hochstrasser. 1999. The Doa4 deubiquitinating enzyme is required for ubiquitin homeostasis in yeast. *Mol Biol Cell*. 10:2583-2594.

Urban, J., A. Soulard, A. Huber, S. Lippman, D. Mukhopadhyay, O. Deloche, V. Wanke, D. Anrather, G. Ammerer, H. Riezman, J.R. Broach, C. De Virgilio, M.N. Hall, and R. Loewith. 2007. Sch9 is a major target of TORC1 in Saccharomyces cerevisiae. *Mol Cell*. 26:663-674.

Wang, T., U. Lao, and B.A. Edgar. 2009. TOR-mediated autophagy regulates cell death in Drosophila neurodegenerative disease. *J Cell Biol*. 186:703-711.

Wang, X., and C.G. Proud. 2009. Nutrient control of TORC1, a cell-cycle regulator. *Trends Cell Biol*. 19:260-267.

Wullschleger, S., R. Loewith, and M.N. Hall. 2006. TOR signaling in growth and metabolism. *Cell*. 124:471-484.

Xiao, W., T. Fontanie, and M. Tang. 1994. UBP5 encodes a putative yeast ubiquitin-specific protease that is related to the human Tre-2 oncogene product. *Yeast*. 10:1497-1502.

Zinzalla, V., D. Stracka, W. Oppliger, and M.N. Hall. 2011. Activation of mTORC2 by association with the ribosome. *Cell*. 144:757-768.